

Bachelor Thesis

Amplifier design for an implementation of
motional feedback in a bass loudspeaker

by

Alexander Avdeev & Hitesh Djalani &
Daniel Vlaardingerbroek

to obtain the degree of Bachelor of Science
at the Delft University of Technology,
to be defended on Monday June 29, 2020.

Student number: 4713753

Project duration:

Thesis committee:

4648153

April 20, 2020 – July 3, 2020

Prof. dr. ir. W.A. Serdijn,

dr. ir. G.J.M. Janssen,

dr. O.A. Krasnov,

4580834

TU Delft, jury chair

TU Delft, supervisor/jury member

TU Delft, jury member

Abstract

The displacement of a loudspeaker cone is not linearly proportional to the voltage/current at its input provided. This is due to electrical and mechanical limitations. The distortion is more noticeable at lower frequencies. This report is one of two reports, that will explain how to minimize this distortion. The motion of the loudspeaker cone will be measured and compared with the input voltage. This way the error in the output can be found. Finally, a system will adjust the current through the voice coil to decrease this error. An accelerometer is used as a sensor and the ADAU1777 is used to compensate for the error in output displacement. Finally, a voltage to current converter is used to convert and amplify the output voltage from the ADAU1777 into a current signal to drive the loudspeaker. This report focuses on the voltage to current amplifier. To begin the design, a problem definition and program of requirements will be given. Usually, loudspeakers are voltage driven. This report begins by first explaining why a current-driven loudspeaker delivers less distortion. Then an attempt is made to build a single operational amplifier (opamp) design that meets the requirements for a real load. For the single opamp design, a simple version of the operational transconductance amplifier (OTA) will be compared against a Howland model based on noise performance and circuit analysis, where it will be shown that the simple OTA has a larger signal to noise ratio and does not need to meet any additional criteria to maintain a high output impedance. However, the simple OTA still does not meet the Signal to Noise (SNR). The simple OTA also did not meet the maximum Total Harmonic Distortion (THD) at 800 Hz. Then, a two opamp design will be constructed using a composite configuration to increase the SNR and decrease the THD. This design does meet the requirements given, at least for a purely resistive load. Then an electrical model of a loudspeaker, which has a complex impedance, will replace the resistive load. Now the composite design for the resistive load needs to be adjusted for the inductive characteristic of a loudspeaker at higher frequencies. The resulting design has a THD of 0.000427%, a PM of 51° and a SNR is 100.92 dB. All results will be given as simulations, because the current pandemic (COVID-19) does not make it possible to physically construct and measure this model. Micro-Cap 12 is used for circuit simulations and Slicap for circuit noise analysis.

Preface

In these challenging times for both the educational staff as well as students, the authors of this report want to express the gratitude for all the help and feedback that was provided by our supervisor Dr.ir. G.J.M Janssen. We are also very grateful for the graduation project coordinator dr.ir. I. E. Lager to organize and deal with the logistics of the graduation project. We would also like to thank our teammates from the control department Richard Eveleens, Mart Haarman en Leila Gottmer to shed the light to the somber mornings in the pas two months.

Many thanks to the people who are involved in this project but are not mentioned here.

*Alexander Avdeev & Hitesh Dialani & Daniel Vlaardingerbroek
Delft, June 2020*

Nomenclature

List of Parameters

μ	Permeability
ϕ	Magnetic flux
A	Input voltage over output voltage of a two-port system with open output
A_v	Gain of the composite amplifier
A_y	Transconductance gain
B	Input voltage over output current of a two-port system with shorted output
C	Input current over output voltage of a two-port system with open output
C_{mes}	Moving mass converted to electrical capacitance
C_{ms}	Suspension compliance
D	Input current over output current of a two-port system with shorted output
$D_{tolerance}$	Deviation due to resistor tolerance
D_{max}	Maximum deviation due resistor tolerances
e	Error signal
F	Feedback factor
F_s	Resonance frequency
G	Open loop voltage gain
H	Transfer function
K_{ms}	Restoring force
L_e	Voice coil inductance
L_{mes}	Enclosure suspension converted to electrical inductance
M_{ms}	Moving mass
O	Output signal
p	Resistor tolerance
R_a	radiation resistance
R_e	Voice coil resistance
R_{es}	Mechanical resistance converted to electrical resistance
R_i	Input resistance
R_{me}	Electrical resistance converted to mechanical resistance
R_{ms}	mechanical resistance of damper
R_o	Output resistance
R_{sense}	Sensing resistance
R_x	Output resistance of the Howland amplifier
S	Input signal
SD	effective cone area
S_v	Output noise voltage of opamps
Q	Quality factor
u	Velocity of the loudspeaker cone
X_1	Power opamp
X_2	Precesion opamp
Z_a	Acoustic impedance
Z_g	Source impedance
Z_{mg}	Electrical source impedance converted into mechanical damper
Z_m	lumped electrical components
Z_s	lumped mechanical components

Abbreviations

BW	Bandwidth
CS	Current source
EMF	Electromotor force
GBWP	Gain Bandwith Product
HD	Harmonic Distortion
IMD	Intermodulated distortion
MFB	Motion Feedback
OpAmp	Operational amplifier
OTA	Operational transconductance amplifier
PoR	Program of Requirements
PM	Phase Margin
SNR	Signal to noise ratio
THD	Total Harmonic Distortion
VCCS	Voltage Controlled Current Source
VCVS	Voltage Controlled Voltage Source
VS	Voltage source

List of Figures

3.1	Cross section of a Woofer, source: https://en.wikipedia.org/wiki/Woofers	5
3.2	Stiffness over distance	6
3.3	Harmonic distortion in sound for stiffness displacement, source: [14]	6
3.4	Force factor	6
3.5	HD and IMD distortion due to Force factor	7
3.6	Displacement of voice coil, source:[14]	7
3.7	HD and IMD distortion due to only Voice Coil displacement	8
3.8	Non-linear relationship between flux Density B and Magnetic field strength H , source:[14]	8
3.9	HD and IMD distortion due to only voice coil current	9
3.10	Loudspeaker driver model, source: http://projectryu.com/wp/2017/07/23/electrical-model-of-loudspeaker-parameters/	9
3.11	Loudspeaker electrical model, source: http://projectryu.com/wp/2017/07/23/electrical-model-of-loudspeaker-parameters/	9
3.12	Equivalent models of loudspeaker	11
4.1	Two-port representations	13
4.2	Derivation of the OTA using nullator and norator.	14
4.3	The simple OTA, with the noise sources added to it.	15
4.4	SPICE circuit of the simple transconductance amplifier with nullor as a controller	16
4.5	Howland two port representation with nullor as a controller	17
5.1	Black model of the simple OTA	19
5.2	Creating composite amplifier	20
5.3	Black model of composite amplifier without noise source added and with noise source added	21
5.4	The finalised circuit for the composite amplifier.	22
5.5	Bode plot of the OPA541, showing that the 0db-point (and its GBW) is set to 922KHz.	24
5.6	The finalised circuit for the composite amplifier.	25
5.7	The finalised circuit of the composite amplifier with the values for all the components.	26
5.9	The bode plot of the amplifier.	27
5.10	The phase plot of the amplifier.	27
6.1	Absolute magnitude plot from measured dipole speaker	28
6.2	The amplifier with the zobel network and electrical model of the loudspeaker added to it.	29
6.3	The bode plots of the the amplifier with the electrical model and Zobel network added to it.	30
6.4	The bode plots of the the amplifier with varying values of the resistor R5.	31
6.5	The finalised circuit of the amplifier, with the Zobel network and realistic load added to it.	32
6.7	The bode plots of the the finalised amplifier.	33
A.1	Absolute magnitude impedance for both subwoofers	39
A.3	Two port representation of the amplifier	41
A.2	Two port circuit	41
A.4	Nullor that consist of a nullator and norator	42
A.5	Representation of operational amplifier	42
A.6	Equivalent model of operational amplifier	43
B.1	Black model [7] of the amplifier where S is the input signal, e is the error signal, G is the open-loop voltage gain, F is the feedback factor and O is the output signal	44
B.2	Black [7] model of the amplifier where S is the input signal, N is the noise signal, e is the error signal, G is the open-loop voltage gain, F is the feedback factor and O is the output signal	45

B.3	Black model [7] of the composite amplifier where S is the input signal, e1 and e2 are the error signals, G1 and G2 are the open-loop voltage gains, F1 and F2 are the feedback factors and O is the output signal	45
B.4	Black model of the composite amplifier where S is the input signal, N1 and N2 are the noise signals, e1 and e2 are the error signals, G1 and G2 are the open-loop voltage gains, F1 and F2 are the feedback factors and O is the output signal	46
B.5	Nodel analysis of composite amplfier without R3 and R4	47
B.6	Nodel analysis of composite amplfier with R3 and R4	49
B.7	The total output noise voltage for a given bandwidth of the amplifier.	51
B.8	A comparison of the results from the inbuilt function and the method that was derived in this section.	51
B.9	The total output noise voltage for a given bandwidth of the amplifier.	52
B.10	Howland two port representation with nullor as a contorller	53
B.11	The phase diagram of the amplifier.	55
B.12	SPICE circuit of the simple transconductance amplifier with nullor as a controller	57
B.13	SPICE circuit of the howland amplifier with nullor as a controller and equivalent noise sources added	57
B.14	SPICE circuit of the composite amplifier with two nullors as controllers and equivalent noise sources added	58
D.1	The SNR of the amplifier.	60
D.2	The THD of the amplifier.	61

List of Tables

3.1	Calculated parameters for loudspeakers	10
5.1	The optimal values for C_1 , R_3 and R_4	26
6.1	The optimal values for R_z and C_z	29
6.2	The optimal values for R_5	31
8.1	Amplifier design requirements	35

Contents

Nomenclature	iv
List of Figures	vi
List of Tables	viii
1 Introduction	1
2 Program of Requirements (PoR)	2
2.1 Problem definition	2
2.1.1 Situation Assessment	2
2.1.2 Scoping analysis.	2
2.1.3 Bounding analysis.	3
2.2 Requirements	3
2.2.1 Total System	3
2.2.2 Amplifier.	3
3 Loudspeaker Theory	5
3.1 Distortions in loudspeakers.	5
3.1.1 $K_{ms}(x)$ Stiffness versus Displacement	5
3.1.2 $Bl(x)$ Force factor versus Displacement	6
3.1.3 $L_e(x)$ Voice coil inductance versus Displacement	7
3.1.4 $L_e(i)$ Voice coil inductance versus Current	8
3.2 Distortion of Current and voltage driven loudspeaker.	9
3.2.1 Electrical loudspeaker model	9
3.2.2 Voltage and current driven electrical model of loudspeaker	10
4 Amplifier structure considerations	12
4.1 Introduction	12
4.2 Basic properties of the VCCS	12
4.3 Simple OTA	13
4.3.1 Circuit derivation	13
4.3.2 Circuit analysis.	14
4.3.3 Noise performance.	14
4.4 Howland	17
4.4.1 Circuit analysis.	17
4.4.2 Noise performance.	17
4.5 Comparison.	17
4.5.1 Circuit structure comparison	18
4.5.2 Noise comparison	18
4.5.3 Circuit choice	18
5 Simple operational Transconductance amplifier and the Composite Amplifier	19
5.1 Control analysis of the simple transconductance amplifier	19
5.1.1 Control analysis	19
5.1.2 Noise analysis	20
5.2 Composite amplifier	20
5.3 Analysis of the composite amplifier	20
5.3.1 Control analysis	21
5.3.2 Noise analysis	21
5.3.3 Stability analysis	22

5.4	Component selection	22
5.4.1	Opamp selection	22
5.4.2	Power amplifier gain	23
5.4.3	Capacitor C_1 and overall amplifier gain	23
5.5	Results	26
5.5.1	Transient Analysis	26
5.5.2	AC Analysis	27
5.5.3	Distortion Analysis.	27
5.5.4	Conclusion.	27
6	Composite amplifier with realistic load	28
6.1	Problem analysis realistic load	28
6.2	Zobel network.	29
6.3	Frequency compensation	30
6.4	Adjustment of overall gain	31
6.5	Results	32
6.5.1	Transient Analysis	32
6.5.2	AC Analysis	32
6.5.3	Distortion Analysis.	33
6.5.4	Conclusion.	33
7	Discussion	34
8	Conclusions, recommendations and future work	35
8.1	Conclusions.	35
8.2	Recommendations	36
8.3	Future Work.	36
	Appendices	37
A	Extra Theory	38
A.1	Finding the equivalent loudspeaker impedance parameters from measured loudspeaker impedance graph	38
A.2	Chain matrix and nullor.	40
A.2.1	Chain matrix.	40
A.2.2	Nullor	42
B	Calculations	44
B.1	Control analysis of the simple transconductance amplifier	44
B.1.1	Control analysis	44
B.1.2	Noise Analysis	45
B.2	Control analysis of the composite amplifier.	45
B.3	Noise analysis of the composite amplifier.	46
B.4	Nodal analysis of the composite amplifier with frequency compensation.	47
B.4.1	Nodal analysis full circuit	47
B.4.2	Derivation of A_v	48
B.5	Nodal analysis of the composite amplifier with frequency compensation when the resistors for the overall gain have been added	49
B.6	Total harmonic distortion calculation using MicroCap	50
B.7	Calculating the SNR using Micro-Cap 12	50
B.7.1	Derivation	50
B.7.2	Calculation of the SNR.	52
B.8	Howland nodal analysis	52
B.9	Noise analysis simple transconductance amplifier	55
B.9.1	Primary analysis	55
B.9.2	SliCAP analysis.	56
B.10	Noise analysis howland	56
B.11	Noise analysis composite amplifier	58

C	Code	59
C.1	SliCap	59
C.1.1	Simple transconductance noise analysis	59
D	Simulations	60
D.1	Composite Amplifier with real load	60
	Bibliography	62

1

Introduction

Audio speakers are mostly implemented by using a moving coil inside a permanent magnetic field. This setup is prone to linear and non-linear distortions. While linear distortions are easy to correct for, the non-linear distortions pose a challenge to deal with. A solution to this problem was proposed by Philips in [13]. It was proposed to use a motional feedback (MFB) system to correct for the distortions at the output. To correct for distortions, the motion of the speaker is measured using a sensor and compared to the input signal. Looking at the input signal, if the measured output signal is not the expected output signal the system will try to correct it by making adaptations to the loudspeaker drive signal, thus it would help "push" the loudspeaker cone through the distortions.

As part of the bachelor university program "Electrical Engineering" at the Technical University of Delft, a group of students is assigned to investigate and implement the MFB system. An accelerometer is used as the sensor and the ADAU1777 [2] is used to compensate for the error in output displacement. Finally, a voltage to current converter is used to convert and amplify the output voltage from the ADAU1777 into a current signal to drive the loudspeaker. The project has been divided into two subgroups: one will implement the control system and the other will implement an amplifier for the loudspeaker. The report of the second group focuses on how the ADAU1777 can create the appropriate control voltage to decrease the error in the loudspeaker displacement, while this report will go in-depth on the design of the amplifier that will be used to drive the loudspeaker. A loudspeaker can consist of a woofer and tweeter, for this project both subgroups will only focus on the woofer. The Woofer consists of two subwoofer. A monopole, which works from 20-80 Hz and a dipole that works from 20-300 Hz. All the requirements will be based on the dipole speaker, since the higher frequencies will lead to more distortions that will have to be dealt with. If the amplifier for the dipole speaker is finished, it is relatively straightforward to change the parameters for the monopole speaker.

Before starting with the design of the amplifier, a detailed comparison of the distortions of a loudspeaker as a function of current and voltage source will be given in Chapter 3. Using this theory and a set of requirements made in Chapter 2 the specifications for the design will be known. First, a single operational amplifier (opamp) design will be explained in Chapter 4. Then a two opamp design for a resistive load that is equal to the nominal impedance of the loudspeaker will be discussed in Chapter 5. Lastly, a two opamp design for the complex electrical model of the loudspeaker will be discussed in Chapter 6. The discussion for this report is located in Chapter 7 and the conclusion, recommendation and future work is located in Chapter 8.

2

Program of Requirements (PoR)

2.1. Problem definition

2.1.1. Situation Assessment

Current state of the problem

Most speakers that are used are based on a coil that moves in a permanent magnetic field. These systems are prone to linear and non-linear distortions, which are easily heard in the sound coming from the loudspeaker since they add harmonic distortions (HD) to the output signal. Linear distortions are easier to deal with than non-linear distortions, because a linear block filter can be designed to compensate for linear distortions. Non-linear distortions come from different sources: the stiffness of the spring system that holds the cone of the loudspeaker in an equilibrium point, the force factor that describes the integral of the flux density over the length of the coil and the non-linear inductance of the voice coil. These sources are briefly discussed in the next sections.

Stiffness

Since the movements of the loudspeaker cone are dictated by an electrical signal, a spring is attached to the cone to center it around some specific equilibrium point. If the displacement of the cone becomes too large, the force that the spring acts on to bring it back to the equilibrium point becomes non-linear.

Force factor

It is possible at some moments in the operation of the speaker for the voice coil to move beyond the plate of the magnet. This results in non-linear behavior of the force factor.

Voice coil

The voice coil moves in a non-homogeneous environment, this means that the magnetic permeability μ changes with position. For large displacements, the coil moves into the open air, which means that the magnetic permeability changes non-linearly at these moments. There is also a second source of non-linearity made by the voice coil which is dependent on the current. That non-linearity is caused by the fact that the permeability saturates at large current level

Future design

The situation to aim for is that the speaker does not experience the non-linearities described above and the distortions are kept at a minimum, this would result in the best listening experience for the user.

2.1.2. Scoping analysis

To solve the non-linearities produced by the speaker, which in turn distorts the sound coming from the speaker, MFB system can be designed. The motion of the speaker cone is measured, which then is fed back to the input stage of the system, where the input signal is subtracted from the output signal that produces the error signal. That error signal is then fed into the amplifier, which amplifies the signal so it can power the loudspeaker. The amplifier for the MFB should add minimal distortions to the signal and if possible prevent sources of distortions of the loudspeaker to occur, while also adding power to the signal.

2.1.3. Bounding analysis

The power supply voltage and power are limited, which means that the operational power of the amplifier can deliver is limited. Also, the input signal power is limited. In this project, the source of the signal is the audio that comes from the digital processing chip, which is used to compensate for the errors. The amplifier must work in the frequency ranges of the audio signal. The audio signal path must not be disturbed with a large delay, as the speed of the MFB system as a whole will largely determine its performance. That is why the amplifier must add minimal delay to the signal in order to maintain good operation of the MFB. The power performance can be found by measuring the output voltage and current. The THD can be determined by connecting sinusoidal signal with a known frequency to the input of the amplifier. Using the frequency spectrum ($\frac{V^2}{Hz}$) of the output of the amplifier, power at the signal frequency is compared to the power at the higher harmonics. By calculating the ratio of power at the higher harmonics and the power at the input signal frequency the THD can be determined. The SNR can be found by measuring the noise spectrum ($\frac{V^2}{Hz}$) over the required bandwidth. From the frequency spectrum, the power in the harmonics can be analyzed and the THD can be determined, which will be the defining parameter for the performance of the amplifier. The power supply voltage and power are limited, which means that the operational power of the amplifier can deliver is limited. Also, the input signal power is limited. In this project, the source of the signal is the audio that comes from the digital processing chip, which is used to compensate for the errors. The amplifier must work in the frequency ranges of the audio signal. The audio signal path must not be disturbed with a large delay, as the speed of the MFB system as a whole will largely determine its performance. The power performance can be found by measuring the output voltage and current. The THD can be determined by connecting sinusoidal signal with a known frequency to the input of the amplifier. Using the frequency spectrum ($\frac{V^2}{Hz}$) of the output of the amplifier, power at the signal frequency is compared to the power at the higher harmonics. By calculating the ratio of power at the higher harmonics and the power at the input signal frequency the THD can be determined. The SNR can be found by measuring the noise spectrum ($\frac{V^2}{Hz}$) over the required bandwidth.

2.2. Requirements

In this chapter, the requirements for the project are described. First, the requirements for the MFB system as a whole are given, after which the requirements that have specifically been set for the amplifier will be discussed.

2.2.1. Total System

2.1. General

- 2.1.1 The system should be bandwidth limited between 20-800 Hz for the dipole loudspeaker.
- 2.1.2 The system should be bandwidth limited between 20-300 Hz for the monopole loudspeaker.
- 2.1.3 Maximum Total Harmonic Distortion (THD) for frequencies under 1 kHz: 0.1%
- 2.1.4 The system's maximum use of power is limited to 70 Watt.
- 2.1.5 The system's audio input should have standard phone aux connection (3.5 mm Jack).
- 2.1.6 The product (excl. speaker) should not cost more than €499.99.
- 2.1.7 The product should not weigh more than 10 kg.

2.2.2. Amplifier

2.1. Environmental Conditions

- 2.1.1. Operation temperature: between -40 to 70 °C

2.2. Given parameters

- 2.2.1. Source peak to peak voltage: 1.5 V
- 2.2.2. Load nominal impedance speaker : 8 Ω
- 2.2.3. Power supply voltage: \pm 40 V

2.3. Performance requirements

2.3.1. Mandatory Requirements

- 2.3.1.1. Output power: 50 W RMS for a sinusoidal signal
- 2.3.1.2. Maximum RMS load current: 2.5 A
- 2.3.1.3. Source voltage to load current transfer: 4.71
- 2.3.1.4. The transfer function must have a deviation of under ± 1 dB for a frequency of under 800 Hz.
- 2.3.1.5. Peak to peak load voltage drive: 80 V
- 2.3.1.6. Peak to peak load current drive: 7 A
- 2.3.1.7. Maximum THD for frequencies under 800 Hz: 0.001%
- 2.3.1.8. Minimum (SNR) for frequencies under 800 Hz: 96 dB
- 2.3.1.9. Minimum Phase Margin (PM): 45°
- 2.3.1.10. The output signal must have a maximum phase deviation of 20° at 800 Hz
- 2.3.1.11. No clipping must occur for frequencies under 800 Hz.

2.3.2. Trade-off Requirements / Objectives

- 2.3.2.1. The output signal should preferably have a maximum phase deviation of 3° at 800 Hz
- 2.3.2.2. The transfer function should preferably have a deviation of under ± 0.3 dB for a frequency of under 800 Hz.
- 2.3.2.3. The SNR at the output of the amplifier for input signal frequencies under 800 Hz should preferably be above 100 dB
- 2.3.2.4. The Phase Margin should be 45° or larger to increase the robustness of the amplifier.

3

Loudspeaker Theory

The focus of this chapter is to explain why a voltage-controlled current source (VCCS) results in less non-linear distortion when driving the loudspeaker, when compared to a voltage-controlled voltage source (VCVS). Section 3.1 explains what causes loudspeakers to distort and Section 3.2 compares the distortion of a loudspeaker if it is driven by a voltage or current source.

3.1. Distortions in loudspeakers

Figure 3.1 shows the cross-section of a Woofer. One of the main requirements for this project is that the total harmonic distortion (THD) of the amplifier should be lower than 0.001%. The loudspeaker contributes to the THD. There are 4 sources of non-linearity present in a loudspeaker [14]. Each of them creates a non-linear distortion, which will be explained in subsection 3.1.1 till subsection 3.1.4.

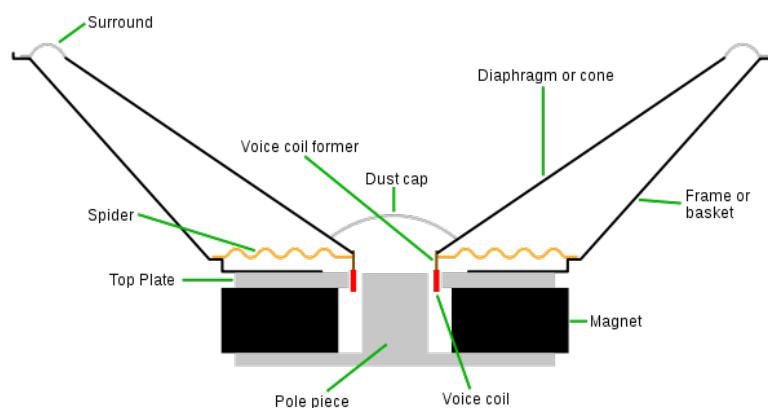


Figure 3.1: Cross section of a Woofer, source: <https://en.wikipedia.org/wiki/Woofer>

3.1.1. $K_{ms}(x)$ Stiffness versus Displacement

Loudspeakers use a suspension system to center a coil in a resting position using a restoring force $K_{ms}(x)$. For small displacements this relationship is almost linear, however for large displacements, this is no longer true [14], as shown in Figure 3.2a. The restoring force is given by the following equation: $F=K_{ms}(x) * x$. K_{ms} is not constant, but depends on the displacement x . Both the Spider and Surround contribute to the total stiffness, this can be seen in Figure 3.2b.

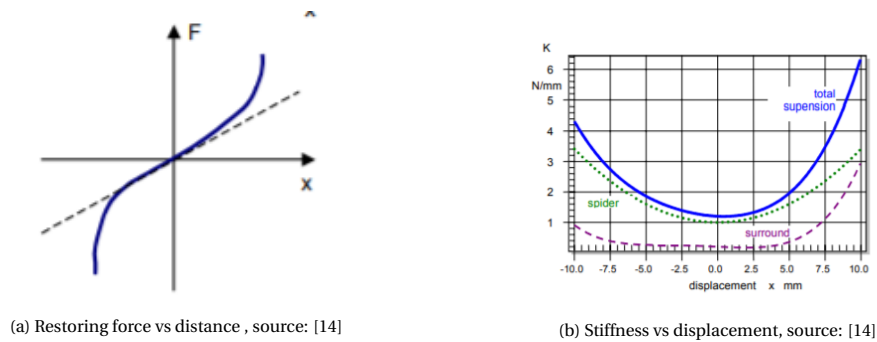


Figure 3.2: Stiffness over distance

The $K_{ms}(x)$ is also frequency-dependent. This has to do with the visco-elastic behavior of the suspension material [14]. This report will not go into detail explaining the cause behind this relationship. Figure 3.3 shows the harmonic distortion in sound as a function of frequency. In this plot, f_s is the resonance frequency. It can be seen that at lower frequencies the distortion is far worse. The stiffness has a low Interharmonic Distortion (IMD) in sound, as well as a low HD and IMD in the current signal [14].

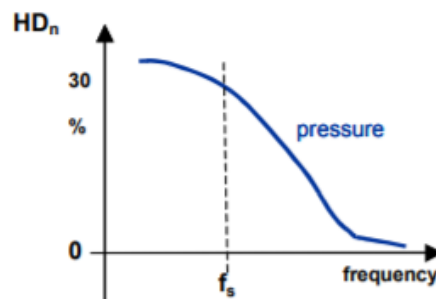


Figure 3.3: Harmonic distortion in sound for stiffness displacement, source: [14]

3.1.2. $Bl(x)$ Force factor versus Displacement

The force factor $Bl(x)$ describes how the mechanical and electrical model can be coupled to each other. This is located at the magnet and pole-piece in Figure 3.1. $Bl(x)$ is the line integral of the magnetic flux density over the voice coil length that is present in the gap between the pole piece and the magnet. Figure 3.4a provides a visual representation. As the voice coil moves to produce sound $Bl(x)$ is constant, as long as the voice coil is fully inside the gap.

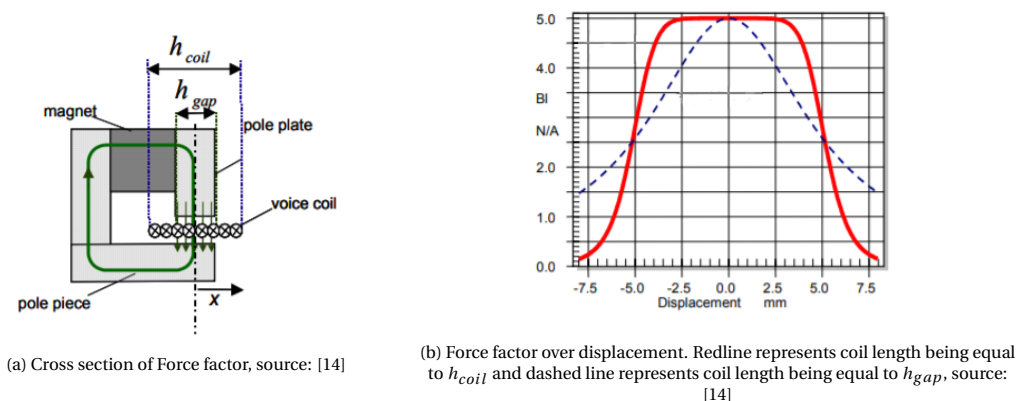


Figure 3.4: Force factor

The electro-magnetic motor produces high HD at lower frequencies as shown in Figure 3.5a, while the HD of the current signal is low [14]. There is a high IMD at lower frequencies as shown with Figure 3.5b [14].

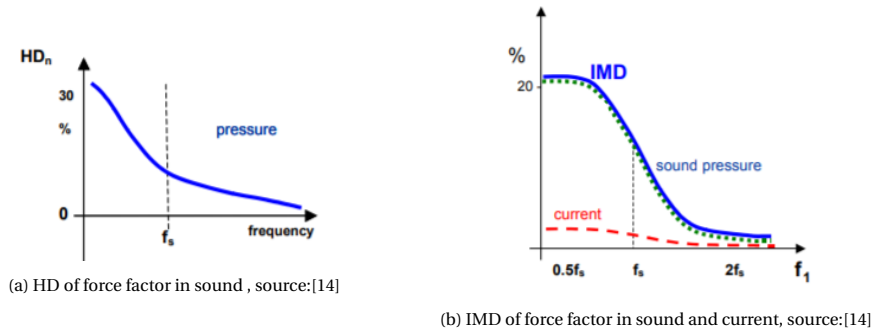


Figure 3.5: HD and IMD distortion due to Force factor

3.1.3. $L_e(x)$ Voice coil inductance versus Displacement

The voice coil moves by moving the cone. It moves from inside the magnet to the outside in the air as can be seen with Figure 3.6.

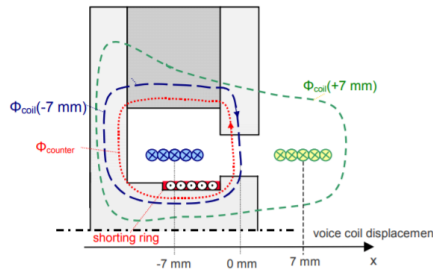


Figure 3.6: Displacement of voice coil, source:[14]

As the voice coil moves to produce sound, it will not constantly be surrounded in the same environments as shown in Figure 3.6. It can either be outside of the magnet in the open air or inside the magnet, surrounded by iron. The inductance is dependent on its environment, more precisely the permeability μ of the environment [14]. Due to the inductance of the coil, an alternating magnetic flux is produced when the coil is provided with an alternating current. When the voice coil is inside the gap of the magnet it produces a larger magnetic flux compared to when it is outside of this gap. This is because the voice coil is then surrounded by metal instead of air. Since this subsection only focuses on the displacement of the coil and not the current through the coil, it is assumed that the magnetic flux $\phi(i)$, given in Equation 3.1, is fixed and can be seen as ϕ . Now, when Equation 3.1 is rewritten by substituting Equation 3.2 and Equation 3.4, the inductance L is no longer dependent on i and it is purely dependent on μ . The inductance can be calculated using Equation 3.1. If for example the magnetic reluctance R increases, the magnet flux will decrease and as a result, the inductance decreases. A mechanical solution for this problem is to increase the voice coil height. Looking back at Figure 3.4a and Figure 3.4b, the red line represents the voice coil height, which is equal to h_{coil} and the blue dash represents the coil height, which is equal to h_{gap} . With a larger voice coil height, the coil will mostly be located inside the gap, while with a smaller coil height it can either be entirely inside the magnet or outside in the air.

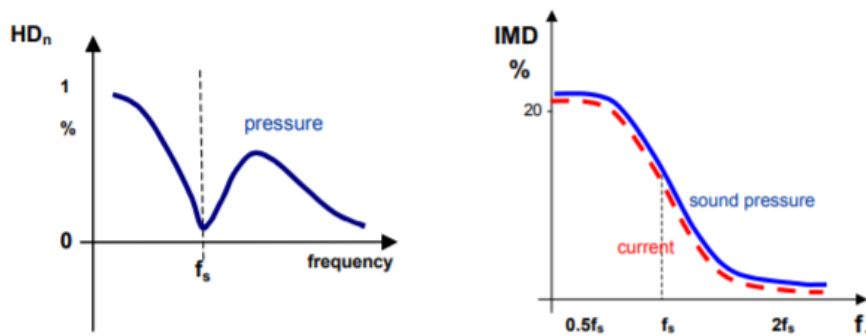
$$L = \frac{\phi(i)}{i} \tag{3.1}$$

$$R = \frac{F}{\phi} \tag{3.2}$$

$$R = \alpha \frac{1}{\mu r} \tag{3.3}$$

$$F = i * N \tag{3.4}$$

Voice coil inductance fluctuations for a fixed current and fluctuating displacements result in HD for both the current signal and displacement, however, this is very small as can be seen in Figure 3.7a. The IMD is however moderate for sound pressure and current as can be seen in Figure 3.7b.



(a) HD of voice coil displacement for both sound pressure and current, source:[14]

(b) IMD of voice coil displacement for both sound pressure and current, source:[14]

Figure 3.7: HD and IMD distortion due to only Voice Coil displacement

3.1.4. $L_e(i)$ Voice coil inductance versus Current

The inductance is given in Equation 3.1. If the change in magnetic flux, due to a fluctuating current, is proportional to the change in input current, then L will remain constant. However, this is not the case. The reason for this is that the relationship between the flux density and the magnetic field is not linear. The relationship between the flux and flux density is given with Equation 3.5 and Equation 3.6. The non-linearity is caused by the fact that the permeability saturates at larger current levels [14]. This relationship can be seen in Figure 3.8.

$$\phi = B * A \quad (3.5)$$

$$B = \mu(i) * H \quad (3.6)$$

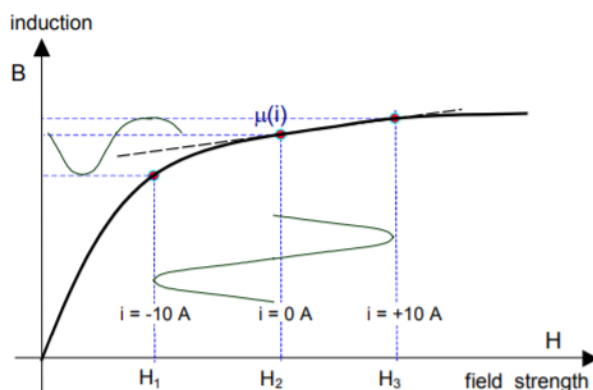


Figure 3.8: Non-linear relationship between flux Density B and Magnetic field strength H, source:[14]

The coil inductance with a fluctuating current causes a moderate HD and IMD for both the sound pressure and current. The HD can be seen from Figure 3.9a and the IMD can be seen from Figure 3.9b. More factors play a role in the non-linearity characteristics of a loudspeaker: Variation of cone geometry, Young's E-modulus, Doppler effect and wave steepening [14]. Distortion caused by these topics will not be discussed here because this chapter is focused on the impedance characteristics of the loudspeaker.

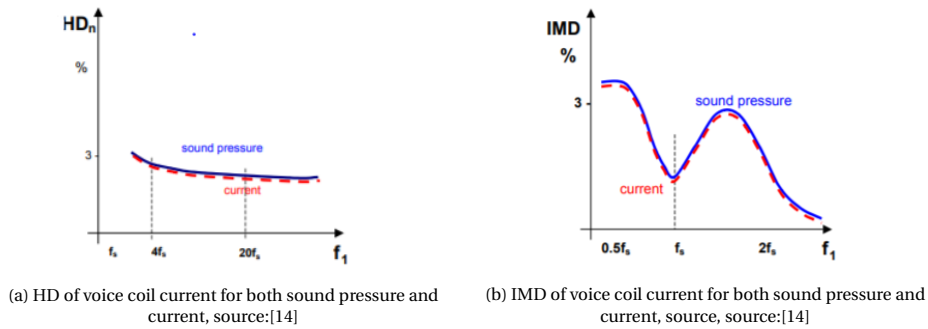


Figure 3.9: HD and IMD distortion due to only voice coil current

3.2. Distortion of Current and voltage driven loudspeaker

To compare the distortion of voltage and current-driven loudspeakers, an electrical model of the loudspeaker model is needed, then the distortion as a function of a voltage and current source can be compared.

3.2.1. Electrical loudspeaker model

The electrical model can be derived from the driver as shown in Figure 3.10. The driver model [1] shows how the electric and mechanical components of a loudspeaker are connected. Starting from the left, the voltage over the voice coil is converted into mechanical force via a gyrator with a ratio of $Bl:1$. Then the mechanical force to the cone is transferred into an acoustic pressure. The transfer of mechanical force into acoustical pressure is done using a transformer with a ratio of $SD:1$, where SD is the effective cone area.

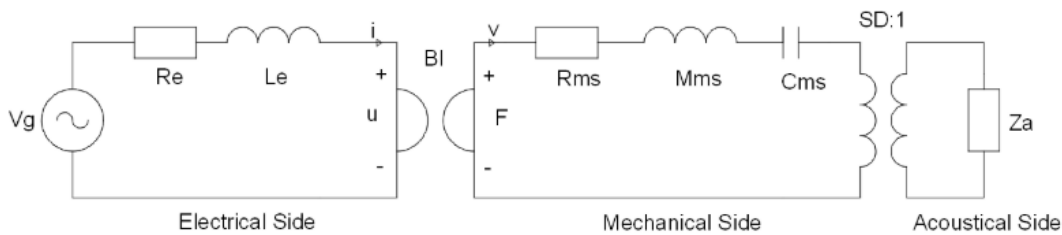


Figure 3.10: Loudspeaker driver model, source: <http://projectryu.com/wp/2017/07/23/electrical-model-of-loudspeaker-parameters/>

The impedance Z_a given in Figure 3.10 corresponds to the radiation resistance for both the front and back of the cone and the enclosure impedance [8]. If no enclosure is modelled then $Z_a = R_a$, where R_a is the radiation resistance, which is frequency-dependent [8]. The acoustic side can be moved over to the mechanical side using impedance reflection [3]. Using impedance reflection the transformer with a ratio of $SD:1$ can be removed and the resistor R_a can be connected in series with the other mechanical components. However, its impedance will be given as $R_a * (SD)^2$. The resistor $R_a * (SD)^2$ will be so much smaller than R_{ms} that for a simplified model it can be ignored [9]. Then after some rewriting using impedance reflection and impedance conversion, the mechanical components can be converted to electrical components [4]. Figure 3.11 represents the electrical model of the loudspeaker.

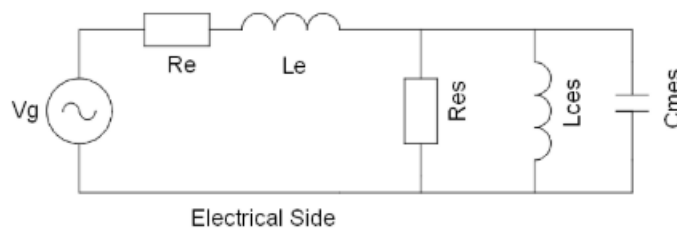


Figure 3.11: Loudspeaker electrical model, source: <http://projectryu.com/wp/2017/07/23/electrical-model-of-loudspeaker-parameters/>

Now that the electrical model of the loudspeaker is given, the next step is to find the parameters of the monopole and dipole loudspeaker that are used for this project. This is not relevant for the comparison of voltage and current sources, but is important for later on in this report when the real load is substituted for the complex loudspeaker load. These parameters are given in Table 3.1. The explanation as to how these values were found is given in section A.1.

Table 3.1: Calculated parameters for loudspeakers

$Z_{monopole}$	Z_{dipole}
$R_e = 4.6 \Omega$	$R_e = 6.3 \Omega$
$L_e = 2.1 \text{ mH}$	$L_e = 2.0 \text{ mH}$
$R_{es} = 34.3 \Omega$	$R_{es} = 42.3 \Omega$
$L_{ces} = 16.9 \text{ mH}$	$L_{ces} = 6.3 \text{ mH}$
$C_{mes} = 0.8 \text{ mF}$	$C_{mes} = 4.4 \text{ mF}$

3.2.2. Voltage and current driven electrical model of loudspeaker

In many loudspeakers, a voltage source is used to drive the components to produce sound. The main focus of this sub-group is to drive the loudspeaker to produce sound using a current source instead.

The reason that a current source (CS) is used instead of a voltage source (VS) is because the speaker will produce less harmonic distortion in its sound quality at lower frequencies [15]. The movement of the cone produces the sound. When using a CS instead of a VS it can be shown that the velocity of the speaker cone will be more linear [15]. To help illustrate this, Figure 3.12 will be used. Some knowledge of impedance analogy [11] is needed to convert electrical impedance into mechanical impedance and vice versa. This was taught in the course Signals and Controls (EE2S21). For this report, only the relevant theory regarding impedance analogy will be repeated. Impedance analogy is converting mechanical impedances such as: mass, spring and damper into its equivalent electrical model: inductor, capacitor and resistor or vice versa. With impedance analogy, a series RLC circuit is equivalent to a mass, spring and damper in parallel and vice versa. Impedance reflection [3] is also needed in order to convert Figure 3.12a into Figure 3.12b or Figure 3.12c. Using all of this, the following general equations will be used to represent mechanical or electrical impedance, the electrical equivalent of mechanical impedance is given as $Z_{electrical} = \frac{(Bl)^2}{Z_{mechanical}}$ and mechanical equivalent of electrical impedance is $Z_{mechanical} = \frac{(Bl)^2}{Z_{electrical}}$.

A few remarks regarding Figure 3.12: The velocity of the cone is given with u . Z_s represents the lumped equivalent impedance of the electrical components. In Figure 3.12b, Z_s is equal to Z_g , R_e and L_e in series and in Figure 3.12c $\frac{(Bl)^2}{Z_s}$ is equal to Z_{mg} , C_{me} and R_{me} in parallel. Z_{mg} is the mechanical impedance equivalent of Z_g , C_{me} is the mechanical impedance equivalent of L_e and R_{me} is the mechanical impedance equivalent of R_e . Z_m is the same as Z_s , but only for the lumped equivalent impedance of the mechanical components. The reasoning behind using Z_m and Z_s is for simplifying Equation 3.7 and Equation 3.8 so that it becomes easier to see why CS delivers less distortion than VS.

Looking at Figure 3.12a, the first step is to convert the mechanical components into electrical components and then pull all components onto the primary side of the transformer. This gives Figure 3.12b, Since Figure 3.12b is the electrical model, Z_m becomes $\frac{(Bl)^2}{Z_m}$, which is in series with Z_s . The voltage over $\frac{(Bl)^2}{Z_m}$ in this circuit is $V_0 * \frac{(Bl)^2}{Z_m} \frac{1}{Z_s + \frac{(Bl)^2}{Z_m}}$. In systems equivalent theory, the force for mechanical components and voltage for electrical components are interchangeable, when swapping from mechanical and electrical [11]. This voltage is equivalent to the force in Figure 3.12a. Now, using Lorentz force for velocity ($|F_L| = |Bl u|$) the cone velocity can be calculated. The cone velocity is given with Equation 3.7.

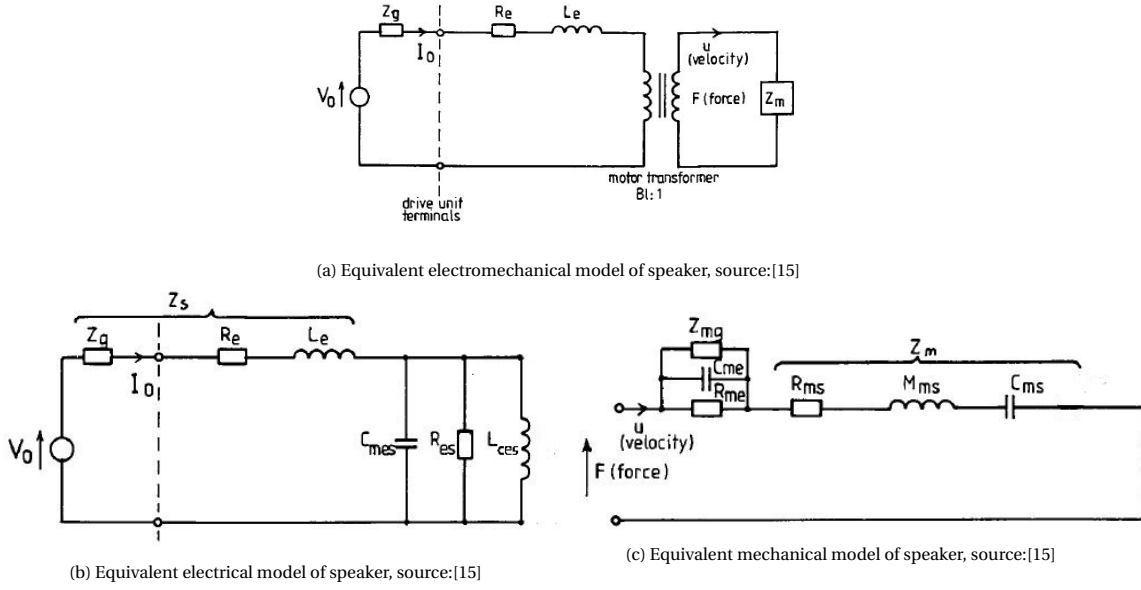


Figure 3.12: Equivalent models of loudspeaker

$$u = \frac{V_0 * Bl}{Z_m * (Z_s + \frac{(Bl)^2}{Z_m})} \quad (3.7)$$

The difference between a VS and a CS is the internal source impedance Z_g . For a voltage source, this should be as small as possible ideally 0 and for a CS it should be as large as possible ideally ∞ . This characteristic will be important when finding the cone velocity as a function of CS. For a VS the Z_g is very small. Z_{mg} , which is given as $Z_{mg} = \frac{(Bl)^2}{Z_g}$, is very large. However, the values for C_{me} and R_{me} are far smaller compared to Z_{mg} , resulting in Z_s not being far larger than $\frac{(Bl)^2}{Z_m}$ in Equation 3.7. For a CS, Z_g is very large. Thus, it results in a very small Z_{mg} : approximately zero. Since Z_{mg} is in parallel with C_{me} and R_{me} , this results in the total impedance being equal to zero. This causes the Z_s given in Equation 3.7 to be zero. Once again, using impedance analogy, $I_0 = \frac{V_0}{Z_m}$. This results in Equation 3.8. When looking at the cone velocity using a VS, the term $\frac{1}{Z_s + \frac{(Bl)^2}{Z_m}}$ is present, while this term is not present when a CS is used. As mentioned in section 3.1, $Bl(x)$, $L_e(x)$, $L_e(i)$ and $K_{ms}(x)$ are all non-linear. The mechanical lumped impedance Z_m has K_{ms} and the electrical lumped impedance Z_s has L_e . This results in the cone velocity equation being more linear when a CS is used instead of a VS. Meaning a CS delivers less distortion than a VS, because the non-linear elements present in $\frac{1}{Z_s + \frac{(Bl)^2}{Z_m}}$ are only present when a VS is used.

$$u = \frac{I_0 * Bl}{Z_m} \quad (3.8)$$

When looking at the electrical side of Figure 3.10, it follows that the voltage goes over the voice coil, which produces alternating current. As a result of this, the cone has enough force to produce sound, the force is proportional to the current $F = Bli$. Non-electrical actions such as the cone movement in a loudspeaker can produce an electrical source. This action is called the electromagnetic force (EMF). For the loudspeaker, there are two causes of EMF. One is the motion EMF, which is caused by the motion of the voice coil and is given as $\epsilon_m = Blu$ [17]. The other one is inductive EMF, which is caused by the lossy inductive characteristic of the voice coil and is given as $\epsilon_i = L * \frac{di}{dt}$ [17]. When a VS is applied over the voice coil, both EMFs will contribute and produce their current. This results in an additional current at the output, which distorts the output current. When a CS is applied, both EMFs do not produce any additional current, due to the fact EMFs are potential energy and need work (voltage) to move electrons. This means that when using a CS the EMFs do not produce any additional current, thus it results in a less distorted output current. Because of this, there is no current modulation due to changing electrical parameters. Given all of these arguments, it has been decided to build a VCCS amplifier. The rest of this report will explain how this circuit was designed, based on theory and simulation.

4

Amplifier structure considerations

4.1. Introduction

In Chapter 3, it was derived that the VCCS is most suitable for this project because it limits the distortions made by the speaker. In this chapter two amplifier structures that implement a VCCS will be presented and analyzed: an operating transconductance amplifier (OTA) in section 4.3 which was renamed to simple OTA to distinguish from other OTAs, and a Howland amplifier [16] in section 4.4. The goal of this chapter is to choose the basic structure which will further be used in the design of the VCCS. To do so, the basic properties of the VCCS will firstly be derived in section 4.2 with the help of the chain matrix. From this, the basic properties of the simple OTA will be derived in subsection 4.3.1 and in subsection 4.3.2 it will be analyzed. In subsection 4.3.3, the noise performance of the OTA will be analyzed. In section 4.4, the Howland amplifier will be introduced and analyzed in the same way as the simple OTA. The chapter will be concluded with the comparison of both circuits in section 4.5: In subsection 4.5.1, both circuits will be compared based on circuit analysis and in subsection 4.5.2 the noise of both circuits will be compared, after which a choice will be made based on these comparisons.

4.2. Basic properties of the VCCS

In this section, the basic properties of the VCCS are discussed with the help of the two-port representation given in Figure 4.1b. The two-port representation is convenient, since this circuit can be analyzed with the help of the chain matrix. The chain matrix describes the two-port as given in Figure 4.1a. The chain matrix equation is given in Equation 4.3. The elements A , B , C and D of the chain matrix are explained in great detail in subsection A.2.1. Briefly explained the elements A , B , C and D in the matrix equation 4.3 can be found with the help of the following equations:

$$V_i = AV_O + BI_O \quad (4.1)$$

$$I_i = CV_O + DI_O \quad (4.2)$$

By opening the circuit at the output in Figure 4.1a the elements A and C are found. By short-circuiting the output ports in Figure 4.1a the elements B and D are obtained.

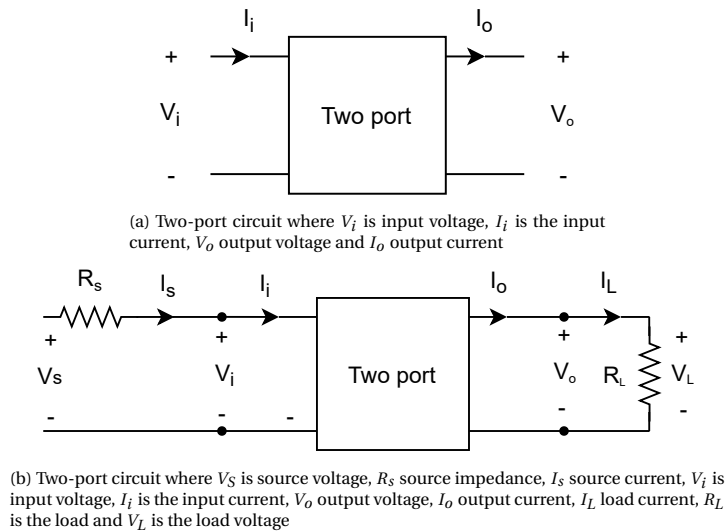


Figure 4.1: Two-port representations

$$\begin{bmatrix} V_i \\ I_i \end{bmatrix} = \begin{bmatrix} A & B \\ C & D \end{bmatrix} \begin{bmatrix} V_o \\ I_o \end{bmatrix} \quad (4.3)$$

The voltage to current gain A_y of the two-port as given in Figure 4.1b, can be expressed in the matrix elements as given in Equation 4.4. As explained in chapter 3, the speaker impedance Z_L is frequency dependent. This is why the chain matrix elements A and C must be set to zero to make the amplifier load-independent, as can be seen from Equation 4.4. Since the value of the source impedance R_s is unknown, the chain matrix element D should be set to zero as well. Thus, the gain of the amplifier must be solely determined by the chain matrix parameter B .

$$A_y = \frac{1}{AR_L + B + CR_LR_s + DR_s} \quad (4.4)$$

The remaining variables that have to be analyzed are the input and output resistance of the circuit. As derived in subsection A.2.1 the input resistance R_i and out resistance R_o can be calculated with the aid of Equation 4.5a and Equation 4.5b respectively. Plugging $A = C = D = 0$ into Equation 4.5a and Equation 4.5b results in an infinite output and input impedance.

$$R_i = \frac{AR_L + B}{CR_L + D} \quad (4.5a) \quad R_o = \frac{DR_s + B}{CR_s + A} \quad (4.5b)$$

4.3. Simple OTA

In this section, the simple OTA will be derived and analyzed for in circuit properties and noise performance.

4.3.1. Circuit derivation

In this subsection, the simple OTA is derived with the aid of the nullor elements: nullator and norator. A nullator is a circuit element that is an open and closed circuit at the same time. The norator is a perfect source that can supply all possible current and voltage combinations. To derive the simple OTA, the nullator is firstly used to nullify the current and pass the input voltage to the resistor as represented in Figure 4.2a. The relation between the output current and input voltage is then:

$$I_R = \frac{V_i}{R_L} \quad (4.6)$$

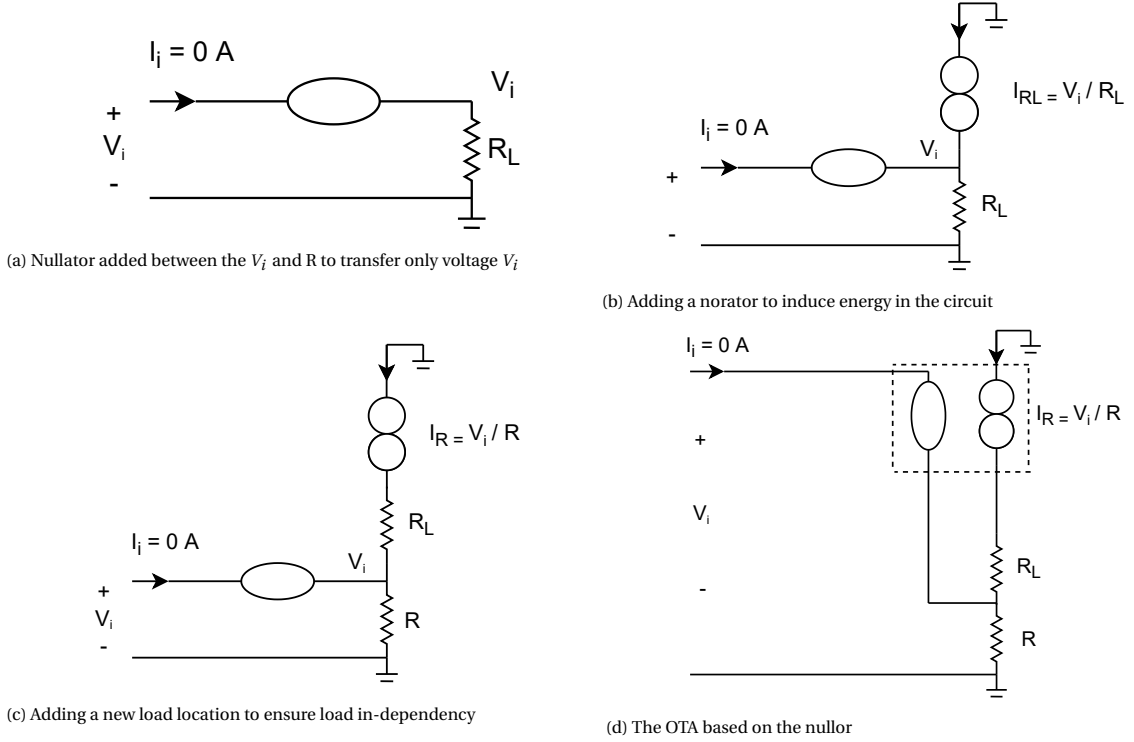


Figure 4.2: Derivation of the OTA using nullator and norator.

Adding a nullator between the load and the source removes all of the power delivered by the source to the load R_L . Since the current through the nullator is zero, an additional power source must be added to power the load R_L , this is done with the norator as given in Figure 4.2b. The current structure of the amplifier is load dependent and as was derived in section 4.2, this should not be the case. To solve this complication, an additional resistor R is placed as illustrated in Figure 4.2c. Now the amplifier is load-independent, since the output current does not depend on R_L , but only on the resistor R . By combining the nullator and norator the nullor is made and the final circuit is represented in Figure 4.2d.

4.3.2. Circuit analysis

To analyze the circuit given in Figure 4.2d, the chain matrix elements are derived with the help of equation 4.6 and using the fact that $I_L = I_R$, $V_i = R_L I_L$ and $I_i = 0$:

$$A = \frac{V_i}{V_L} |_{I_L=0} = 0 \quad (4.7a)$$

$$B = \frac{V_i}{I_L} |_{V_L=0} = \frac{V_i}{\frac{V_i}{R}} = R \quad (4.7b)$$

$$C = \frac{I_i}{V_L} |_{I_L=0} = 0 \quad (4.7c)$$

$$D = \frac{I_i}{I_L} |_{V_L=0} = 0 \quad (4.7d)$$

Equations 4.7a, 4.7b, 4.7c and 4.7d prove that the obtained amplifier is indeed a OTA since only the B parameter is set and the other elements are 0.

4.3.3. Noise performance

The noise analysis will be performed on the circuit given in Figure 4.2d. To model the noise of the amplifier, voltage sources have been added for each resistor, a voltage source has been added for the opamp (E_{op}) to simulate the input voltage noise density and two current sources (I_{n+} and I_{n-}) have been added to the opamp for the current noise density as given in Figure 4.3, this opamp circuit noise model has been taken from [20]. These noise sources are in the following units: $\frac{V}{\sqrt{Hz}}$ or $\frac{A}{\sqrt{Hz}}$.

The goal is to find an expression for the noise power density for both the output and the input signal of

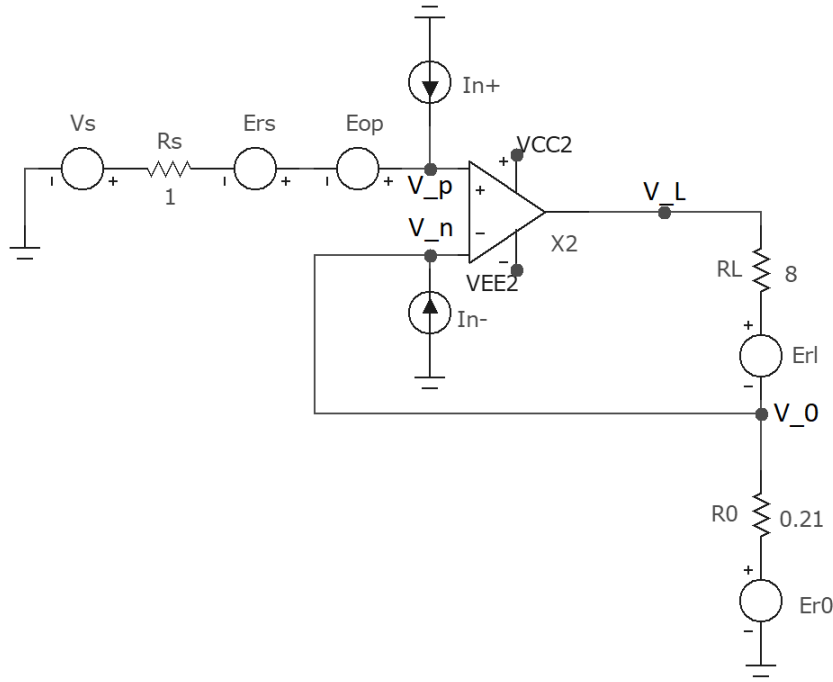


Figure 4.3: The simple OTA, with the noise sources added to it.

the amplifier. In order to do this, an expression for the output voltage V_L with the noise sources (E_L) added to it will have to be found first. The full derivation can be found in subsection B.9.1, but the expression for $V_L + E_L$ is given below:

$$V_L + E_L = \left(1 + \frac{R_L}{R_0}\right)(V_s + E_{rs} + E_{op} + I_{n+}R_s) - I_{n-}R_L + E_{rl} + \frac{R_L}{R_0}E_{R_0} \quad (4.8)$$

With this equation, the noise power density can be found at the output of the amplifier. Because the goal is to find an expression for the noise power density the input source V_s is set to zero. This means that V_L is also zero since there is a linear relationship between the two, given by $V_L = \left(1 + \frac{R_L}{R_0}\right)V_s$. Considering that the RMS value is wanted, all terms in the equation have to be squared and summed, this is possible since all noise sources are independent from each other. This results in Equation 4.9, which shows the noise power density at the output of the amplifier.

$$E_L^2 = \left(1 + \frac{R_L}{R_0}\right)^2 (E_{rs}^2 + E_{op}^2 + I_{n+}^2 R_s^2) + I_{n-}^2 R_L^2 + E_{rl}^2 + \left(\frac{R_L}{R_0}\right)^2 E_{R_0}^2 \quad (4.9)$$

To get the noise power density at the input of the amplifier, Equation 4.9 needs to be divided by the gain, given by $\left(1 + \frac{R_L}{R_0}\right)^2$. This results in the following equation, which is the noise power density at the input of the amplifier.

$$E_{in}^2 = E_{rs}^2 + E_{op}^2 + I_{n+}^2 R_s^2 + \frac{I_{n-}^2 R_L^2 + E_{rl}^2 + \left(\frac{R_L}{R_0}\right)^2 E_{R_0}^2}{\left(1 + \frac{R_L}{R_0}\right)^2} \quad (4.10)$$

Given that $S = E^2$ and that $S_i = I_{n+}^2 = I_{n-}^2$, Equation 4.10 can be rewritten as follows:

$$S_{in} = S_{rs} + S_{op} + S_I R_s^2 + \frac{S_i R_L^2 + S_{rl} + \left(\frac{R_L}{R_0}\right)^2 S_{R_0}}{\left(1 + \frac{R_L}{R_0}\right)^2} \quad (4.11)$$

This equation shows that the noise at the input of the amplifier is mostly dominated by the noise sources of the opamp, since typically speaking S_{op} is larger than the other terms in the equation.

To confirm the calculation of the noise power density, an external computer tool was used. In the course Structured Electronics Design the tool SliCap, developed by the TU Delft professor Anton Montagne, was

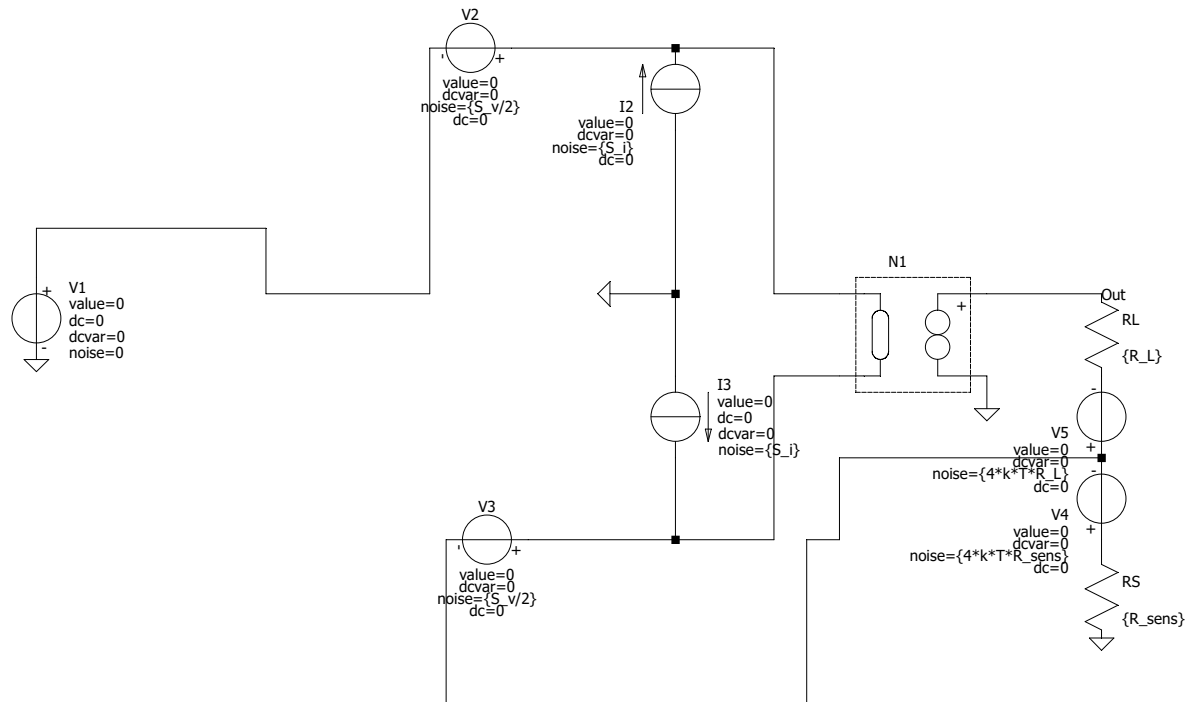


Figure 4.4: SPICE circuit of the simple transconductance amplifier with nullor as a controller

taught and it is also covered in [18]. With this tool, the circuit can be calculated symbolically. Thus, also the noise can be calculated symbolically. First, the amplifier with the noise sources modeled in it must be built in a SPICE circuit simulator [5]. The circuit from Figure 4.3 was recreated but with a nullor instead of the opamp. This circuit is given in figure 4.4. By running the code given in Appendix C.1.1 the resulting input-referred noise of the simple OTA is obtained as given in equation 4.12.

$$S_{src} \approx S_v + R_{sense}^2 S_i + \frac{4TkR_{sense}^2}{R_L} + 4TkR_{sense} \text{ if } R_L \gg R_{sense} \quad (4.12)$$

From Equation 4.12 it can be seen that the noise at the input of the amplifier is mostly dominated by the noise power density of the opamp, since typically speaking $S_v \gg S_i$. R_{sense} must also be smaller than one to get the gain of the amplifier larger than one as dictated by Equation 4.7b. All the other terms in both equations are negligibly small. This backs up the hand-calculated equation and gives an extra confirmation that it is correct. As performing noise analysis on the other circuits is very tedious, SliCAP will be used in the future to perform this analysis.

4.4. Howland

The Howland circuit [16] is an alternative to the simple OTA, as derived in the previous section. The Howland circuit is given in Figure 4.5.

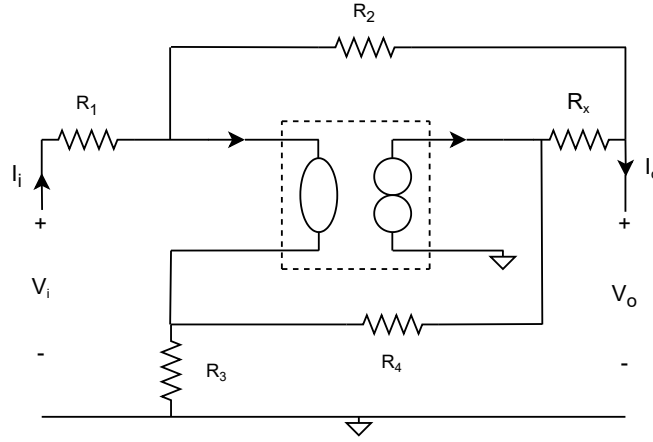


Figure 4.5: Howland two port representation with nullor as a controller

4.4.1. Circuit analysis

In Appendix B.8, the nodal analysis of the derived Howland circuit is presented. The chain matrix elements A , B , C and D are the following:

$$A = \frac{R_1}{R_2} \left(\frac{\beta}{\alpha} - 1 \right) \quad (4.13a) \quad B = \frac{R_x R_1 \beta}{R_2 \alpha} \quad (4.13b)$$

$$C = \frac{(1 - \alpha)}{\alpha R_2} \quad (4.13c) \quad D = \frac{R_x}{\alpha R_2} \quad (4.13d)$$

It was already derived that the matrix elements A , C and D must be equal to zero in order to create a VCCS. When it is assumed that $R_2, R_1 \gg R_x$ holds true, the chain matrix elements C and D are set to zero by ensuring that $R_2 \gg R_x$, $|1 - \alpha| \gg 0$ and element A is set to zero if the following equality (as derived in section B.8) is valid:

$$\frac{R_2}{R_1} = \frac{R_4}{R_3} \quad (4.14)$$

4.4.2. Noise performance

In appendix B.10 the calculation of the input referred noise is given for the circuit as given in Figure B.13. The resulting input referred equation is given as Equation B.75, which for case $R_1, R_2, R_3, R_4 \gg R_0, R_L$ becomes:

$$S_{src} = S_v + \frac{R_1^2 R_2^2 S_i}{(R_1 + R_2)^2} + \frac{4kTR_1 R_2^2}{(R_1 + R_2)^2} + \frac{4kTR_1^2 R_0^2}{R_4 (R_1 + R_2)^2} + \frac{4kTR_1^2 R_o}{(R_1 + R_2)^2} \quad (4.15)$$

The equation is further reduced by assuming that $R_1, R_2, R_3, R_4 \approx R$:

$$S_{src} = S_v + \frac{R^2 S_i}{2} + 2kTR + \frac{2kTR_o^2}{R} + 2kTR_o \quad (4.16)$$

Since $R \gg 0$, the contribution to $\frac{R^2 S_i}{2}$ and S_v are dominant.

4.5. Comparison

In this section the simple OTA structures as present in section 4.3 and section 4.4 are compared. First, the circuit structures are compared using the circuit analysis from subsection 4.3.2 and subsection 4.4.1. Then, the noise performance from 4.3.3 and 4.4.2 are compared. At the end of this section the simple OTA structure is chosen on which the further design will be based.

4.5.1. Circuit structure comparison

From the circuit analysis of the Howland amplifier it is observed that in order to set the chain matrix A equal to zero, Equation 4.14 needs to be fulfilled. The output resistance is dependent on the value of A . The output resistance becomes,

$$R_o = \frac{B}{A} = \frac{R_x \beta}{\beta - \alpha} \quad (4.17)$$

using Equations 4.13a and 4.13b. In order for R_o to approach infinity, A in Equation 4.17 must approach zero. That is the case if the relation given in Equation Equation 4.18 is met. Real resistors have tolerance, this means that the equality as given in Equation 4.18 changes to Equation 4.19 where D is the deviation from zero value and p the tolerance of the resistor. Due to this deviation the denominator $\beta - \alpha$ of Equation 4.17 changes to non-zero value and thus the R_o decreases. By maximizing the term $\frac{R_2}{R_1}$ and minimizing the term $\frac{R_4}{R_3}$ in Equation 4.19 the maximum deviation as given in Equation 4.20 is obtained. The full derivation of the equation 4.20 is given in section B.8.

$$\frac{R_2}{R_1} - \frac{R_4}{R_3} = 0 \quad (4.18)$$

$$D_{tolerance} = \frac{R_2(1 \pm p)}{R_1(1 \pm p)} - \frac{R_4(1 \pm p)}{R_3(1 \pm p)} \quad (4.19)$$

$$D_{max} = 4p \frac{R_2}{R_1} \quad (4.20)$$

Plugging the maximum deviation D_{max} from Equation 4.20 into Equation 4.17 results in the following output resistance:

$$R_o = \frac{R_x R_1 \beta}{R_2 4p} \quad (4.21)$$

From Equation 4.21 it becomes clear that a very small tolerance p of the values of the resistor is needed to maintain a high output resistance.

4.5.2. Noise comparison

The terms S_v and S_i are dominant in Equation 4.16 for the Howland current pump. For the simple OTA, only the term S_v in Equation 4.12 is dominant. Meaning that the simple OTA adds less noise to the signal than the Howland circuit.

4.5.3. Circuit choice

It was decided to base the design of the VCCS on the simple OTA because its noise performance is better and there are no additional requirements needed on the circuit elements to maintain a high output impedance. In the upcoming chapter, the simple OTA is analyzed as a control system and ways to improve the performance of the amplifier will be introduced.

5

Simple operational Transconductance amplifier and the Composite Amplifier

This chapter will start off with a noise- and control analysis for the simple OTA, which was chosen as the best suitable choice for this VCCS in the previous chapter since it has better noise performance and does not impose any additional requirements on the circuit. Then in section 5.2, the conclusions of these analyses will be used to create an enhanced version of the simple OTA. More analysis will be performed on this enhanced version in section 5.3, to find out if this amplifier can be optimized for its SNR, THD and stability. Then in section 5.4, components will be chosen for the amplifier, after which the amplifier will be simulated and validated in section 5.5.

5.1. Control analysis of the simple transconductance amplifier

By using the black model [7], the amplifier circuit with the operational amplifier as a controller can be modeled as a control system and control theory can be used to analyze the stability and noise performance. Control theory was taught in the course Systems and Control (EE2S21) and the derivations below and in section 5.3 are based on [11].

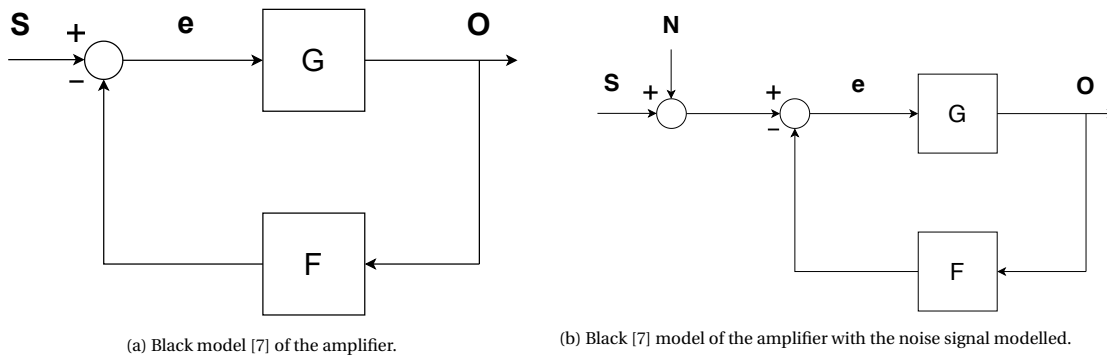


Figure 5.1: Black model of the simple OTA

5.1.1. Control analysis

The black model [7] of the operational amplifier is presented in Figure 5.1a, in this model the S is the input signal, e is the error signal, G is the open-loop voltage gain, F is the feedback factor and O is the output signal. The derivation of the transfer function H of this model, given in Equation 5.1, is provided in appendix B.1.1:

$$H = \frac{O}{S} = \frac{G}{1 + GF} \quad (5.1)$$

$$\lim_{G \rightarrow \infty} H = \frac{1}{F} \quad (5.2)$$

If the open-loop gain is larger than zero, the transfer function approaches the reciprocal of the feedback gain as given in Equation 5.2. Since for the opamp the open-loop voltage is finite, the error made by the amplifier is given by the following equation (the full derivation can be found in Equation B.1.1).

$$Error \approx \frac{1}{GF^2} \text{ if } G \gg 0 \quad (5.3)$$

From Equation 5.3 it follows that to minimize distortion the open-loop voltage gain needs to be high.

5.1.2. Noise analysis

The calculation of the noise of the , as given in Figure 5.1b, is presented in subsection B.1.2, where the noise source from the opamp and the input noise is modeled into the system as N . The conclusion of this calculation, namely the transfer function with the added noise, is given in equation 5.4.

$$H_N = \frac{O}{N} = \frac{G}{1 + GF} \approx \frac{1}{F}, \text{ if } G \gg 0 \quad (5.4)$$

The noise at the output will behave the same as the transfer function of the model given in Figure 5.1a and the noise will be multiplied with the gain as given in equation 5.4. Thus the noise at the output is proportional by the overall gain of the amplifier. And since the gain $1/F$ is fixed, the only means to decrease the noise at the output is by reducing the noise at the input.

5.2. Composite amplifier

As concluded above, the THD of the amplifier can be improved by increasing the open-loop gain. A way of increasing this open-loop gain is to create a composite amplifier. A composite amplifier is an amplifier where a second opamp has been added inside the feedback loop, the output of this opamp feeds into the input of the original power opamp. By doing this, the open-loop gain of the total amplifier will have increased significantly, which in turn reduces the error in the output signal, as derived in subsection 5.1.1.

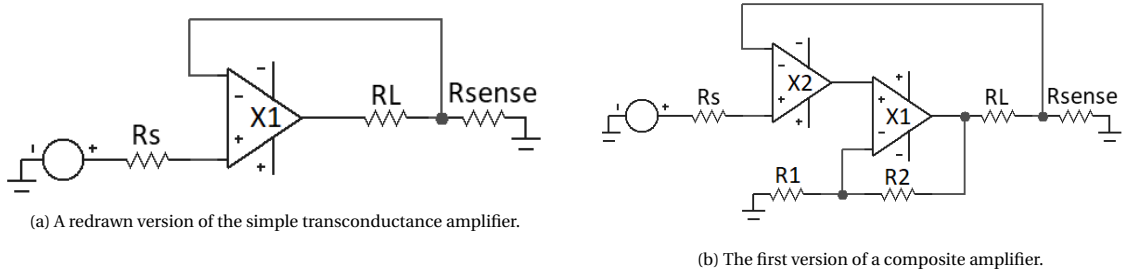
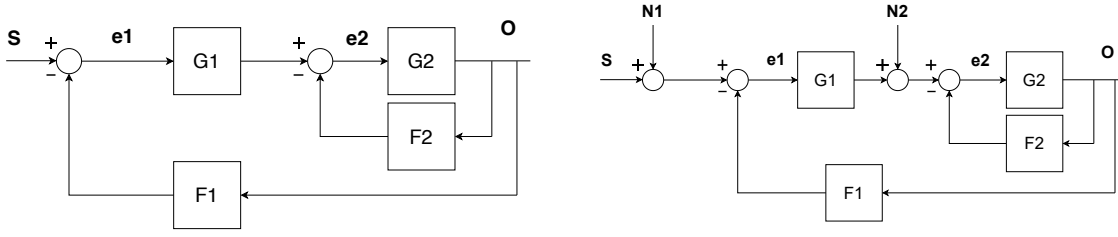


Figure 5.2: Creating composite amplifier

In Figure 5.2b, a redrawn version of the simple OTA is given. Next to it, the opamp X_2 has been added to the amplifier, including the resistors R_1 and R_2 for the power opamp. While the overall voltage to current gain of the amplifier is still given by $\frac{1}{R_{sense}}$, the distribution of this gain over the opamps can be adjusted manually with the resistors R_1 and R_2 , since the original opamp X_1 has become a voltage amplifier. This will be used at a later stage in the design process to optimize the amplifier.

5.3. Analysis of the composite amplifier

In this section, control analysis, noise analysis and stability analysis will be carried out on the composite amplifiers, as given in Figure 5.2b. By doing this a better understanding of the circuit will be obtained, with which a better choice for the selection of components can be made.



(a) Black [7] model of the composite amplifier where S is the input signal, e_1 and e_2 are the error signals, G1 and G2 are the open-loop voltage gains, F1 and F2 are the feedback factors and O is the output signal
 (b) Black model of the composite amplifier where S is the input signal, N1 and N2 are the noise signals, e_1 and e_2 are the error signals, G1 and G2 are the open-loop voltage gains, F1 and F2 are the feedback factors and O is the output signal

Figure 5.3: Black model of composite amplifier without noise source added and with noise source added

5.3.1. Control analysis

In Figure 5.3a the black model [7] of the composite amplifier is presented. If this model is compared with Figure 5.2b, it can be seen that G1 and G2 model the open-loop voltage gains of the opamp X_2 and X_1 respectively. By using the transfer function of this model, an equation for the error in the output signal can be derived. The full analysis can be found in subsection B.1.1. The equation for the error can be seen below:

$$Error = \frac{1 + G_2 F_2}{F_1 (1 + G_1 G_2 F_1 + G_2 F_2)} \quad (5.5)$$

$$\approx \frac{G_2 F_2}{G_1 G_2 (F_1)^2} \text{ if } G_1 \gg G_2 \gg 0 \text{ or } G_1 \approx G_2 \gg 0 \quad (5.6)$$

$$Error \approx \frac{F_2}{G_1 (F_1)^2} \text{ if } G_1 \gg G_2 \gg 0 \text{ or } G_1 \approx G_2 \gg 0 \quad (5.7)$$

According to Equation 5.7 the error in the output gets smaller if the feedback-gain F2 decreases. Since the feedback gain F1 determines the overall gain of the system, this gain is fixed at a value of 4.71 as given in the program of requirements. On the other hand, F2 can be chosen freely since this only impacts the individual closed-loop gain of each opamp, but not the overall gain. Thus, F2 can be used to minimize the distortions in the output signal. The open-loop gain G1 can also be used to lower the distortions, this will then have to be as high as possible.

5.3.2. Noise analysis

When adding the noise coming from the two opamps to the model in Figure 5.3a, this results in the model given by Figure 5.3b. Using this model, an equation for the noise present in the output signal can be derived. The full analysis can be found in section B.3, but the concluding equation is given below in the case that the open-loop voltage gain of the two opamps are in the same range:

$$O \approx \frac{G_1 G_2 N_1}{G_1 G_2 F_1} + \frac{G_2 N_2}{G_1 G_2 F_1} \quad (5.8)$$

$$= \frac{N_1}{F_1} + \frac{N_2}{G_1 F_1} \approx \frac{N_1}{F_1} \text{ Since } G_1 \gg 0 \quad (5.9)$$

$$\frac{O}{N_1} \approx \frac{1}{F_1} \text{ if } G_1 \approx G_2 \gg 0 \quad (5.10)$$

Equation 5.10 shows that the noise at the output of the signal is mostly dependent on the noise coming from the first opamp, provided that the open-loop voltage gain of both opamps are in the same range. This shows that for the power amplifier, given by G2, noise is not of as much importance. On the other hand, the precision opamp given by G1, must have as little noise as possible.

To confirm this result, SliCAP has been used to analyze this circuit. The circuit and result from SliCAP can be found in section B.11. From the given equation it can be seen that most of the noise in the circuit comes from the first opamp (shown as G1 in Figure 5.3b). This confirms the notion that the noise in the first opamp should be as low as possible.

5.3.3. Stability analysis

To make sure that the THD is as low as possible, the gain factor for the power amplifier should be as high as possible. Given the fact that the gain-bandwidth product (GBWP) for every opamp is fixed, this will cause the bandwidth (BW) of the power opamp to decrease as its gain increases. If the bandwidth of the precision opamp is larger than the BW of the power opamp there will be delays due to the power opamp, since the power opamp cannot keep up with the precision opamp. This delay can cause overshooting. Large overshoot delivers an underdamped system, which can cause the output to oscillate, thus distorting the output current. Now there are additional criteria that need to be taken into account when choosing the precision opamp, which is that the BW of the precision opamp needs to be smaller than the BW of the power opamp.

This new criteria for the precision opamp can be troublesome, since the precision opamp needs a GBWP that is smaller than the GBWP of the power opamp. The GBWP of the precision opamp has to be small enough that its BW is still smaller than the BW of the power opamp with a high gain, which restricts the design to opamp manufacturers. There is a way to remove the low GBWP criteria, this can be done by creating a feedback loop for the precision opamp with a capacitor in it. By adding this capacitor, a pole is introduced in the feedback loop of the precision opamp which will cause the opamp to have a lower gain at higher frequencies. This effectively lowers the bandwidth of the opamp and resolves the oscillation caused by the power opamp with the low BW. This capacitor has been added in the circuit as can be seen in Figure 5.4.

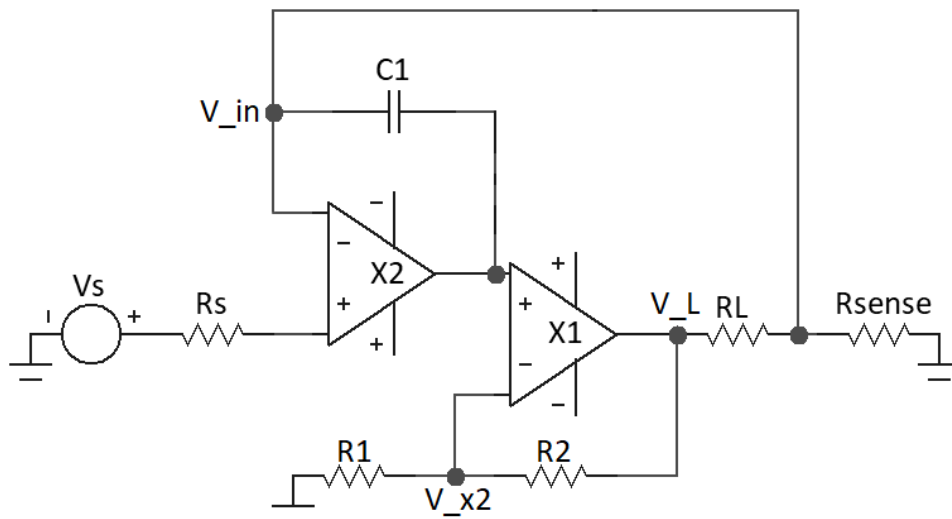


Figure 5.4: The finalised circuit for the composite amplifier.

5.4. Component selection

Now that the composite amplifier has been analyzed extensively and conclusions have been drawn, values can be selected for the components of the finalized circuit, which is given in Figure 5.4. The requirements given in item 2.3. of the PoR are especially of importance for this.

5.4.1. Opamp selection

In the composite amplifier two opamps are present: A power opamp (X_1) and a precision opamp (X_2). For the power opamp, it is important that it can deliver at least 7 A peak to peak to a purely resistive load of 8 Ω . This would require the opamp to be able to output at least 56 V peak to peak, but the peak of the output signal will need to be a few volts below the limit of the opamp to avoid clipping, so it has been decided to go with an opamp that can output 80V peak to peak. To accommodate these limitations it was decided to go with the OPA541 [21] as the power opamp. The OPA541 can output 10 A and 80V peak to peak, so it will be able to fulfill the requirements of item 2.3.1.5. and item 2.3.1.6..

The opamp X_2 needs to be of high quality: A low noise, high precision, high gain and high GBW is wanted. As discussed in subsection 5.3.2, the noise is mostly dependent on the opamp X_2 , while the high gain of the opamp aids in the reduction of the error in the output signal, as discussed in subsection 5.1.1. It also

does not need a high output voltage, because according to subsection 5.3.1 the closed-loop voltage gain of the power opamp should be as large as possible to lower the THD. Since the closed-loop voltage gain of the overall amplifier is fixed, the gain of the precision opamp will automatically be low if a high gain is chosen for the OPA541. The GBW of the opamp is also not as much of importance since the BW of the opamp will be limited by the capacitor C_1 . For the precision opamp, the LME49860 [19] has been chosen. It has a typical noise voltage density of $2.7 \text{ nV}/\sqrt{\text{Hz}}$ and a THD+N of 0.00003%, which make it a low-noise and high-precision opamp.

5.4.2. Power amplifier gain

As discussed in subsection 5.3.1, the gain of the power opamp should be as high as possible to reduce the error in the output signal. This gain is set by the following equation, where A_p is the voltage gain of the power opamp:

$$A_p = 1 + \frac{R_2}{R_1} \quad (5.11)$$

There is one limitation to the gain of the power opamp: the precision opamp should not have a gain smaller than one, as this will cause the opamp to have a positive phase shift, which can cause stability issues. This limits the gain of the opamp to the voltage gain of the composite amplifier, which is set to the following equation, where A_v is the voltage gain of the whole composite amplifier (see subsection B.4.2 for the full derivation):

$$A_v = 1 + \frac{R_L}{R_{sense}} = 1 + R_L g_m \quad (5.12)$$

In order to find the values for R_2 and R_1 for which the precision opamp will act as a voltage follower, A_v should be equal to A_p . If Equation 5.11 is set equal to Equation 5.12 the following equation is obtained:

$$\frac{R_2}{R_1} = R_L g_m \quad (5.13)$$

It is known that the transconductance g_m of the amplifier should be set to 4.71 (item 2.3.1.3 of PoR) and R_L is set to 8Ω . According to Equation 5.13, $\frac{R_2}{R_1}$ would then be set to 38, this means that R_2 should be 38 times as large as R_1 . These resistors should not be too large, as it would otherwise add unnecessary noise to the circuit, but on the other hand, they should not be too small to avoid a high power dissipation by R_1 . For these reasons it has been decided to go with $R_1 = 100 \Omega$ and $R_2 = 3.8 \text{ k}\Omega$.

5.4.3. Capacitor C_1 and overall amplifier gain

As discussed in subsection 5.3.3, the goal of the capacitor C_1 is to reduce the unity gain BW of the precision opamp so that it is lower than the BW of the power opamp. It does this by adding a pole to the feedback loop of the precision opamp. Since the closed-loop voltage gain of the power opamp has been decided, a value for the BW of the power opamp can be found. As can be seen in Figure 5.5, the GBW of the OPA541 is set to 922 kHz. Since the closed-loop voltage gain of the OPA541 is set to 41, the BW of the OPA541 is 22.5 kHz. This means that the value of the capacitor should be set in such a way that the pole is located at 20 kHz. To find the value for the capacitor, a transfer function of the composite amplifier is needed. The nodal analysis that has been done to find this transfer function can be found in Figure B.4.1, the result of this analysis is the following transfer function:

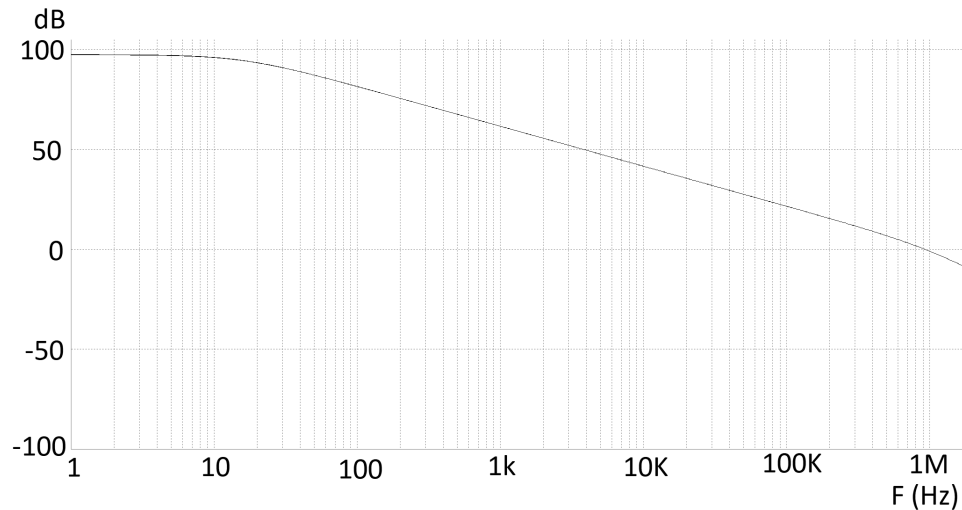


Figure 5.5: Bode plot of the OPA541, showing that the 0db-point (and its GBW) is set to 922KHz.

$$H = \frac{\frac{1}{R_{sense}} - sC_1 \left(\frac{1}{1 + \frac{R_2}{R_1}} - 1 \right)}{1 + sC_1 \frac{R_L}{1 + \frac{R_2}{R_1}}} \quad (5.14)$$

From this equation it can be seen that a pole is present at the following frequency:

$$s = -\frac{1 + \frac{R_2}{R_1}}{C_1 R_L} \quad (5.15)$$

Since a value has to be found for the capacitance C_1 , the equation is rewritten as follows:

$$C_1 = \frac{A_p}{R_L s} \quad (5.16)$$

The value for the voltage gain A_p has already been set in subsection 5.4.2 using Equation 5.11 and R_L is fixed to 8Ω . To obtain a pole at a frequency of 20Khz, the previously mentioned numbers and $s = 2\pi * 20kHz$ can be used, this results in $C_1 = 40.8\mu F$. This capacitor will cause an increase in THD, where the THD will increase with the value of the capacitor, so it is important to try and make this value as small as possible. It is possible to make the value of the capacitor smaller and have the pole stay in the same place. This is done by adding two extra resistors (R_3 and R_4) to the amplifier as displayed in Figure 5.6.

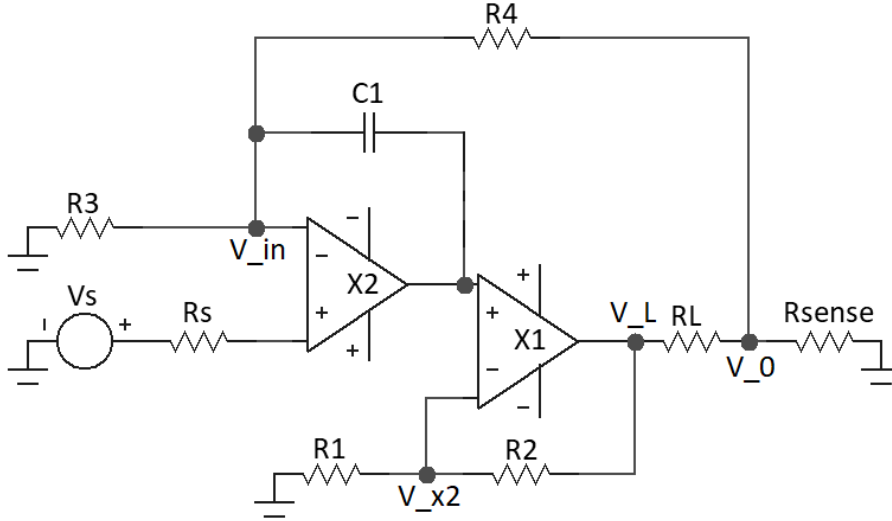


Figure 5.6: The finalised circuit for the composite amplifier.

By adding these two resistors, the transfer function of the amplifier is now given by Equation 5.17. The full derivation of this this transfer function can be found in section B.5.

$$H = \frac{1}{R_{sense}} \frac{(1 + \frac{R_4}{R_3}) + R_4 s C_1}{1 + \frac{R_4 s C_1}{R_{sense}} \frac{R_L}{1 + \frac{R_2}{R_1}}} \quad (5.17)$$

The equation for the value of the capacitance for a pole at a frequency s is now given by the following equation:

$$C_1 = \frac{R_{sense} A_p}{R_4 R_L s} \quad (5.18)$$

The value for A_p has already been set in subsection 5.4.2 using Equation 5.11 and R_L is fixed to 8Ω . This shows that the value for C_1 is now dependent on R_{sense} and R_4 . These two resistors also set the gain for the overall amplifier as follows (this equation is obtained by setting $s = 0$ for Equation 5.17):

$$H = \frac{1}{R_{sense}} \left(\frac{R_4}{R_3} + 1 \right) \quad (5.19)$$

As Equation 5.18 and the equation above show, there is a trade-off in the value of capacitor C_1 and resistors R_{sense} and R_4 . Increasing R_4 can allow C_1 to be lower and still have the same pole location and vice-versa, there is an inversed relation between R_4 and C_1 . The effect of R_{sense} on this trade-off is not significant, since an increase of R_{sense} will lead to a higher R_4 and a lower C_1 and vice-versa, so the net results in THD/SNR will be roughly similar. Since it does not impact the result that much, R_{sense} will be set to 1Ω to make the calculations simpler.

Since the transconductance of the amplifier is fixed, R_3 will have to increase if the value for R_4 increases, according to Equation 5.19. As R_{sense} is set to 1Ω , R_4 has to be 3.7 times as large as R_3 (item 2.3.1.3 of PoR). Since the noise added by R_3 gets multiplied by the voltage gain A_v , the SNR goes down considerably if these resistor values get higher. On the other hand, an increase in C_1 will lead to high values for the THD, which is also unwanted. As this amplifier is going to be used for a speaker, the THD of the amplifier is more important, since this impacts listening quality more than the SNR does. Thus, minimizing the THD while remaining above the limit for the SNR as set in item 2.3.1.8. of the PoR will be the main concern. This trade-off between the SNR and THD of the amplifier does end eventually if the resistor values keep increasing, so there is a sweet spot of resistor values that give the best THD possible. These resistor values have been found using simulations for a pole located at $s = 2\pi * 20k Hz$ and are as follows:

Table 5.1: The optimal values for C_1 , R_3 and R_4

C_1	1.4 nF
R_3	8 k Ω
R_4	29.7 k Ω

As can be seen, the value for C_1 is down by a factor of 29000. The added resistors will cause the SNR to drop, but there will be an even more significant drop in THD, which makes this design choice the right one.

5.5. Results

The finalized circuit can be found in Figure 5.7, in this circuit X_1 , is the OPA541 and X_2 is the LME49860. To test and validate the amplifier, three types of analysis have been done: transient analysis, AC analysis, and distortion analysis. By doing this it can be checked if the requirements set in the PoR have been met.

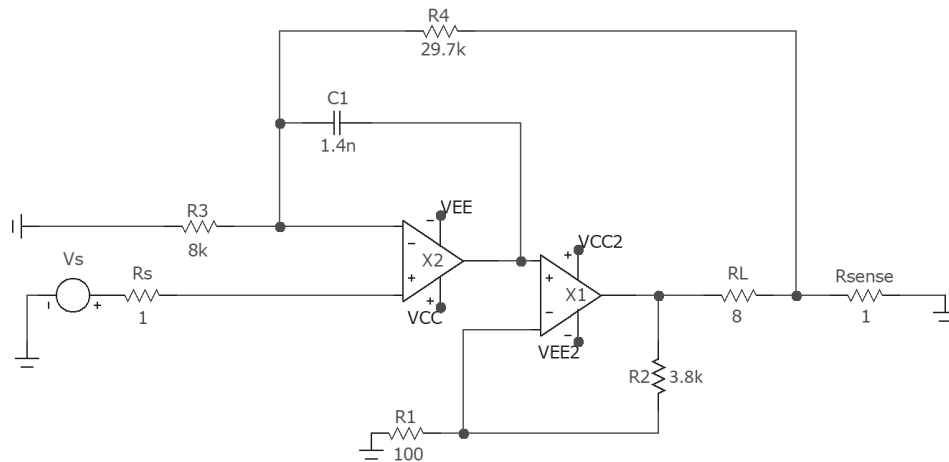
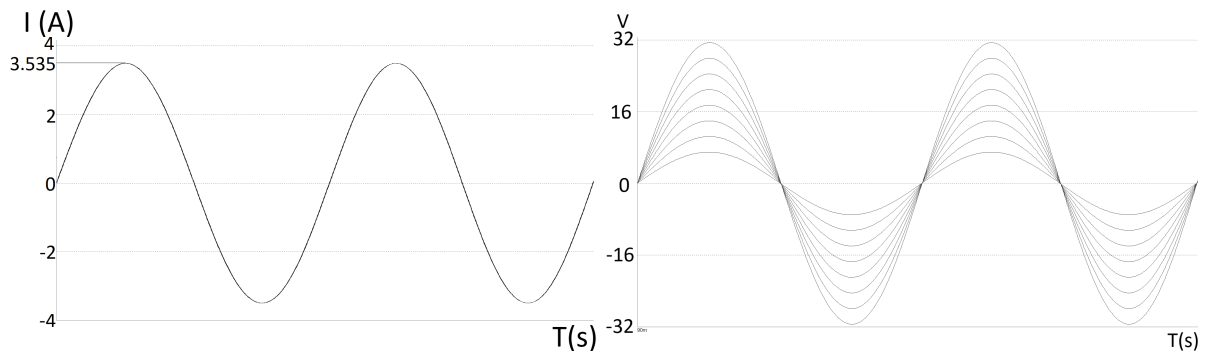


Figure 5.7: The finalised circuit of the composite amplifier with the values for all the components.

5.5.1. Transient Analysis

For the transient analysis, a 300 Hz signal with a voltage of 1.5 V peak to peak has been used. With this signal as input, the output current (Figure 5.8b) and the output voltage (Figure 5.8b) have been plotted. From these results, it can be seen that the transconductance of the amplifier is equal to $4.71 = \left(\frac{3.535}{0.75}\right)$. From Figure 5.8b it can be seen that the amplifier is load-independent since the voltage changes linearly with the load to ensure that the output current does not change, this also then shows that the output impedance of the amplifier is very high, since a change in load does not affect the output current. These results show that the resistor values R_3 , R_4 and R_{sense} were set correctly.



(a) A simulation of the output current when the input voltage is 1.5V peak to peak. (b) A simulation of the output voltage for loads of 1-8 Ω when the input voltage is 1.5V peak to peak.

5.5.2. AC Analysis

For the AC analysis, two plots have been made: the bode plot of the amplifier and the phase plot. These plots can show the -3 dB points of the output signal, the gain at a range of frequencies and the phase margin. According to Figure 5.9, the -3 dB point of the amplifier is at 57 kHz and the bode plot is flat for a frequency of under 800 Hz, as set in item 2.3.1.4 of the PoR. This means that the system has a flat response in the range of the speaker. At 800 Hz, the phase of the amplifier is -100° , which is better than the maximum of 3° that was set in item 2.3.1.10 of the PoR. The 0 dB point of the amplifier is at 178 kHz, with this value the Phase Margin (PM) of the amplifier can be found. From Figure 5.10 it can be seen that at a frequency of 178 kHz the phase is -93° . This shows that the PM of the amplifier is 87° , which means that the amplifier is stable, since it is above 45° .

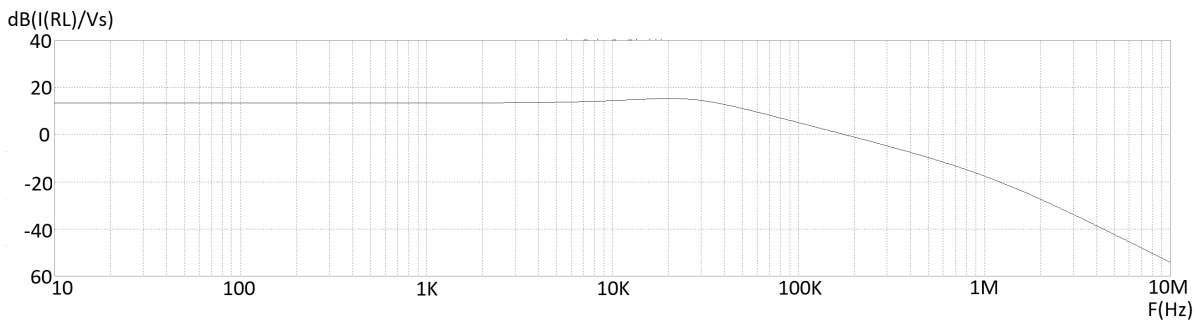


Figure 5.9: The bode plot of the amplifier.

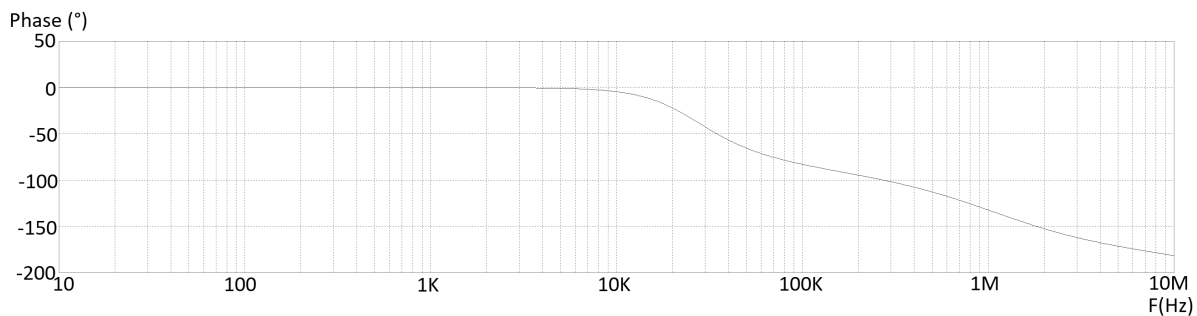


Figure 5.10: The phase plot of the amplifier.

5.5.3. Distortion Analysis

For the distortion analysis, the SNR and the THD of the amplifier have been plotted over a frequency range of 10-1000 Hz, these plots can be found in D.1. The SNR is fixed at 102.47 dB, which is more than the 100 dB that was set as a minimum in item 2.3.1.11. of the PoR. The THD is 293u% at 1kHz, which is lower than the minimum of 0.001% set in item 2.3.1.7. of the PoR. Both these values has been found using an inbuilt function of Micro-Cap 12.

5.5.4. Conclusion

These results show that all requirements set in the PoR were met for a resistive load of $8\ \Omega$. The resistors were set to the right value for the transconductance, the AC analysis showed that the amplifier is stable, that the phase difference over the frequency range of the speaker is minimal and the distortion analysis showed that the SNR and THD were a lot better than were set in the requirements. This means that for a purely resistive load the amplifier works well. In the next chapter, this amplifier will be tested with an electrical model of the loudspeaker (subsection 3.2.1) as load.

t

6

Composite amplifier with realistic load

Now that the design for the amplifier for a purely resistive load has been finished, the load can be replaced with the electrical model of a loudspeaker. The loudspeaker model is given in Figure 3.11 and the parameters are given in Table 3.1. The challenge with this realistic load is that the loudspeaker is inductive by nature, which causes the impedance of the loudspeaker to increase with higher frequencies. This impedance will have to be compensated for to avoid a too high output voltage that can cause clipping. Considering that the dipole speaker is used for the higher bass frequencies, this model will be used for the design. If this design fits the requirements given in the program of requirements, it can be assumed that it will also work for the monopole speaker. This chapter will start with a problem analysis, then a way to solve this problem will be given and applied, after which the circuit will be optimized for stability, SNR and THD of the amplifier. This amplifier will then be simulated to check whether all set requirements are met.

6.1. Problem analysis realistic load

The electrical model that will be used to simulate the loudspeaker was derived in subsection 3.2.1. The loudspeaker is inductive by nature, thus the impedance increases with a higher frequency, as can be seen in Figure 6.1. The rising impedance forms a problem, because the amplifier is a VCCS, this means it will try to keep the same output current by increasing the output voltage. The power opamp OPA541 is limited to an output voltage of ± 40 V, which means that clipping will occur if the impedance becomes too large, this clipping will cause for deformations in the output signal and will cause the THD to increase significantly. In Figure 6.1, a resonant frequency at around 40 Hz can also be seen. This resonant frequency will not have to be dealt with, because the MFB system will be able to compensate for this.

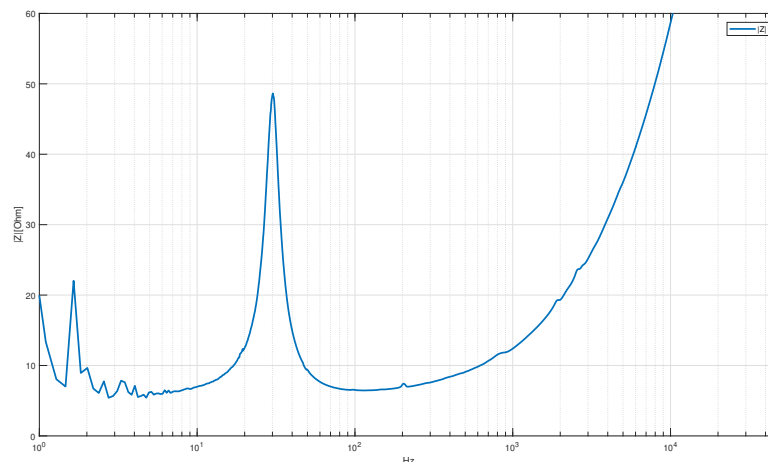


Figure 6.1: Absolute magnitude plot from measured dipole speaker

6.2. Zobel network

A way to compensate for this inductive nature is by adding a Zobel network to the amplifier, this Zobel network is an RC circuit that is placed in parallel with the load, as can be seen in Figure 6.2. This RC circuit introduces a pole which can compensate for the zero that the inductive load places. In the model given in Figure 3.11, R_{es} , L_{ces} and C_{mes} cancel each other out for frequencies above 100 Hz. This means that the load places a zero at the frequency given by the Equation 6.1a.

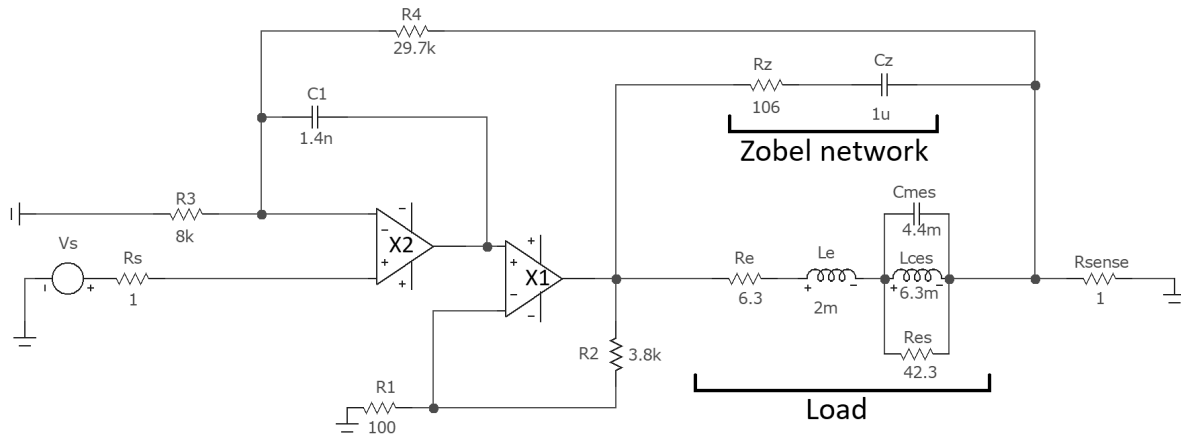


Figure 6.2: The amplifier with the zobel network and electrical model of the loudspeaker added to it.

$$s = \frac{R}{L} \tag{6.1a}$$

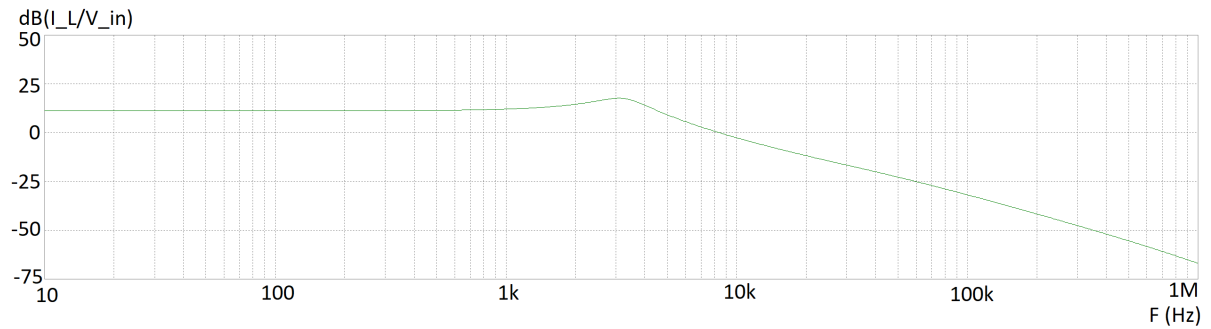
$$s = \frac{1}{RC} \tag{6.1b}$$

Using values from Table 3.1 for speaker inductance $L_e = 2.0mH$ and speaker resistance $R_e = 6.3\Omega$ and filling them in Equation 6.1a, results in a zero at 501 Hz. Because this amplifier is a VCCS, the amplifier will change its output voltage to keep the output current steady. While the Zobel network will cause the output voltage to remain stable, the current through the load will decrease, because the impedance of the load will still increase with higher frequencies. The transfer function should be as flat as possible over the frequency range of the MFB system (20-800Hz). For this reason, the frequency of the pole is set at 1.5 kHz. This should make sure that the current output remains stable over the range of the loudspeaker. The values for the RC circuit should then be based on Equation 6.1b, where $s = 2\pi * 1500Hz$. The ideal values for the RC circuit have been found using a simulation in Micro-Cap 12, they have been optimized for the minimum phase deviation at a frequency of 1kHz and the flattest response for frequencies that are less than 1 kHz, while still having the pole located at 1500 Hz. These values are as follows:

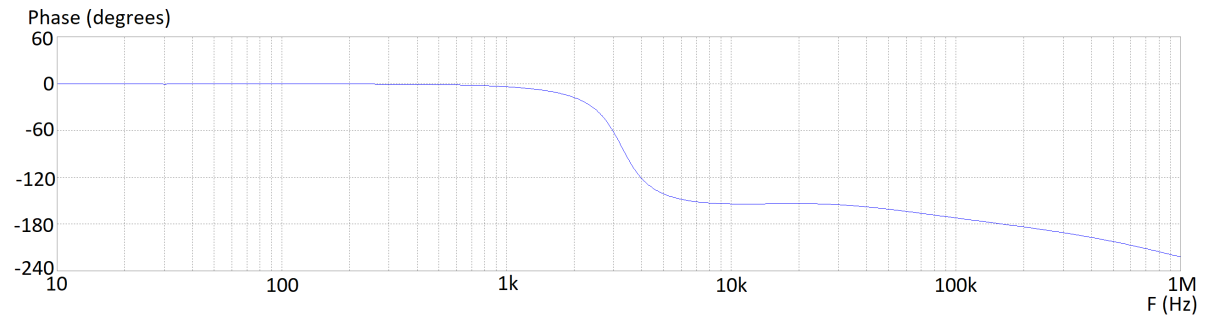
Table 6.1: The optimal values for R_z and C_z

C_z	1 μ F
R_z	106 Ω

In Figure 6.3a and Figure 6.3b, the bode plot and phase plot of the circuit as given in Figure 6.2 have been plotted respectively. From these plots, it can be seen that the transfer function is flat for frequencies that are less than 800 Hz, with a max deviation of +- 0.5 dB. The phase deviation at 800 Hz is -2.7°. These results both meet the PoR. The downside is that the PM is too low, which is set at 27°. This can be solved by using frequency compensation, which will be discussed in the next section.



(a) The transfer plot of the amplifier with the electrical model and Zobel network added to it.



(b) The phase plot of the amplifier with the electrical model and Zobel network added to it.

Figure 6.3: The bode plots of the the amplifier with the electrical model and Zobel network added to it.

6.3. Frequency compensation

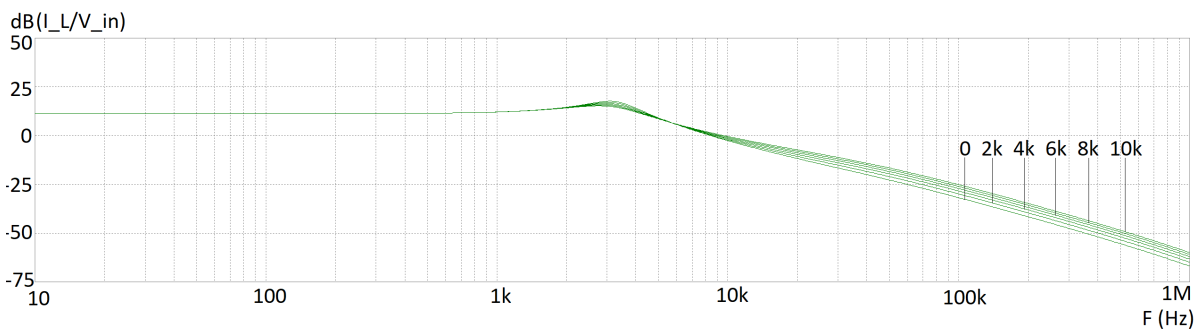
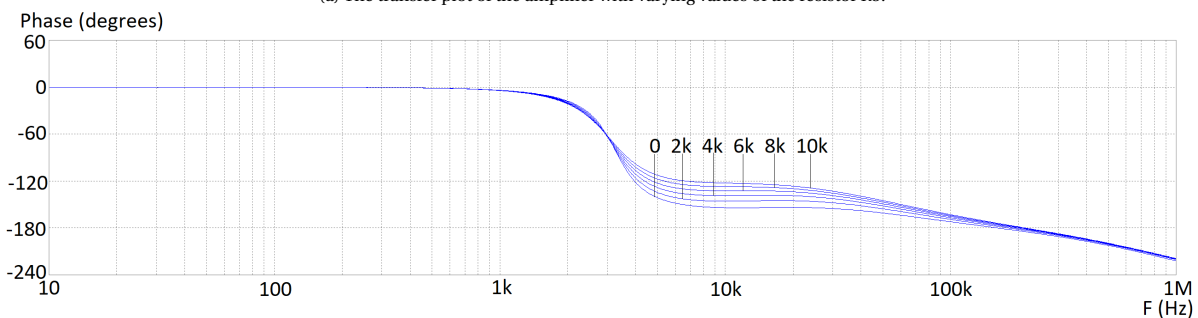
Now that the Zobel network has been added there is a flat current response up to 800 Hz, however the PM is less than 45° . Frequency compensation will need to be performed to increase the PM. When looking at the phase of the current design given with Figure 6.3b, it can be seen that the phase quickly shifts from 0° to -145° between 2 kHz and 5 kHz. The speed in which this phase shift happens implies that there is peaking present around that frequency range, which can be seen with Figure 6.3a. By making the phase shifts from 0° to -145° happen in a larger bandwidth it can increase the phase of the system at the 0 dB frequency because the 0-dB point of the bode plot will stay in roughly the same position, which causes the PM to be larger. The speed in which the phase shift occurs is dependent on how large the peaking is, the larger the peak the faster the phase shift occurs [6]. Therefore, decreasing the peak that is present on the resonance will result in a better PM. The first step in solving this is by finding out what causes the peaking. The output current of the power opamp goes through the electrical loudspeaker model and the Zobel network, which is then indirectly fed back into the precision opamp by R_{sense} . Since the peak happens at 3.3 kHz, looking at Figure 6.1 it is safe to assume that the loudspeaker's L_e is significant enough to affect the system. The parallel components R_{es} , L_{ces} and C_{mes} can be replaced with a wire for a frequency of 3.3 kHz, since the frequency is high enough that C_{mes} will be short-circuited. Also looking at the precision opamp's feedback circuit at around 3.3 kHz the capacitor C_1 will be in the signal path.

The peaking at around 3.3 kHz has to be the result of the loudspeaker load R_e and L_e , together with the Zobel network and the filter C_1 of the precision opamp. The next step is to figure out where the frequency compensation should be added. Placing the frequency compensation around the load is undesirable, since the component noise will contribute a lot to the total noise of the system, furthermore output power will be lost because it is used by the frequency compensation components. Adding the frequency compensation at the Zobel network is also not desirable, because the new component can remove the flat current response at the output of amplifier. This only leaves the filter of the opamp. The only requirement for the precision opamp filter is that high frequencies should be removed from its BW. Now that the location of the frequency compensation is known, the next step is to find out what components should be used, in what configuration, and what value it should have. Seeing that zeros can cancel poles, placing a zero at the resonance frequency will decrease the peak value, which results in the phase shifts from 0° to -145° to happen in a larger bandwidth, thus resulting in a better PM. Adding additional poles can deliver new complications, therefore the

frequency compensation component should preferably only deliver an addition zero and no poles. Keeping this in mind, together with the fact that only high frequencies need to be removed from a precision opamp, this will result in the frequency compensation component being a resistor in series with the capacitor. The new RC circuit will have a zero located at $s = -\frac{1}{RC}$, adds no new poles in the system, and only filters out the high frequencies for the precision opamp. Finding the value for the new resistor mathematically is extremely troublesome given all the variables that play a role, therefore it was decided to find the resistor by looking at the bode- and phase plot with different resistor values. The plots can be found in Figure 6.4, where Figure 6.4a is the bode plot and Figure 6.4b is the phase plot. The best value for the resistor is the smallest value where the PM is above 45° , since a large value should be avoided because it would add a lot of noise to the circuit. Based on these plots, the optimal value was found to be the following, which results in a PM of 46.2° :

Table 6.2: The optimal values for R_5

R_5	5.5 k Ω
-------	----------------

(a) The transfer plot of the amplifier with varying values of the resistor R_5 .(b) The phase plot of the amplifier with varying values of the resistor R_5 .Figure 6.4: The bode plots of the the amplifier with varying values of the resistor R_5 .

6.4. Adjustment of overall gain

To avoid a decrease in current in frequencies less than 800 Hz, it was decided in section 6.2 to place a pole at a frequency of 1500 Hz. This does mean that the impedance will increase for the frequencies less than 1500 Hz, thus the voltage will increase too. Since the MFB system works up till 800Hz, it is also required that no clipping occurs for these frequencies (item 2.3.1.11. of PoR). The current overall gain of the amplifier, as set in subsection 5.4.3, has been based on an impedance of 8 Ω . For a maximum input signal with frequencies above 550 Hz, the voltage required to drive the load is above the limit of the OPA541. To accommodate these frequencies too, the overall gain of the amplifier will have to be lowered. To avoid clipping of the voltage in all cases, the overall gain had to be set to a value of 3.48. To avoid changing the locations of the pole set by C_1 , R_3 had to be increased to set this gain. To set the gain, Equation 5.19 has been used. Keeping R_4 and R_{sense} the same, calculating for the new value for R_3 resulted in a value of 12 k Ω .

Now that the adjustments to accommodate the realistic load have been made, the circuit can be simulated and validated. This will happen in the next section.

6.5. Results

The finalized circuit can be found in Figure 6.5, in this circuit X_1 is still the OPA541 and X_2 is the LME49860. To test and validate the amplifier, three types of analysis have been done: transient analysis, AC analysis, and distortion analysis. By doing this it can be checked if the requirements set in the PoR have been met.

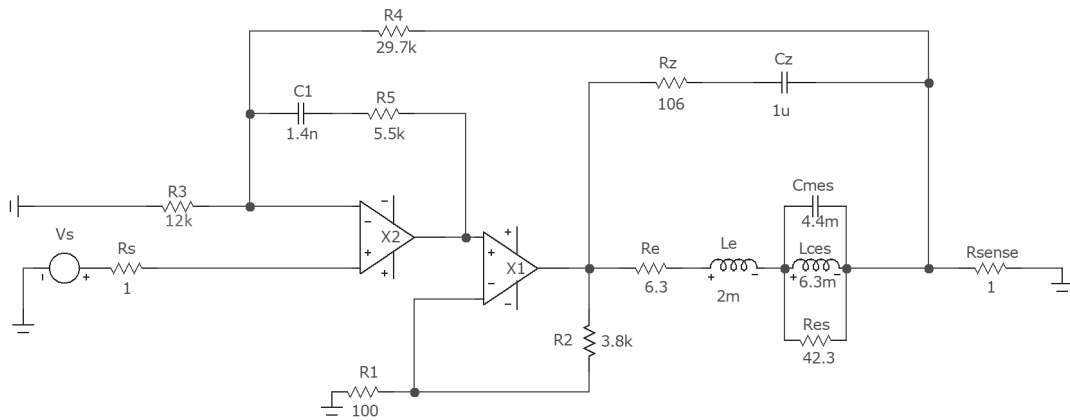
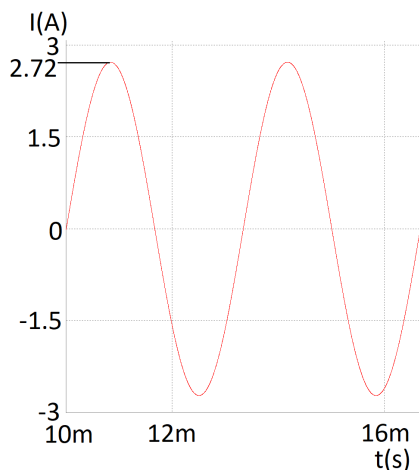


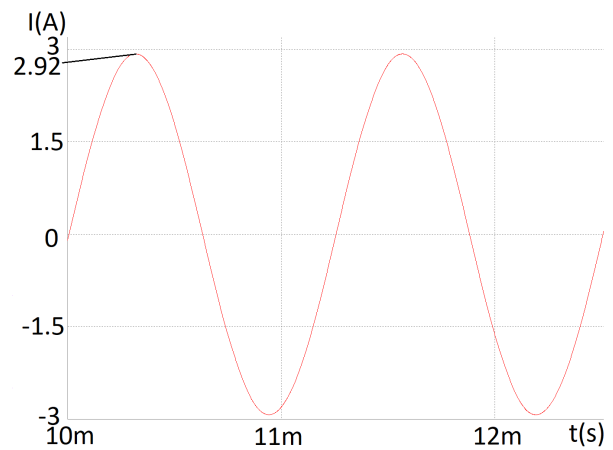
Figure 6.5: The finalised circuit of the amplifier, with the Zobel network and realistic load added to it.

6.5.1. Transient Analysis

For the transient analysis, the output current is shown for two input signals of 1.5 V peak to peak. The first signal has a frequency of 300 Hz (Figure 6.6a) and the second one a frequency of 800 Hz (Figure 6.6b). Now that the gain has been adjusted in section 6.4, no clipping occurs when the input signal is 800 Hz, as can be seen in Figure 6.6b. A very noticeable thing is that there is a difference in the transfer function of 0.62 dB between 300 Hz and 800 Hz. As stated in item 2.3.2.2. of the PoR, this is above the requirement that was originally set in the trade-off requirements. This is because there is a trade-off between the stability of the circuit and the location of the ringing. It would be possible to adjust C_z and R_z in such a way that the ringing shifts to the right and that the deviation would become less, but that would cause the peak of the ringing to increase and thus also the phase shift. Considering that the requirement is in the list of Trade-off Requirements (ToR), it has been decided that this 0.62 dB deviation is acceptable with the stability that it brings.



(a) A simulation of the output current when the input voltage is 1.5 V peak to peak with a frequency of 300 Hz.

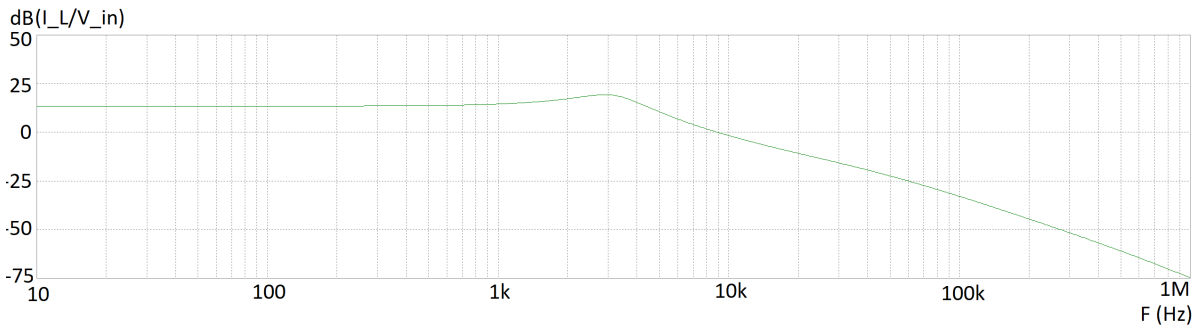


(b) A simulation of the output current when the input voltage is 1.5 V peak to peak with a frequency of 800 Hz.

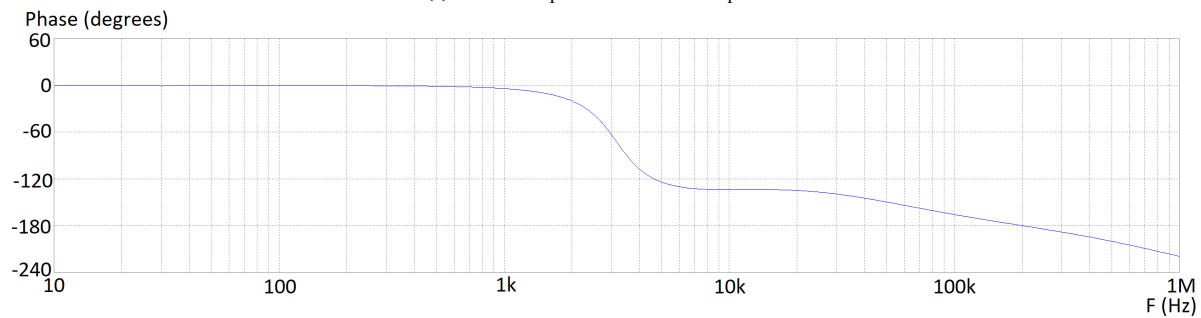
6.5.2. AC Analysis

For the AC analysis, two plots have been made: the bode plot of the amplifier and the phase plot. At 800 Hz, the phase of the amplifier is -2° , which is better than the maximum of 3° that was set in item 2.3.1.10 of the PoR. The 0-dB point of the amplifier is at 8 kHz, with this value the Phase Margin (PM) of the amplifier can be

found. From Figure 6.7b it can be seen that at a frequency of 8 kHz the phase is -129° . This shows that the PM of the amplifier is 51° , which means that the amplifier is stable, since it is above 45° .



(a) The transfer plot of the finalised amplifier.



(b) The phase plot of the finalised amplifier.

Figure 6.7: The bode plots of the the finalised amplifier.

6.5.3. Distortion Analysis

For the distortion analysis of the SNR and the THD of the amplifier, the inbuilt function in Micro-Cap 12 could not be used because the load consisted of more than one component. This means that both the SNR/THD have to be calculated manually. For the THD, this could be done using the HARM() function of Micro-Cap 12. This function plots all harmonics present in the signal, from which the THD can be calculated by measuring all the peaks and using the following equation:

$$THD = \frac{\sqrt{V_2^2 + V_3^2 + V_4^2 + \dots}}{V_1} * 100\% \quad (6.2)$$

In this equation, V_1 stands for the RMS value of the fundamental frequency, and the others stand for the higher harmonics. When the harmonics are plotted and plugged into Equation 6.2, a THD of 0.000432% was found. Which is lower than the 0.001% set in item 2.3.1.7 of the PoR.

The SNR of the amplifier is set to 100.92 dB, the whole calculation can be found in subsection B.7.1. According to PoR item 2.3.1.8 the SNR is allowed to be 96 dB, thus the amplifier meets all requirements.

6.5.4. Conclusion

These results show that all requirements set in the PoR were met for the electrical model of the loudspeaker. The AC analysis showed that the amplifier is stable at all times and that the phase difference over the frequency range of the speaker is minimal and the distortion analysis showed that the THD was better than was set in the requirements. A method has been found to calculate the SNR, which resulted in a SNR that is above the one set in the PoR. This all shows that the amplifier works for the electrical model for the loudspeaker, which will be the final design of the amplifier for the MFB system.

7

Discussion

The results which were given in section 6.5 show that the amplifier works as intended and performs better than was set in the PoR, except for the SNR, which is unknown at this date. This should be the case since the results will most likely not be as good in a real prototype. Due to the restriction given by the current pandemic (COVID-19), it was not possible to construct and measure the circuit throughout this entire project. By doing this, more design flaws might have been found, which do not show up in simulations. In the finished prototype of the amplifier, extra distortions might also be present which could reduce the performance of the amplifier.

It was stated that the amplifier is supplied by a $\pm 40V$ power source. However, different voltages were needed for the VCC and VEE of the precision opamp. In simulations, one can simply change the VCC and VEE supply voltage for the opamp to the required value. For the real prototype, voltage regulator or a buck converter would need to be used to achieve the $\pm 22V$ necessary for the precision opamp.

The results of the simulations show that the THD is 0.000432 % which is less than the required THD. Even with the above-mentioned distortions that might occur, it is expected that the SNR and THD will both still be better than was originally required in PoR, but it was not possible to confirm this.

8

Conclusions, recommendations and future work

8.1. Conclusions

The focus of this report is on the design of a voltage controlled current source (VCCS) amplifier for a loudspeaker. The goal of the design is to meet the requirements as given in Table 8.1. First, the type of amplifier is chosen by using an in-depth analysis of the distortions coming from the loudspeaker. With a current source (CS) for the speaker, there is no current modulation due to (non-)linear impedance modulation, while with a voltage source (VS) there is. Looking at the relationship between the net force $F = m * a$ and the Lorentz force $F = Bli$, it can be seen that the acceleration is proportional to the current. By not adding current modulation the system will be more linear. That is why a voltage-controlled current source (VCCS) was chosen.

Table 8.1: Amplifier design requirements

THD	0.001 %
SNR	100 dB
Phase margin (PM)	45°
Phase at 800 Hz	3°

The design is based on operational amplifiers (opamp) and it was started with an operational transconductance amplifier (OTA), which was renamed to simple OTA, and a Howland amplifier. They have been compared to one another based on their noise analysis and circuit analysis, from which it was concluded that the OTA was the better choice for this VCCS because it had better noise performance and did not pose any additional requirements on circuit elements. The noise of the simple OTA is dependent on the input voltage noise of the power opamp S_v , while the noise of the Howland is dependent on both the input current and voltage noise of the power opamp (S_v and S_i). The performance of the OTA did not meet the requirements as given in Table 8.1, as its THD was too high and its SNR too low.

A second opamp, a precision opamp, has been added inside the feedback loop of the power opamp from the first design, to make a composite amplifier. This greatly enhances the SNR and THD of the amplifier. To get a low THD the gain of the power opamp should be as high as possible, causing its bandwidth (BW) to decrease. Because the overall gain of the composite amplifier is fixed to 4.71, the gain of the precision opamp will decrease, causing its BW to increase. If the BW of the precision opamp is larger than that of the power opamp it will overshoot and start to oscillate. A way to solve this problem was by using a filter in the feedback of the precision opamp, effectively lowering its BW.

After optimizing the resistive load circuit for its components and performing frequency compensation the design met all requirements given in Table 8.1. The SNR is 102.47 dB, which meets the required 100 dB. The THD is 0.000293 %, which is lower than the required 0.001%. The phase margin is 87 °, which is larger than

45°, meaning that the amplifier is stable and robust. And the output current at 1Khz has a phase shift of 0° compared to the input voltage, which is lower than the 31° that is given in Table 8.1. The fact that all requirements were met means that for a purely resistive load the amplifier works well: it is stable, robust, with a high SNR and low THD.

Since the loudspeaker does not behave as a resistive load but has an inductive nature, the speaker model was derived. This inductive nature results in a high impedance as seen from the amplifier for high frequencies. Meaning that to maintain the same output current the amplifier has to deliver a larger voltage. The voltage of a power supply of the amplifier is limited to ± 40 V. That is why to counteract the increase of impedance at higher frequencies where the amplifier starts to run out of the supply voltage, a Zobel network was designed. The Zobel network counteracts the increase of the impedances seen by the amplifier, but it has adds an unwanted phase shift at 800 Hz causing peaking. To increase the phase at 800 Hz a resistor and a capacitor were added as a feedback of the precision amplifier. This added a zero near the peaking which decreased the peaking and thus increased the phase at 800 Hz. The design with the loudspeaker model as a load has a THD of 0.000427 %, PM of 51° and phase at 800 Hz of -2°. A SNR of 100.9 dB. By comparing this values with Table 8.1 the amplifier met all the requirements.

8.2. Recommendations

Calculation of THD and SNR were done in the circuit simulating program MicroCap. This calculation is easy to do when dealing with a real load. But it becomes more cumbersome to do when using complex impedance as a load. The reason being that Micro-cap can only simulate the THD and SNR of a one component load, which the complex loudspeaker is not.

8.3. Future Work

In this amplifier design, all the theory and the simulation is an approximation of the real world, and unfortunately the proof of the pudding is in the eating. That is why to measure the performance of the proposed amplifier, the amplifier has to be build and tested. Protection circuits were not added in the design. To name a few: an over current protection circuit is needed for the output and a protection method which stops the amplifier from working if no load is attached.

The designed amplifier in this report acts as a class A amplifier, meaning that it conducts for the whole period of the cycle. The other op amp classes can be investigated. For example, a very efficient class D amplifier, which has switching transistors in order to modulate the signal into the desired gain. Since the transistors are fully on or fully off during a fixed period of time they consume less power due to the fact that in that mode transistors have the lowest resistance. It might be interesting to see how this amplifier concept would perform in a different class, since the power efficiency will then be greatly enhanced.

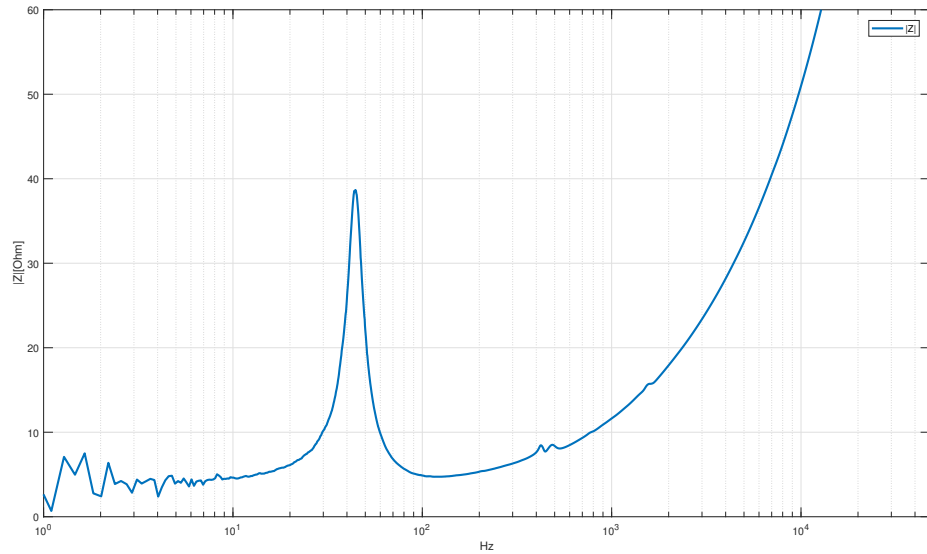
Appendices

A

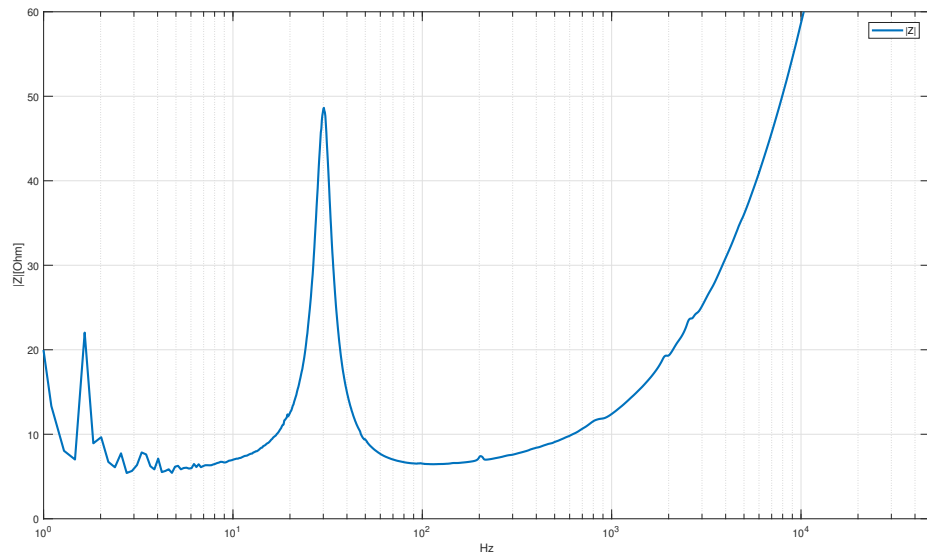
Extra Theory

A.1. Finding the equivalent loudspeaker impedance parameters from measured loudspeaker impedance graph

Now that the electrical model is given, it is time to find the values for the model. The impedance measurement for both monopole and dipole speakers were done and can be seen at Figure A.1a and Figure A.1b.



(a) Absolute magnitude plot from measured monopole speaker



(b) Absolute magnitude plot from measured dipole speaker

Figure A.1: Absolute magnitude impedance for both subwoofers

The values for the electrical model can be found using Figure 3.11, Figure A.1 and the Epo1 manual [10]. The first thing to notice is that R_{es} , L_{ces} and C_{mes} are all connected in parallel and thus can be seen as one impedance that is frequency-dependent. The total impedance for the RLC circuit is given with Equation A.1, At a low frequency the total impedance for the parallel circuit is approximately 0, leaving only the impedance of the voice coil. The characteristic impedance for an inductor at low frequencies is also approximately 0. Thus meaning that at low frequency (below the resonance frequency) the measured impedance of the loudspeaker is equal to R_e [10].

The next interesting frequency to look at is the resonant frequency. Seeing that there is only one RLC circuit present. This circuit causes the resonant characteristic of the speaker. At resonant frequency there is no imaginary load, meaning the total impedance of Z_{RLC} is equal to R_{es} . L_e is approximately 0, once again using the fact that the characteristic impedance of an inductor is approximately zero at low frequencies. This means

that the measured impedance at the resonant frequency is equal to $R_e + R_{es}$ [10]. Next, at high frequencies, Equation A.1 is once again approximately zero. This time the L_e is not approximately 0 and it is noticeable when comparing its magnitude with R_e . Thus at higher frequencies, the absolute measured impedance is equal to the $|R_e + j\omega L_e|$ [10]

Now that it is known how the circuits impedance changes at different frequencies it is time to find the values. The easiest value to find is R_e . In theory simply look at the impedance of the speaker at around 0 Hz as it should be constant. In practice it is very difficult to measure around 0 Hz, as can be seen from Figure A.1. Thus instead look for the first point after 0 Hz where the impedance is flat.

The next value to find is R_{ces} . As mentioned before at the resonant frequency the measured impedance is equal to $R_{ces} + R_e$. R_e is already known thus R_{ces} is also known. Next are the C_{mes} and L_{ces} values. The resonance caused by these two will be used to find their values. First using the resonance frequency. By simply finding at which frequency $Y_{L_{ces}} + Y_{C_{mes}}$ is equal to zero the resonance frequency equation can be found. This is given with Equation A.2. The next characteristic of the resonance that will be used is the bandwidth. The bandwidth in which the impedance is equal to $\frac{R_e + R_{es}}{\sqrt{2}}$. The bandwidth can be calculated using Equation A.3 [6]. For a parallel circuit the quality factor is given with Equation A.4 [6]. Now combining Equation A.2 up to Equation A.4 the Equation A.5 can be derived. By measuring the resonance bandwidth and using equation Equation A.5, C_{mes} can be found. Then using Equation A.2, L_{ces} can be found.

$$Z_{RLC} = (Y_{R_{es}} + Y_{L_{ces}} + Y_{C_{mes}})^{-1} \Rightarrow \frac{1}{\frac{1}{R_{es}} + \frac{1 - \omega^2 LC}{j\omega L}} \quad (\text{A.1})$$

$$f_s = \frac{1}{2\pi\sqrt{L_{ces}C_{mes}}} \quad (\text{A.2})$$

$$BW = \frac{f_s}{Q} \quad (\text{A.3})$$

$$Q = R_{es}\sqrt{\frac{L_{ces}}{C_{mes}}} \quad (\text{A.4})$$

$$BW = \frac{1}{2\pi R_{es}C_{mes}} \quad (\text{A.5})$$

As mentioned before, the absolute impedance of the loudspeaker at high frequencies is given as $Z_{measured} = |R_e + j\omega L_e|$. Now rewriting the equation to remove the absolute sign and the imaginary part of the impedance results in Equation A.6. In theory this value is constant at higher frequencies. In practice this is not so looking at Figure A.1 if 1kHz was chosen it would have a different value for L_e than if 5kHz was chosen. This can be seen by extrapolating the graph using only frequencies up to 2-3 kHz. Seeing that the CS only needs to work at low frequencies the inductance at around 2-3 kHz was chosen.

$$L_e = \sqrt{\frac{Z_{measured}^2 - R_e^2}{4\pi^2 f^2}} \quad (\text{A.6})$$

Now the values for R_e , L_e , L_{ces} , R_e , and C_{mes} for both monopole and dipole L_e speakers can be found.

A.2. Chain matrix and nullor

The following sections are based on [12] which is part of the bachelor course EE1C31.

A.2.1. Chain matrix

The chain matrix as given in matrix equation A.7 describes two ports element which is illustrated in Figure A.2.

$$\begin{bmatrix} V_i \\ I_i \end{bmatrix} = \begin{bmatrix} A & B \\ C & D \end{bmatrix} \begin{bmatrix} V_o \\ I_o \end{bmatrix} \quad (\text{A.7})$$

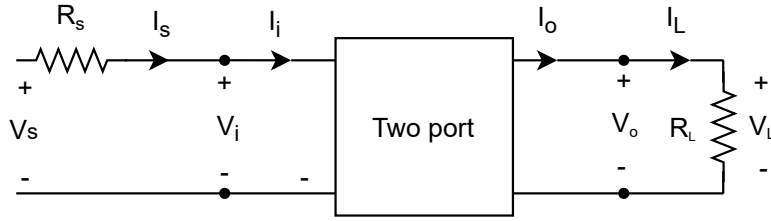


Figure A.3: Two port representation of the amplifier

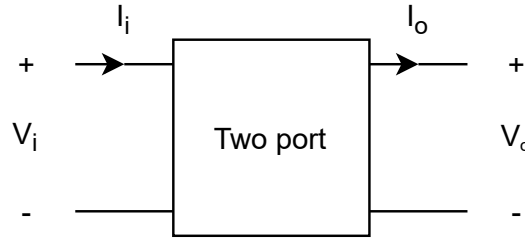


Figure A.2: Two port circuit

The elements A, B, C and D in matrix equation A.7 can be found with the help of the following equations:

$$V_i = AV_o + BI_o \quad (\text{A.8})$$

$$I_i = CV_o + DI_o \quad (\text{A.9})$$

The elements A and C can be found by cutting the output port as given in A.10 and A.12. The elements B and D can be found by short circuit the output as given in equations A.11 and A.13.

$$A = \frac{V_i}{V_o} |_{I_o=0} \quad (\text{A.10})$$

$$B = \frac{V_i}{I_o} |_{V_o=0} \quad (\text{A.11})$$

$$C = \frac{I_i}{V_o} |_{I_o=0} \quad (\text{A.12})$$

$$D = \frac{I_i}{I_o} |_{V_o=0} \quad (\text{A.13})$$

With the help of the chain matrix the input and output resistance can be calculated. The impedance of the source and the resistance of the load are added to the diagram A.2 and the total diagram is given in Figure A.3. By substituting $V_o = I_o R_L$ in equations A.8 and A.9 we obtain the two following equations:

$$V_i = (AR_L + B)I_o \quad (\text{A.14})$$

$$I_i = (CR_L + D)I_o \quad (\text{A.15})$$

By dividing equation A.14 by the equation A.15 the input resistance is obtained and it is given in equation A.16.

$$R_i = \frac{AR_L + B}{CR_L + D} \quad (\text{A.16})$$

The output resistance is calculated by first taking the matrix inverse of matrix given in equation A.17:

$$\begin{bmatrix} V_i \\ I_i \end{bmatrix} = \begin{bmatrix} A & B \\ C & D \end{bmatrix}^{-1} \begin{bmatrix} V_i \\ I_i \end{bmatrix}$$

$$\begin{bmatrix} V_o \\ I_o \end{bmatrix} = \frac{1}{AD - BC} \begin{bmatrix} D & -B \\ -C & A \end{bmatrix} \begin{bmatrix} V_i \\ I_i \end{bmatrix} \quad (\text{A.17})$$

From matrix equation A.17 the following equations are extracted:

$$(AD - BC)V_O = DV_i - BI_i \quad (\text{A.18})$$

$$(AD - BC)I_O = -CV_i + AI_i \quad (\text{A.19})$$

Then by substituting in equations A.18 and A.19 $V_i = -RSI_i$ the following equations are obtained:

$$(AD - BC)V_O = -(DR_s + B)I_i \quad (\text{A.20})$$

$$(AD - BC)I_O = (CR_s + A)I_i \quad (\text{A.21})$$

To calculate the output resistance the output voltage is divided by the reverse of the output current:

$$\frac{V_o}{-I_o}$$

Thus by dividing equation A.20 and equation A.21 and the multiplying it by -1 the output resistance is obtained and it is given in equation A.22

$$R_o = \frac{DR_s + B}{CR_s + A} \quad (\text{A.22})$$

A.2.2. Nullor

Nullor and the components it is made of are given in Figure A.4. The nullor is an element that nullifies the current and voltage for all input voltages and currents values. Norator is the circuit element that can deliver any voltage for any current and vice versa.

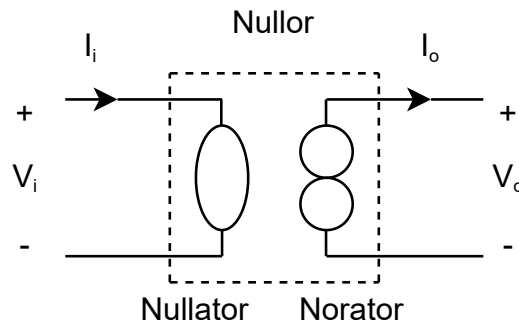


Figure A.4: Nullor that consist of a nollator and norator

We can describe the nullor with the chain matrix since the nullor is a two port element.

From the equations A.10, A.11, A.12 and A.13 it is obvious that the nullor chain matrix elements A, B, C and D are equal to zero. That is because the V_i and I_i in equations A.10, A.11, A.12 and A.13 are set to zero by the nullator.

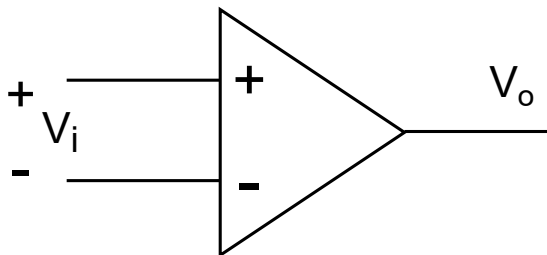


Figure A.5: Representation of operational amplifier

What real component can replace the nullor? One of the candidates is the operational amplifier that is

presented in Figure A.5. The ideal OPAMP has the following input/output relation:

$$V_o = A(V_+ - V_-) \quad A \text{ is the open-loop gain} \quad (\text{A.23})$$

$$V_+ = V_- \quad (\text{A.24})$$

$$I_i = 0 \text{ A} \quad (\text{A.25})$$

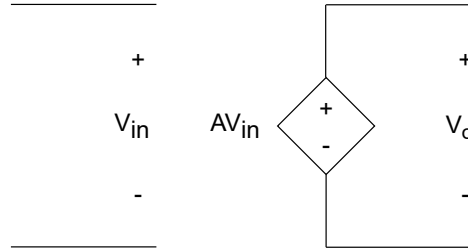


Figure A.6: Equivalent model of operational amplifier

Based on the equations A.23, A.24 and A.25, the equivalent circuit of the opamp is derived using the voltage-dependent-voltage-source. The equivalent circuit of the OPAMP is given in Figure A.6. The chain matrix of the circuit in Figure A.6 is derived by taking into account equation A.25 and $V_o = AV_i$:

$$A = \frac{V_i}{V_o} \Big|_{I_o=0} = \frac{V_i}{AV_i} = \frac{1}{A_v}$$

$$B = \frac{V_i}{I_o} \Big|_{V_o=0} = \frac{A_v 0}{A_v V_i} = 0$$

$$C = \frac{I_i}{V_o} \Big|_{I_o=0} = 0$$

$$D = \frac{I_i}{I_o} \Big|_{V_o=0} = 0$$

For an ideal amplifier A_v goes to infinity and thus A goes to 0. Meaning that the chain matrix is the same as that for the nullor. Since the gain of the real opamp is finite the operational amplifier can only approximate the nullor if $A_v \gg 0$.

B

Calculations

B.1. Control analysis of the simple transconductance amplifier

B.1.1. Control analysis

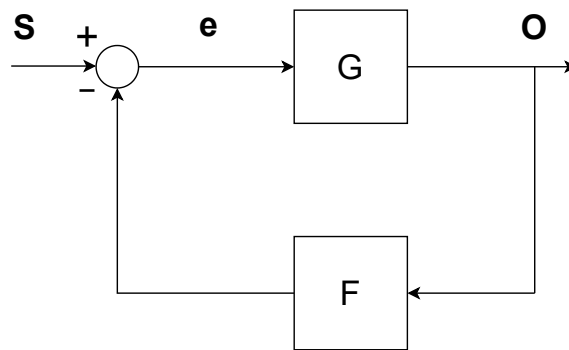


Figure B.1: Black model [7] of the amplifier where S is the input signal, e is the error signal, G is the open-loop voltage gain, F is the feedback factor and O is the output signal

The transfer function of the model given in Figure B.1 goes as follows:

$$\begin{aligned}e &= S - OF \\O &= Ge \\O &= G(S - OF) \\O(1 + GF) &= GS \\O &= \frac{GS}{1 + GF}\end{aligned}$$

By dividing both sides of the equation by s the total transfer function is derived and given in equation 5.1.

$$H = \frac{O}{S} = \frac{G}{1 + GF} \quad (\text{B.1})$$

When the gain goes to infinity the overall gain is given in equation 5.2.

$$\lim_{G \rightarrow \infty} H = \frac{1}{F} \quad (\text{B.2})$$

The following calculation is for the error made by the amplifier:

$$\begin{aligned}
 \text{Error} &= \frac{1}{F} - \frac{G}{1+GF} \\
 &= \frac{1+GF - GF}{F(1+GF)} \\
 &= \frac{1}{F} \\
 &= \frac{1}{1+GF}
 \end{aligned}$$

B.1.2. Noise Analysis

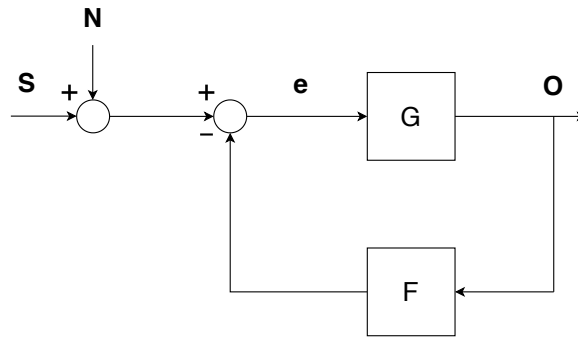


Figure B.2: Black [7] model of the amplifier where S is the input signal, N is the noise signal, e is the error signal, G is the open-loop voltage gain, F is the feedback factor and O is the output signal

In the model given in Figure B.1, a noise source is added as represented in Figure B.2. The derivation of the transfer function with added noise sources goes as follows:

$$\begin{aligned}
 e &= (S + N - OF) \\
 O &= Ge \\
 O &= G(S + N - OF) \\
 O &= GS + GN - GFO \\
 O(1 + GF) &= GS + GN \\
 O &= \frac{G}{1 + GF}(S + N)
 \end{aligned}$$

If the signal S is set to zero and both sides are divided by N we get the transfer function of the noise and it is given in equation B.3.

$$H_N = \frac{O}{N} = \frac{G}{1 + GF} \tag{B.3}$$

B.2. Control analysis of the composite amplifier

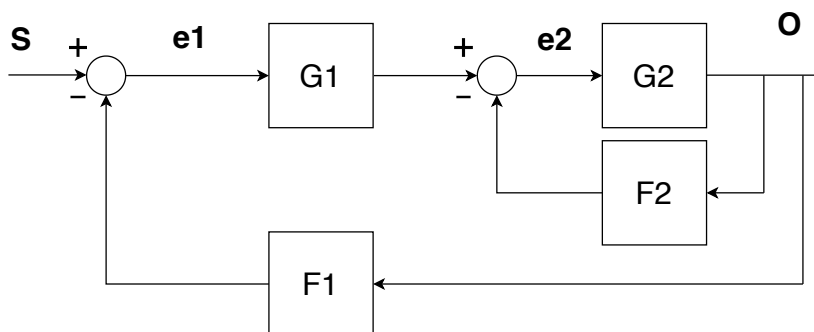


Figure B.3: Black model [7] of the composite amplifier where S is the input signal, e1 and e2 are the error signals, G1 and G2 are the open-loop voltage gains, F1 and F2 are the feedback factors and O is the output signal

The transfer function of this model is calculated as follows:

$$\begin{aligned}
 e1 &= (S - OF1) \\
 e2 &= G1e1 - OF2 \\
 O &= G2e2 \\
 O &= G2(G1e1 - OF2) \\
 O &= G2(G1(S - OF1) - OF2) \\
 O &= G1G2S - G1G2OF1 - G2OF2 \\
 O(1 + G1G2F1 + G2F2) &= G1G2S \\
 O &= \frac{G1G2S}{1 + G1G2F1 + G2F2}
 \end{aligned}$$

By dividing both sides with S the transfer function is obtained and is given in equation B.4.

$$H = \frac{G1G2}{(1 + G1G2F1 + G2F2)} \quad (\text{B.4})$$

The gain of the composite amplifier only determined by F1 as given in equation B.5.

$$\lim_{G1, G2 \rightarrow \infty} H = \frac{G1G2}{G1G2F1} = \frac{1}{F1} \quad (\text{B.5})$$

The error made at the output by the amplifier because of the finite gain is:

$$\begin{aligned}
 Error &= \frac{1}{F1} - \frac{G1G2}{1 + G1G2F1 + G2F2} \\
 &= \frac{1 + G1G2F1 + G2F2 - G1G2F1}{F1(1 + G1G2F1 + G2F2)} \\
 &= \frac{1 + G2F2}{F1(1 + G1G2F1 + G2F2)}
 \end{aligned}$$

The error made at the output by the amplifier if the gain G1 and G2 are much greater than 1.

$$\begin{aligned}
 Error &= \frac{1 + G2F2}{F1(1 + G1G2F1 + G2F2)} \\
 &\approx \frac{G2F2}{G1G2(F1)^2} \text{ if } G1 \gg G2 \gg 0 \text{ or } G2 \approx G2 \gg 0
 \end{aligned}$$

$$Error \approx \frac{F2}{G1(F1)^2} \text{ if } G1 \gg G2 \gg 0 \text{ or } G2 \approx G2 \gg 0 \quad (\text{B.6})$$

B.3. Noise analysis of the composite amplifier

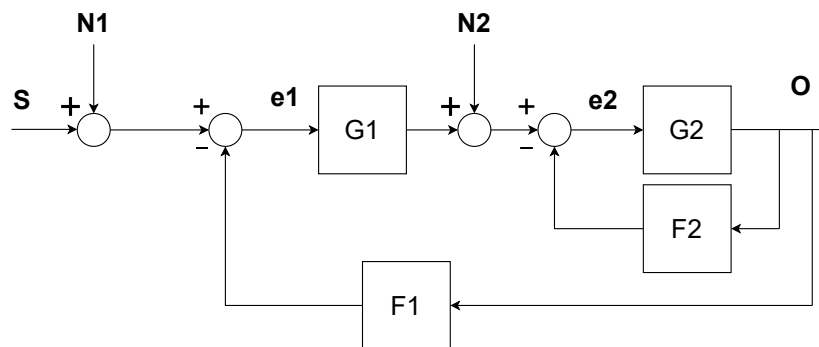


Figure B.4: Block model of the composite amplifier where S is the input signal, N1 and N2 are the noise signals, e1 and e2 are the error signals, G1 and G2 are the open-loop voltage gains, F1 and F2 are the feedback factors and O is the output signal

The transfer function of the model is calculated as follows:

$$\begin{aligned}
 e1 &= (S + N1 - OF1) \\
 e2 &= (G1e1 + N2 - OF2) \\
 O &= G2e2 \\
 O &= G2(G1e1 + N2 - OF2) \\
 O &= G2(G1(S + N1 - OF1) + N2 - OF2) \\
 O &= G1G2S + G1G2N1 - G1G2OF1 + G2N2 - G2F2O \\
 O(1 + G1G2F1 + G2F2) &= G1G2S + G1G2N1 + G2N2 \\
 O &= \frac{G1G2S + G1G2N1 + G2N2}{1 + G1G2F1 + G2F2}
 \end{aligned}$$

By setting the signal to zero the following equation is obtained:

$$O = \frac{G1G2N1}{1 + G1G2F1 + G2F2} + \frac{G2N2}{1 + G1G2F1 + G2F2} \tag{B.7}$$

Equation B.7 can be analyzed for different values of the open-loop gain. Important case is if $G1 \approx G2 \gg 0$. In that case equation B.7 becomes:

$$\begin{aligned}
 O &\approx \frac{G1G2N1}{G1G2F1} + \frac{G2N2}{G1G2F1} \\
 &= \frac{N1}{F1} + \frac{N2}{G1F1} \approx \frac{N1}{F1} \text{ Since } G1 \gg 0 \\
 \frac{O}{N1} &\approx \frac{1}{F1} \text{ if } G1 \approx G2 \gg 0 \tag{B.8}
 \end{aligned}$$

B.4. Nodal analysis of the composite amplifier with frequency compensation

B.4.1. Nodal analysis full circuit

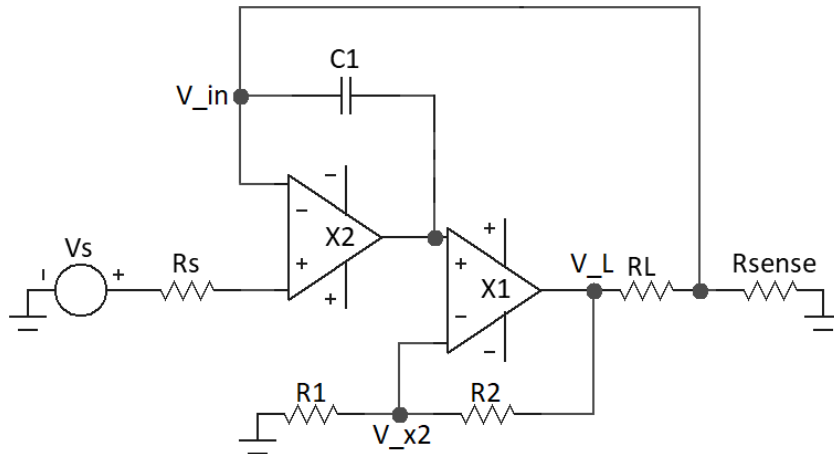


Figure B.5: Nodal analysis of composite amplifier without R3 and R4

This is the nodal analysis performed on the figure above, with the goal to obtain its transfer function. First of all, the equation for the node V_{in} will be given and rewritten to obtain O_L .

$$\frac{V_{in}}{R_{sense}} = \frac{V_L - V_{in}}{R_L} + \frac{V_{x2} - V_{in}}{Z} \tag{B.9}$$

$$\frac{V_{in}}{R_{sense}} = I_L + \frac{V_{x2} - V_{in}}{Z} \tag{B.10}$$

$$I_L = \frac{V_{in}}{R_{sense}} - \frac{V_{x2} - V_{in}}{Z} \quad (\text{B.11})$$

The following equation for V_{x2} will get substituted in to the previous equation:"

$$V_{x2} = \frac{V_L}{1 + \frac{R_2}{R_1}} = \frac{I_L R_L + V_{in}}{1 + \frac{R_2}{R_1}} \quad (\text{B.12})$$

This results in:

$$I_L = \frac{V_{in}}{R_{sense}} - \frac{1}{Z} \left(\frac{I_L R_L + V_{in}}{1 + \frac{R_2}{R_1}} - V_{in} \right) \quad (\text{B.13})$$

$$I_L \left(1 + \frac{1}{Z} \frac{R_L}{1 + \frac{R_2}{R_1}} \right) = \frac{V_{in}}{R_{sense}} - \frac{1}{Z} \left(\frac{V_{in}}{1 + \frac{R_2}{R_1}} - V_{in} \right) \quad (\text{B.14})$$

$$I_L \left(1 + \frac{1}{Z} \frac{R_L}{1 + \frac{R_2}{R_1}} \right) = \frac{V_{in}}{R_{sense}} - \frac{V_{in}}{Z} \left(\frac{1}{1 + \frac{R_2}{R_1}} - 1 \right) \quad (\text{B.15})$$

$$\frac{I_L}{V_{in}} = \frac{\frac{1}{R_{sense}} - \frac{1}{Z} \left(\frac{1}{1 + \frac{R_2}{R_1}} - 1 \right)}{\left(1 + \frac{1}{Z} \frac{R_L}{1 + \frac{R_2}{R_1}} \right)} \quad (\text{B.16})$$

$$H = \frac{\frac{1}{R_{sense}} - \frac{1}{Z} \left(\frac{1}{1 + \frac{R_2}{R_1}} - 1 \right)}{\left(1 + \frac{1}{Z} \frac{R_L}{1 + \frac{R_2}{R_1}} \right)} \quad (\text{B.17})$$

For $Z = \frac{1}{sC}$:

$$H = \frac{\frac{1}{R_{sense}} - sC \left(\frac{1}{1 + \frac{R_2}{R_1}} - 1 \right)}{\left(1 + sC \frac{R_L}{1 + \frac{R_2}{R_1}} \right)} \quad (\text{B.18})$$

This concludes the analysis, since an equation has been found for the transfer function H.

B.4.2. Derivation of A_v

This derivation is done by using $Z = \frac{1}{sC}$ and setting s to zero, meaning the signal will be a DC signal. After this is done, the equation will be rewritten to get the voltage gain factor, as follows:

$$\frac{V_{in}}{R_{sense}} = \frac{V_L - V_{in}}{R_L} + \frac{V_{x2} - V_{in}}{Z} \quad (\text{B.19})$$

$$\frac{V_{in}}{R_{sense}} = \frac{V_L - V_{in}}{R_L} \quad (\text{B.20})$$

$$\frac{V_{in} R_L}{R_{sense}} = V_L - V_{in} \quad (\text{B.21})$$

$$a_v = \frac{V_L}{V_{in}} = 1 + \frac{R_L}{R_{sense}} \quad (\text{B.22})$$

B.5. Nodal analysis of the composite amplifier with frequency compensation when the resistors for the overall gain have been added

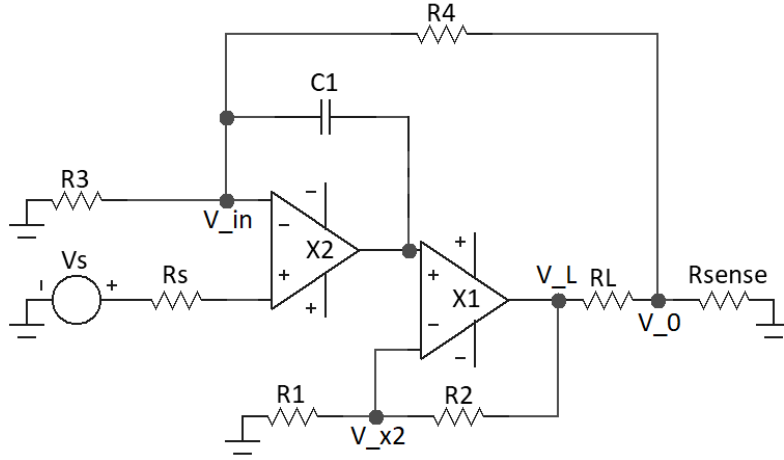


Figure B.6: Nodal analysis of composite amplifier with R3 and R4

This is the nodal analysis performed on the figure above, with the goal to obtain its transfer function. First of all, the equation for the node V_{in} will be given and rewritten to obtain V_0 .

$$\frac{V_{in}}{R_3} = \frac{V_0 - V_{in}}{R_4} + \frac{V_{x2} - V_{in}}{Z} \quad (\text{B.23})$$

$$\frac{R_4}{R_3} V_{in} = V_0 - V_{in} + \frac{R_4}{Z} (V_{x2} - V_{in}) \quad (\text{B.24})$$

$$V_0 = V_{in} \left(1 + \frac{R_4}{R_3}\right) - \frac{R_4}{Z} (V_{x2} - V_{in}) \quad (\text{B.25})$$

Now the node at V_0 will be rewritten to obtain an equation for I_L .

$$\frac{V_0}{R_{sense}} + \frac{V_0 - V_{in}}{R_4} = \frac{V_L - V_0}{R_L} = I_L \quad (\text{B.26})$$

$$I_L R_{sense} = V_0 + \frac{R_{sense}}{R_4} (V_0 - V_{in}) \quad (\text{B.27})$$

$$I_L R_{sense} = V_0 \left(1 + \frac{R_{sense}}{R_4}\right) - V_{in} \frac{R_{sense}}{R_4} \quad (\text{B.28})$$

If it is assumed that $R_1, R_2, R_3, R_4 \gg \gg R_{sense}$ then the following equation is obtained:

$$I_L = \frac{V_0}{R_{sense}} \quad (\text{B.29})$$

If Equation B.25 is substituted into Equation B.29 the following equation is obtained:

$$I_L = \frac{V_{in}}{R_{sense}} \left(1 + \frac{R_4}{R_3}\right) - \frac{R_2}{R_{sense} Z} (V_{x2} - V_{in}) \quad (\text{B.30})$$

$$V_{x2} = \frac{V_L}{1 + \frac{R_2}{R_1}} = \frac{I_L R_L - V_0}{1 + \frac{R_2}{R_1}} \quad (\text{B.31})$$

$$I_L = \frac{V_{in}}{R_{sense}} \left(1 + \frac{R_4}{R_3}\right) - \frac{R_4}{R_{sense} Z} \left(\frac{I_L R_L - V_0}{1 + \frac{R_2}{R_1}} - V_{in}\right) \quad (\text{B.32})$$

$$I_L \left(1 + \frac{R_4}{R_{sense} Z} \frac{R_L}{1 + \frac{R_2}{R_1}}\right) = \frac{V_{in}}{R_{sense}} \left(1 + \frac{R_4}{R_3}\right) + \frac{R_4}{R_{sense} Z} \left(\frac{V_0}{1 + \frac{R_2}{R_1}} + V_{in}\right) \quad (B.33)$$

If it is assumed that $1 + \frac{R_4}{R_3} \gg V_0$, then it turns into the following equation:

$$I_L = \frac{V_{in}}{R_{sense}} \frac{\left(1 + \frac{R_4}{R_3}\right) + \frac{R_4}{Z}}{1 + \frac{R_4}{R_{sense} Z} \frac{R_L}{1 + \frac{R_2}{R_1}}} \quad (B.34)$$

$$H = \frac{1}{R_{sense}} \frac{\left(1 + \frac{R_4}{R_3}\right) + \frac{R_4}{Z}}{1 + \frac{R_4}{R_{sense} Z} \frac{R_L}{1 + \frac{R_2}{R_1}}} \quad (B.35)$$

This concludes the analysis, since an equation has been found for the transfer function H. <https://www.overleaf.com/pro>

B.6. Total harmonic distortion calculation using MicroCap

In this section a way on how to calculate the THD with the help of the circuit simulator MicroCap is given. In the same manner as described in this appendix the THD will be calculated for the final design in the report.

An AC sinusoidal voltage source of known frequency is connected to the input of the circuit. Then the output is simulated in time domain for the chosen quantity using 'Transient analysis' tool in Micro Cap. Since due to internal workings of the MicroCap it takes couple of periods of the signal to charge all the capacitances. In 'Transient analysis limits' window the time region of the output signal can be selected. By selecting one of the last periods in the output. Fourier transform of this last period is calculated using 'FFT' macro provided by MicroCap. Then the power at the natural frequency and the harmonics frequencies is derived from the plot. With this values THD is calculated by dividing the power in harmonics by the power in the natural frequency.

B.7. Calculating the SNR using Micro-Cap 12

B.7.1. Derivation

Since the inbuilt function of Micro-Cap 12 could not be used, a different method had to be found for this calculation. This calculation has been done using the following two equations:

$$SNR = 20 \log_{10} \left(\frac{V_{out}}{V_{noise}} \right) \quad (B.36)$$

$$V_{noise} = \sqrt{\int ONOISE^2 df} \quad (B.37)$$

In Equation B.37 a variable called ONOISE is present, this is an inbuilt variable in Micro-Cap 12 which plots the sum of all noise sources, this is given in $\frac{V}{\sqrt{Hz}}$. This variable then gets squared ($\frac{V^2}{Hz}$), integrated over the bandwidth of the amplifier (V^2) and then the square root is taken from it (V). This results in the total noise voltage at the output of the amplifier. To validate this calculation, it has been performed on the amplifier for a purely resistive load (Figure 5.7). The results are given in Figure B.7.

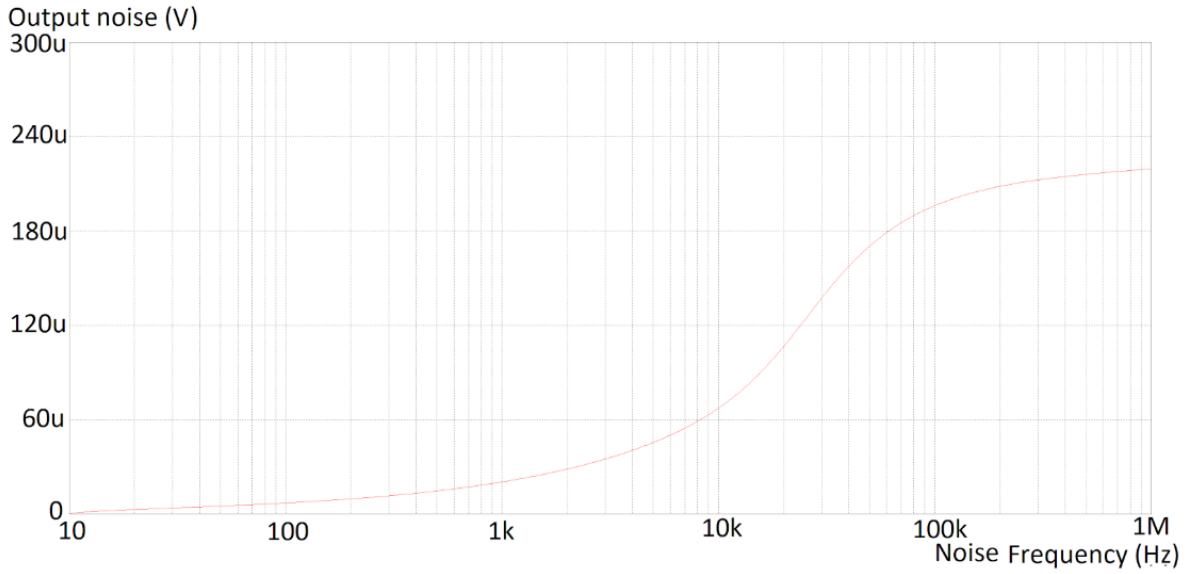


Figure B.7: The total output noise voltage for a given bandwidth of the amplifier.

From these noise values and the output voltage of the amplifier, the SNR has been calculated for different bandwidths of the amplifier. This SNR has then been compared to the SNR from the inbuilt function in Micro-Cap 12, these two plots have been given in Figure B.8.

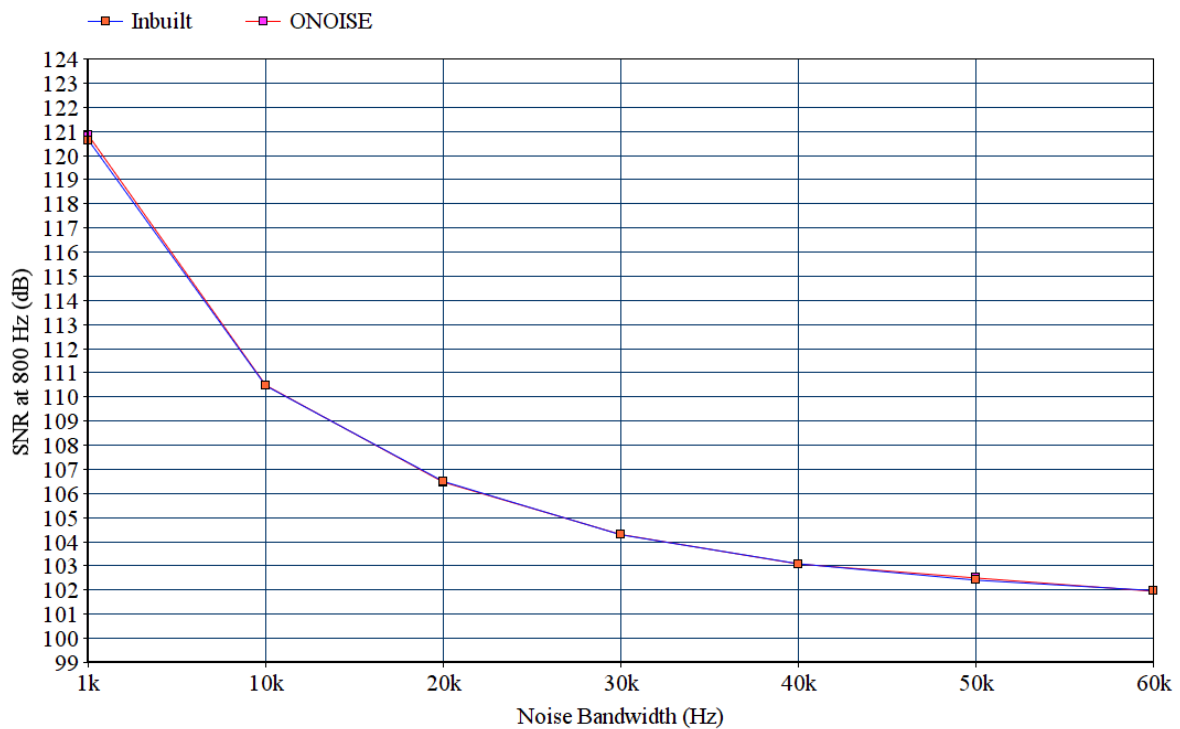


Figure B.8: A comparison of the results from the inbuilt function and the method that was derived in this section.

This plot shows that the results are identical, which confirms that this method works as intended and can be used to determine the SNR for the amplifier with an electrical model of the loudspeaker as load.

B.7.2. Calculation of the SNR

For this calculation, three variables are needed: The BW of the amplifier, the output voltage and the total noise voltage. From Figure 6.7a it can be seen that the BW (-3dB point) is 4.86Khz. It has been measured that at this frequency the output voltage is 24.8V RMS.

If Equation B.37 is used to calculate the output noise for this amplifier, the result is as follows:

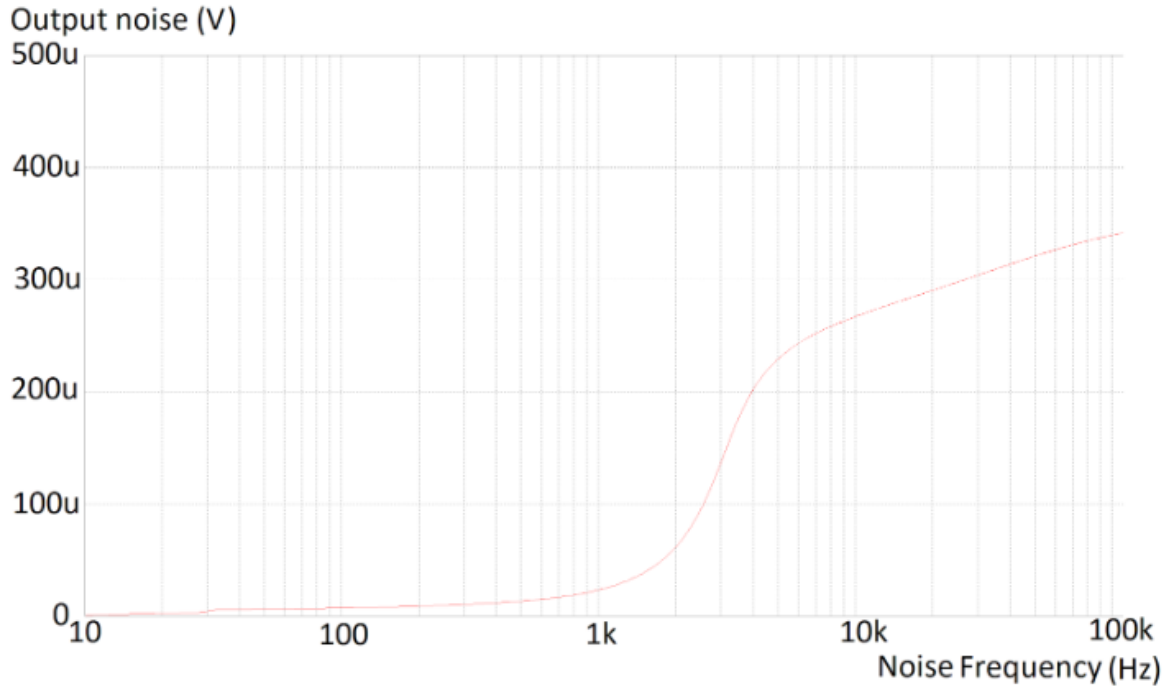


Figure B.9: The total output noise voltage for a given bandwidth of the amplifier.

It can be seen that at a frequency of 4.86Khz, the output noise voltage is 223 μV . With this result and the output voltage of 24.8V RMS, Equation B.36 can be used to calculate the SNR. If these values are plugged into Equation B.36, it results in a SNR of 100.92dB.

B.8. Howland nodal analysis

[H]

Kirchhoff current law (KCL) at node 1:

$$\frac{V_x - V_o}{R_x} - \frac{V_o - V^+}{R_2} - I_L = 0 \quad (\text{B.38})$$

Since $R_2 \gg R_x$ the term $\frac{V_o - V^+}{R_2}$ is negligible in equation B.38. The equation B.38 becomes:

$$I_o \approx \frac{V_x - V_o}{R_x} \text{ if } R_2 \gg R_x \quad (\text{B.39})$$

The voltage at V^- is determined by V_x and the voltage divider which is determined by R_3 and R_4 :

$$\begin{aligned} V^- &= V_x \frac{R_3}{R_3 + R_4} \\ &= V_x \frac{1}{\alpha}, \text{ where } \alpha \text{ is } \frac{R_3 + R_4}{R_3} \end{aligned}$$

Rewriting V_x in terms of V^- :

$$V_x = \alpha V^- \quad (\text{B.40})$$

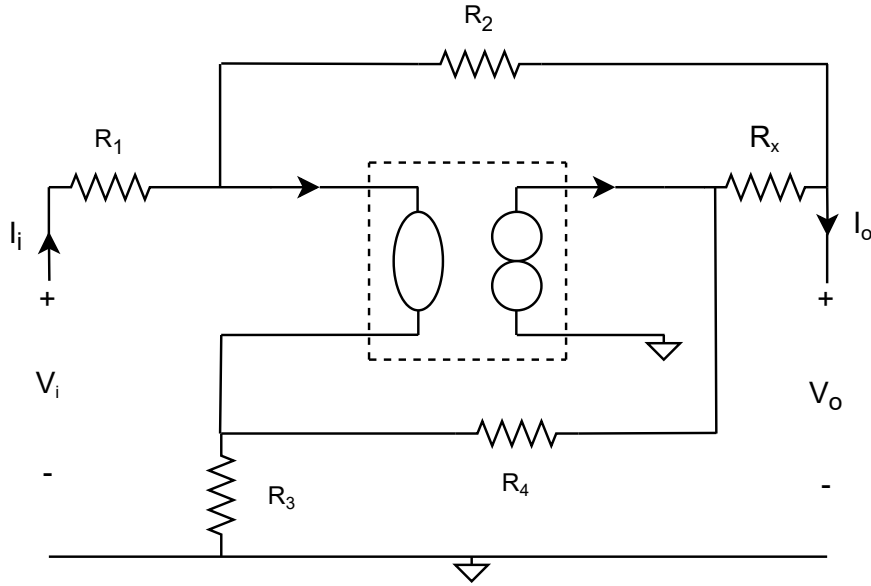


Figure B.10: Howland two port representation with nullor as a controller

KCL at node 2:

$$\frac{V_{in} - V^+}{R_1} + \frac{V_o - V^+}{R_2} = 0 \quad (\text{B.41})$$

eliminating V^+ :

$$\begin{aligned} V_+ \left(\frac{1}{R_1} + \frac{1}{R_2} \right) &= \frac{V_{in}}{R_1} + \frac{V_o}{R_2} \\ V_+ &= \frac{\frac{V_{in}}{R_1} + \frac{V_o}{R_2}}{\left(\frac{1}{R_1} + \frac{1}{R_2} \right)} \\ V_+ &= \frac{V_{in}R_2}{R_1 + R_2} + \frac{V_oR_1}{R_1 + R_2} \end{aligned}$$

$$V_+ = \frac{V_{in}R_2}{R_1\beta} + \frac{V_o}{\beta}, \text{ where } \beta \text{ is } \frac{R_1 + R_2}{R_1} \quad (\text{B.42})$$

By observing that term $\frac{V_{in} - V^+}{R_1} = I_{in}$ in equation B.41 V^+ can be expressed in I_{in}

$$\begin{aligned} I_{in} + \frac{V_o - V^+}{R_2} &= 0 \\ I_{in} + \frac{V_o}{R_2} &= \frac{V^+}{R_2} \end{aligned}$$

$$V^+ = I_{in}R_2 + V_o \quad (\text{B.43})$$

$V^+ = V^-$ because of the nullator. By substituting the equations B.42 and B.43 into equation B.40 the following two equations are acquired:

$$V_x = \alpha \left(\frac{V_{in}R_2}{R_1\beta} + \frac{V_o}{\beta} \right) \quad (\text{B.44})$$

$$V_x = \alpha (I_{in}R_1 + V_o) \quad (\text{B.45})$$

By substituting the equations B.44 I_o is expressed in V_o and V_{in} as given in equation B.46.

$$I_o \approx \frac{1}{R_x} \left(\alpha \left(\frac{V_{in} R_2}{R_1 \beta} + \frac{V_o}{\beta} \right) \right) - \frac{V_o}{R_x}$$

$$I_o \approx \frac{R_2 \alpha}{R_x R_1 \beta} V_{in} + \frac{V_o}{R_x} \left(\frac{\alpha}{\beta} - 1 \right) \quad (\text{B.46})$$

By substituting the equations B.45 I_o is expressed in V_o and I_{in} as given in equation B.47.

$$I_o \approx \frac{1}{R_x} \left(\alpha (I_{in} R_2 + V_o) \right) - \frac{V_o}{R_x}$$

$$I_o \approx \alpha \frac{R_2}{R_x} I_{in} + \frac{V_o}{R_x} (\alpha - 1) \quad (\text{B.47})$$

With the help of Equation B.46 and Equation B.47 the chain matrix elements can be found and the chain matrix elements are given in Equation B.48, Equation B.49, Equation B.50 and Equation B.51.

$$A = \frac{V_{in}}{V_o} \Big|_{I_o=0} = \frac{1 - \frac{\alpha}{\beta}}{R_x} \frac{\beta R_x R_1}{R_2 \alpha} = \frac{R_1}{R_2} \left(\frac{\beta}{\alpha} - 1 \right) \quad (\text{B.48})$$

$$B = \frac{V_{in}}{I_o} \Big|_{V_o=0} = \frac{1}{\frac{R_2 \alpha}{R_x R_1 \beta}} = \frac{R_x R_1 \beta}{R_2 \alpha} \quad (\text{B.49})$$

$$C = \frac{I_{in}}{V_o} \Big|_{I_o=0} = \frac{\frac{(1-\alpha)}{R_x}}{\alpha \frac{R_2}{R_x}} = \frac{(1-\alpha)}{\alpha R_2} \quad (\text{B.50})$$

$$D = \frac{I_{in}}{I_o} \Big|_{V_o=0} = \frac{1}{\alpha \frac{R_2}{R_x}} = \frac{R_x}{\alpha R_2} \quad (\text{B.51})$$

$$(\text{B.52})$$

To set A element the equality in Equation B.58 must be valid.

$$\frac{\beta}{\alpha} - 1 = 0 \quad (\text{B.53})$$

$$\frac{\beta}{\alpha} = 1 \quad (\text{B.54})$$

$$\beta = \alpha \quad (\text{B.55})$$

$$1 + \frac{R_4}{R_3} = 1 + \frac{R_2}{R_1} \quad (\text{B.56})$$

$$\frac{R_2}{R_1} = \frac{R_4}{R_3} \quad (\text{B.57})$$

$$\frac{R_2}{R_1} = \frac{R_4}{R_3} \quad (\text{B.58})$$

Due to the resistors tolerance Equation B.58 can have a specific deviation. The maximum deviation is when the term $\frac{R_2}{R_1}$ is maximized and the term $\frac{R_4}{R_3}$ is minimized. The derivation of the maximum deviation of equality B.58 due to resistor tolerance p is given below.

$$\frac{R_2(1+p)}{R_3(1-p)} - \frac{R_4(1-p)}{R_3(1+p)} \approx \frac{R_2}{R_1}(1+p)^2 - \frac{R_4}{R_3}(1-p)^2, \text{ using } \frac{1}{1 \pm p} \approx 1 \mp p \text{ iff } p \ll 1$$

$$\frac{R_2}{R_1}(1+p)^2 - \frac{R_4}{R_3}(1-p)^2 \approx \frac{R_2}{R_1}((1+2p) - (1-2p)) = 4p \frac{R_2}{R_1}, \text{ iff } R_1 \approx R_2 \approx R_3 \approx R_4 \text{ and } p \ll 1$$

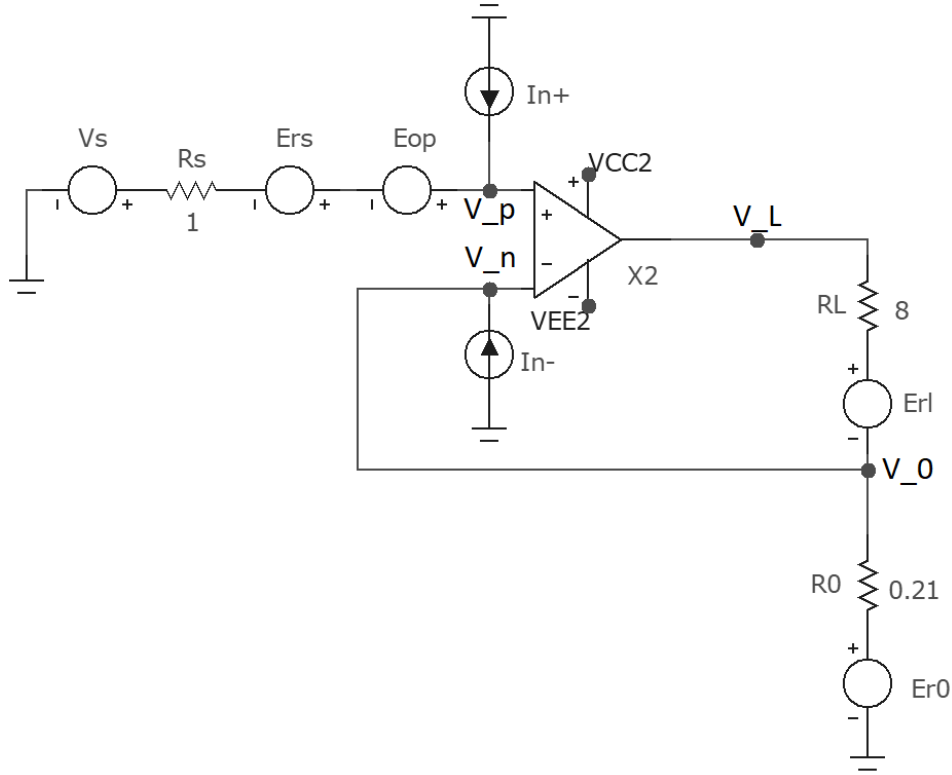


Figure B.11: The phase diagram of the amplifier.

B.9. Noise analysis simple transconductance amplifier

B.9.1. Primary analysis

Calculations of the noise in the simple transconductance amplifier given in Figure B.11.

$$V_L = A(V_p - V_n) \text{ A the open-loop voltage} \quad (\text{B.59})$$

$$V_p = V_s + E_{rs} + E_{op} + I_{n+} R_s \quad (\text{B.60})$$

$$V_n = V_0 \quad (\text{B.61})$$

$$I_{n-} + \frac{(V_L + E_{rl}) - V_0}{R_l} = \frac{V_0 - E_{R0}}{R_0} \quad (\text{B.62})$$

If Equation B.61 and Equation B.60 are substituted in Equation B.59 it results in the following equation:

$$V_L = A(V_s + E_{rs} + E_{op} + I_{n+} R_s - V_0) \quad (\text{B.63})$$

The only unknown variable in this equation is V_0 , but this one can be found if Equation B.62 gets rewritten as follows:

$$I_{n-} R_L + V_L + E_{rl} - V_0 = \frac{R_L}{R_0} (V_0 - E_{R0}) \quad (\text{B.64})$$

$$V_0 \left(1 + \frac{R_L}{R_0}\right) = I_{n-} R_L + V_L + E_{rl} + \frac{R_L}{R_0} E_{R0} \quad (\text{B.65})$$

$$V_0 = \frac{I_{n-} R_L + V_L + E_{rl} + \frac{R_L}{R_0} E_{R0}}{1 + \frac{R_L}{R_0}} \quad (\text{B.66})$$

If V_0 in Equation B.63 gets substituted by Equation B.66 it results in the following equation:

$$V_L = A(V_s + E_{rs} + E_{op} + I_{n+}R_s - \frac{I_{n-}R_L + V_L + E_{rl} + \frac{R_L}{R_0}E_{R0}}{1 + \frac{R_L}{R_0}}) \quad (B.67)$$

$$V_L \left(\frac{1}{A} + \frac{1}{1 + \frac{R_L}{R_0}} \right) = V_s + E_{rs} + E_{op} + I_{n+}R_s - \frac{I_{n-}R_L + E_{rl} + \frac{R_L}{R_0}E_{R0}}{1 + \frac{R_L}{R_0}} \quad (B.68)$$

If it is assumed that A will be very large, $\frac{1}{A}$ will be close to 0. In that case Equation B.68 can be rewritten as follows:

$$\frac{V_L}{1 + \frac{R_L}{R_0}} = V_s + E_{rs} + E_{op} + I_{n+}R_s - \frac{I_{n-}R_L + E_{rl} + \frac{R_L}{R_0}E_{R0}}{1 + \frac{R_L}{R_0}} \quad (B.69)$$

$$V_L = \left(1 + \frac{R_L}{R_0}\right)(V_s + E_{rs} + E_{op} + I_{n+}R_s) - I_{n-}R_L + E_{rl} + \frac{R_L}{R_0}E_{R0} \quad (B.70)$$

$$E_L^2 = \left(1 + \frac{R_L}{R_0}\right)^2(E_{rs}^2 + E_{op}^2 + I_{n+}^2R_s^2) + I_{n-}^2R_L^2 + E_{rl}^2 + \left(\frac{R_L}{R_0}\right)^2E_{R0}^2 \quad (B.71)$$

To get the noise voltage density at the input of the amplifier, this equation above will need to be divided by the gain, given by $\left(1 + \frac{R_L}{R_0}\right)^2$:

$$E_{in}^2 = \frac{E_L^2}{\left(1 + \frac{R_L}{R_0}\right)^2} \quad (B.72)$$

$$E_{in}^2 = E_{rs}^2 + E_{op}^2 + I_{n+}^2R_s^2 + \frac{I_{n-}^2R_L^2 + E_{rl}^2 + \left(\frac{R_L}{R_0}\right)^2E_{R0}^2}{\left(1 + \frac{R_L}{R_0}\right)^2} \quad (B.73)$$

This concludes this analysis, since an equation for the noise voltage density at the output (Equation B.71) and input (Equation B.72) of the amplifier have been found.

B.9.2. SliCAP analysis

$$S_{src} = S_v + \frac{R_L^2 R_{sens}^2 S_i}{(R_L + R_{sens})^2} + \frac{4TkR_LR_{sens}^2}{(R_L + R_{sens})^2} + \frac{4TkR_L^2 R_{sens}}{(R_L + R_{sens})^2} \quad (B.74)$$

B.10. Noise analysis howland

Using the same code in Appendix C.1.1 on the circuit given in Figure B.13. The source referred noise signal is given in equation B.75

$$S_{src} = \frac{R_4^2 S_v (R_1 + R_2)^2}{(R_1 R_4 + R_2 R_4 + R_1 R_o)^2} + \frac{R_1^2 R_2^2 R_4^2 S_i}{(R_1 R_4 + R_2 R_4 + R_1 R_o)^2} + \frac{4kTR_1 R_2^2 R_4^2}{(R_1 R_4 + R_2 R_4 + R_1 R_o)^2} + \frac{4kTR_1^2 R_4 R_o^2}{(R_1 R_4 + R_2 R_4 + R_1 R_o)^2} + \frac{4kTR_1^2 R_4^2 R_o}{(R_1 R_4 + R_2 R_4 + R_1 R_o)^2} \quad (B.75)$$

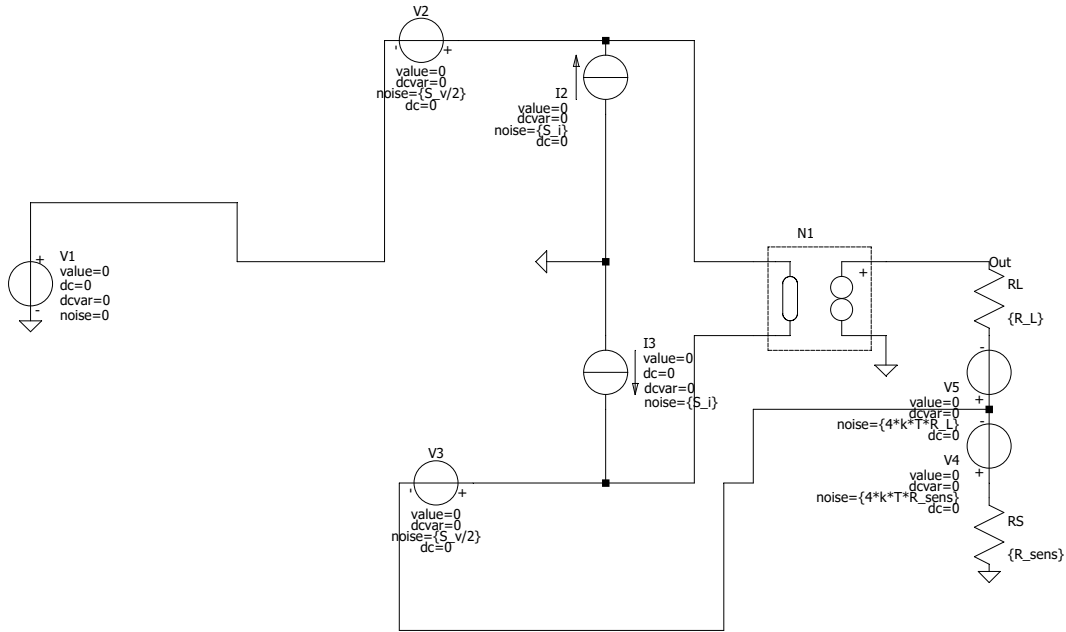


Figure B.12: SPICE circuit of the simple transconductance amplifier with nullor as a controller

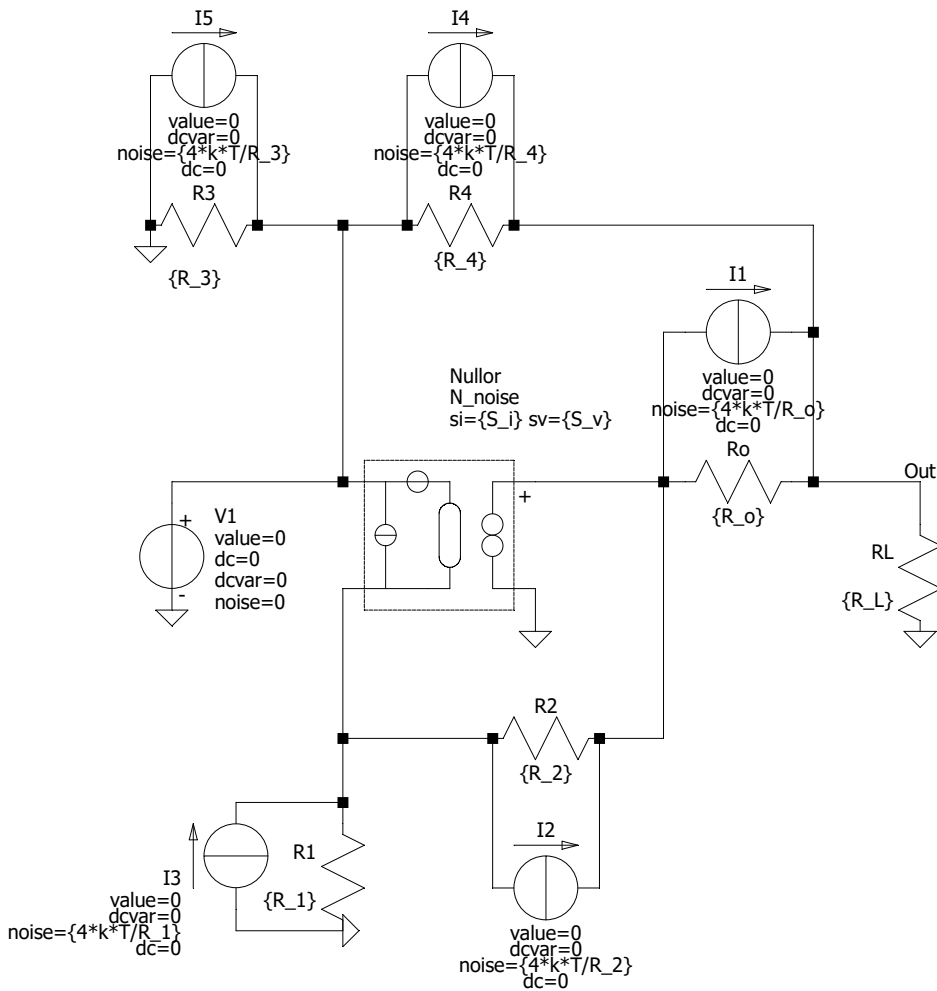


Figure B.13: SPICE circuit of the howland amplifier with nullor as a controller and equivalent noise sources added

B.11. Noise analysis composite amplifier

Using the same code in Appendix C.1.1 on the circuit given in Figure B.14. The source referred noise signal is given in equation B.76

$$S_{\text{SRC}} = S_{v1} + \frac{R_4^2 S_{i1} (R_3 R_L + R_3 R_{\text{sens}} + R_L R_{\text{sens}})^2}{(R_3 R_L + R_4 R_L + R_3 R_{\text{sens}} + R_4 R_{\text{sens}} + R_L R_{\text{sens}})^2} + \frac{4 T k R_4 (R_3 R_L + R_3 R_{\text{sens}} + R_L R_{\text{sens}})^2}{(R_3 R_L + R_4 R_L + R_3 R_{\text{sens}} + R_4 R_{\text{sens}} + R_L R_{\text{sens}})^2} + \frac{4 T k R_3 R_4^2 (R_L + R_{\text{sens}})^2}{(R_3 R_L + R_4 R_L + R_3 R_{\text{sens}} + R_4 R_{\text{sens}} + R_L R_{\text{sens}})^2} + \frac{4 T k R_4^2 R_L^2 R_{\text{sens}}}{(R_3 R_L + R_4 R_L + R_3 R_{\text{sens}} + R_4 R_{\text{sens}} + R_L R_{\text{sens}})^2} \quad (\text{B.76})$$

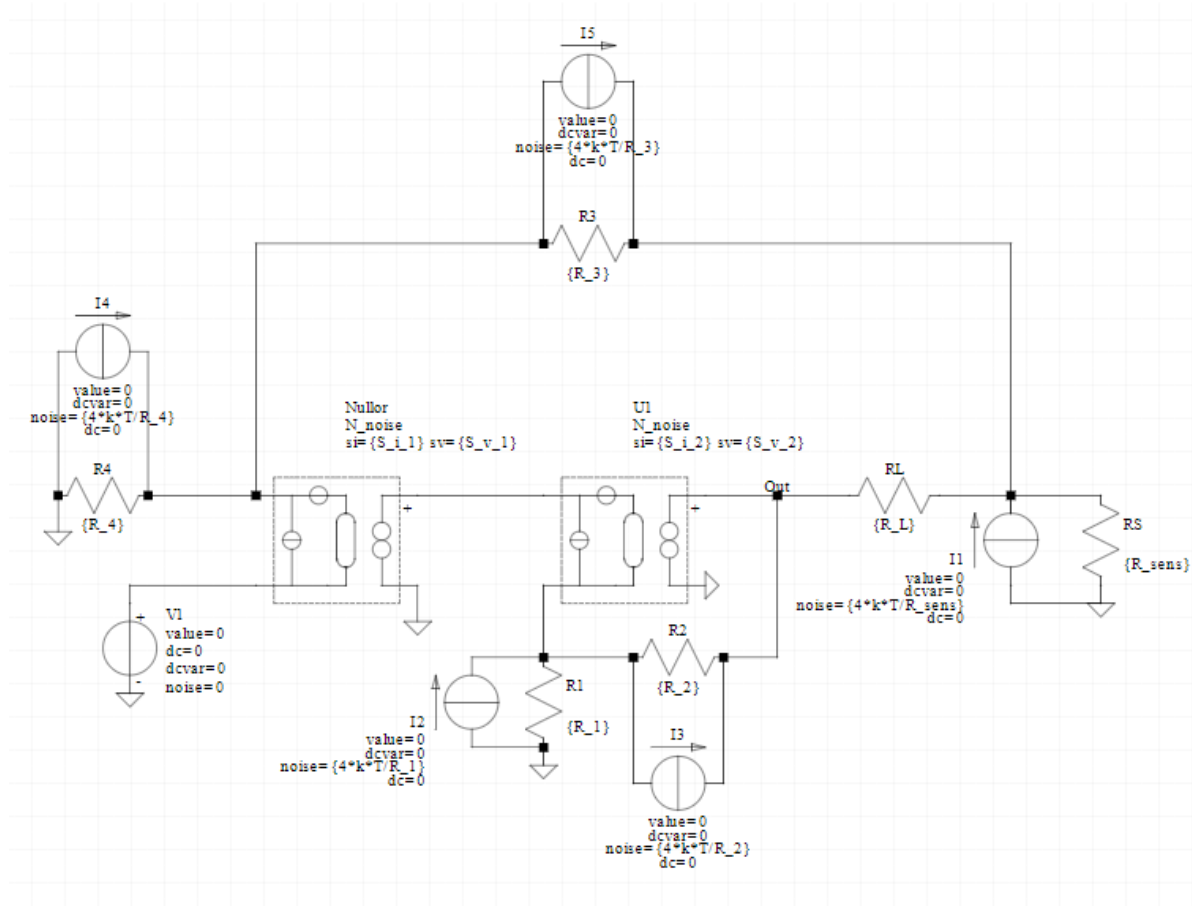


Figure B.14: SPICE circuit of the composite amplifier with two nullors as controllers and equivalent noise sources added

C

Code

C.1. SliCap

C.1.1. Simple transconductance noise analysis

```
%% Variables
fileName = 'simpleY';
%%
checkCircuit(fileName);
htmlPage('Circuit data');
img2html([fileName, '.svg'], 760);
netlist2html(fileName);

%%
htmlPage('Noise analysis');
text2html(['The symbolic analysis of noise']);
simType('symbolic');
gainType('vi');
dataType('noise');
source('V1');
detector('V_Out');
noiseResults = execute();
noise2html(noiseResults);
stophtml();
```

D

Simulations

D.1. Composite Amplifier with real load

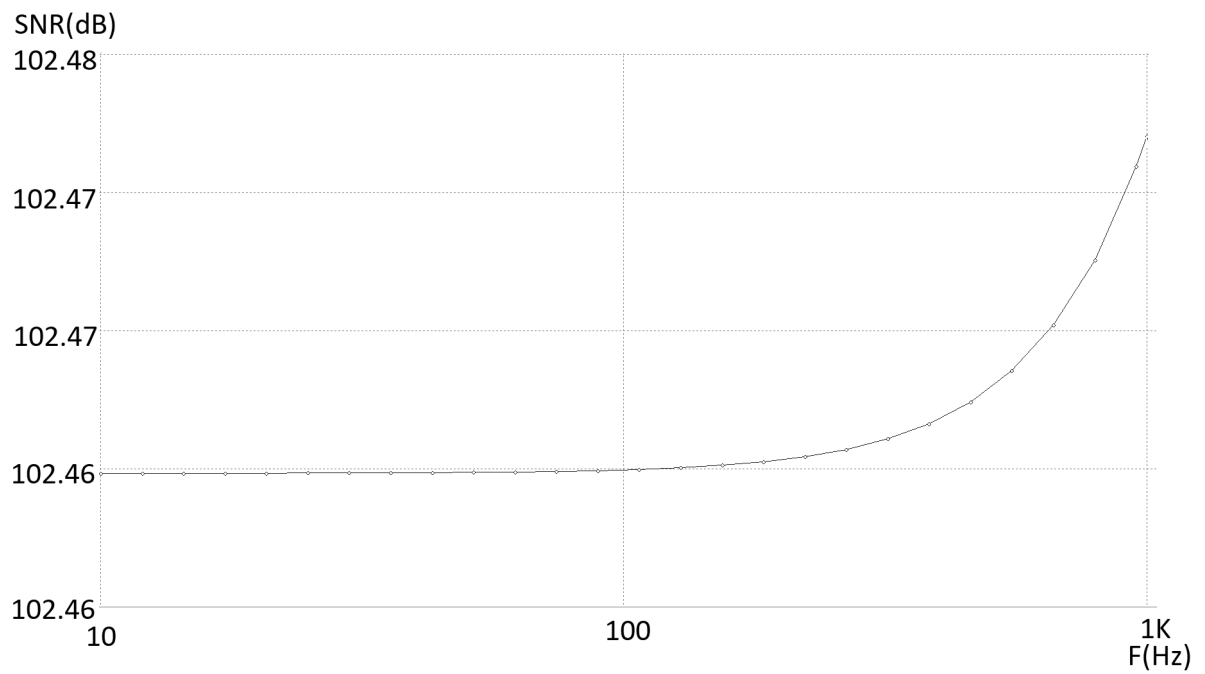


Figure D.1: The SNR of the amplifier.

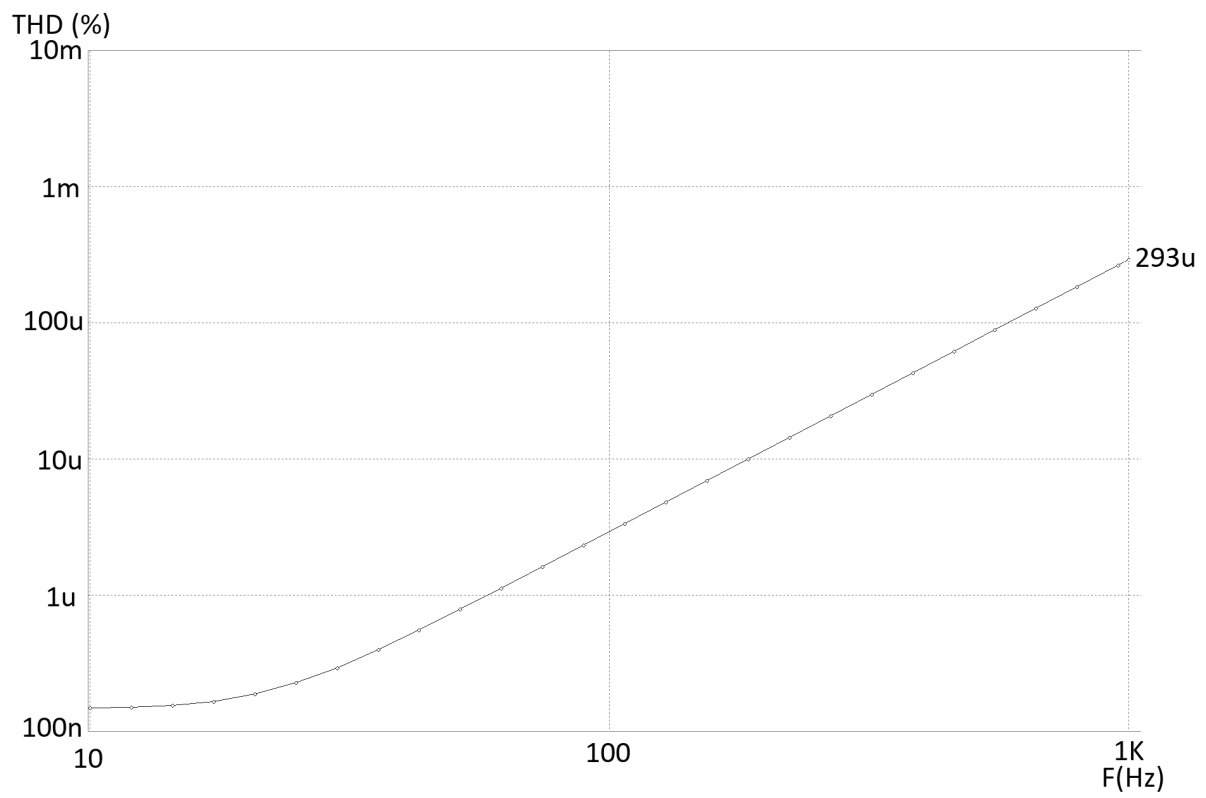


Figure D.2: The THD of the amplifier.

Bibliography

- [1] Loudspeakers' Electric Models for Study of the Efforts in Audio Power Amplifiers. URL https://www.researchgate.net/publication/282705311_Loudspeakers'_Electric_Models_for_Study_of_the_Efforts_in_Audio_Power_Amplifiers.
- [2] ADAU1777 Datasheet and Product Info | Analog Devices. URL <https://www.analog.com/en/products/adau1777.html>.
- [3] Understanding electrical transformers: Chapter 5 - impedance matching and power transfer: Power electronics textbook. URL <https://eepower.com/power-electronics-textbook/vol-i-electrical-power-systems-design/chapter-5-impedance-matching-and-power-transfer/understanding-electrical-transformers/>.
- [4] Electrical Mechanical Analogs - Erik Cheever. URL <https://lpsa.swarthmore.edu/Analog/ElectricalMechanicalAnalog.html>.
- [5] Ltspice. URL <https://www.analog.com/en/design-center/design-tools-and-calculators/ltspice-simulator.html>.
- [6] Charles K. Alexander and Matthew N. O. Sadiku. *Fundamentals of electric circuits*. McGraw-hill Education, New York, NY, sixth edition edition, 2017. ISBN 9780078028229.
- [7] H. S. Black. Stabilized feedback amplifiers*. *Bell System Technical Journal*, 13(1):1-18, 1934. doi: 10.1002/j.1538-7305.1934.tb00652.x. URL <https://onlinelibrary.wiley.com/doi/abs/10.1002/j.1538-7305.1934.tb00652.x>.
- [8] Rosalfonso Bortoni and Homero Sette Silva. Loudspeakers' electric models for study of the efforts in audio power amplifiers. In *Audio Engineering Society Convention 115*. Audio Engineering Society, 2003.
- [9] John Borwick, editor. *Loud speaker and headphone handbook*. Focal Press, Oxford ; Boston, 3rd ed edition, 2001. ISBN 9780240515786.
- [10] J. Creemer M. Gibescu I. Lager N. van der Meijs S. Vollebregt R. Roodenburg J. Hoekstra D. Djairam, G. Janssen and X. van Rijnsoeve. *Student Manual - Lab Course EE Semester 1*. TU Delft, 2017-2018.
- [11] Gene F. Franklin, J. David Powell, and Abbas Emami-Naeini. *Feedback control of dynamic systems*. Pearson, Boston, seventh edition edition, 2015. ISBN 9780133496598.
- [12] Dr. J. Hoekstra. *Versterkerschakelingen*. TU Delft, 12 2014.
- [13] S.H. de Koning J.A. Klaassen. *Bewegingstegenkoppeling bij luidsprekers*.
- [14] Wolfgang Klippel. Loudspeaker nonlinearities—causes, parameters, symptoms. In *Audio Engineering Society Convention 119*. Audio Engineering Society, 2005.
- [15] E. Meriläinen. Comparative measurements on loudspeaker distortion: Current vs. voltage control. *Archives of Acoustics*, 42(1):71-81, 2017. URL https://www.researchgate.net/publication/315508245_Comparative_Measurements_on_Loudspeaker_Distortion_Current_vs_Voltage_Control.
- [16] E. Meriläinen. A large current source with high accuracy and fast settling. *Analog Dialogue*, 52(10), 2018. URL <https://www.analog.com/media/en/analog-dialogue/volume-52/number-4/a-large-current-source-with-high-accuracy-and-fast-settling.pdf>.
- [17] Esa T Merilainen. *Current-driving of loudspeakers: eliminating major distortion and interference effects by the physically correct operation method*. E. Merilainen, United States, 2010. ISBN 9781450544009.

-
- [18] A.J.M. Montagne. *Structural Electronic Design, a conceptual approach to amplifier design*. Delft Academic Press, 1.1 edition, 2019. ISBN 97890-6562-4277.
- [19] *LME49860 44V Dual High Performance, High Fidelity Audio Operational Amplifier*. Texas Instrument, 6 2007.
- [20] *Noise Analysis in Operational Amplifier Circuitser*. Texas Instrument, 2007.
- [21] *OPA541 High Power Monolithic Operational Amplifier*. Texas Instrument, 1 2016.